

The *Kepler* Follow-Up Observation Program. II. Stellar Parameters from Medium- and High-Resolution Spectroscopy

E. FURLAN,¹ D. R. CIARDI,¹ W. D. COCHRAN,² M. E. EVERETT,³ D. W. LATHAM,⁴ G. W. MARCY,⁵ L. A. BUCHHAVE,⁶
M. ENDL,² H. ISAACSON,⁵ E. A. PETIGURA,^{7,*} T. N. GAUTIER, III,⁸ D. HUBER,^{9,10,11,12} A. BIERYLA,⁴ W. J. BORUCKI,¹³
E. BRUGAMYER,² C. CALDWELL,² A. COCHRAN,² A. W. HOWARD,¹⁴ S. B. HOWELL,¹³ M. C. JOHNSON,^{2,15}
P. J. MACQUEEN,² S. N. QUINN,⁴ P. ROBERTSON,^{2,16,†} S. MATHUR,^{17,18,19} AND N. M. BATALHA¹³

¹*IPAC, Mail Code 314-6, Caltech, 1200 E. California Blvd., Pasadena, CA 91125, USA*

²*Department of Astronomy and McDonald Observatory, The University of Texas at Austin, Austin, TX 78712, USA*

³*National Optical Astronomy Observatory, Tucson, AZ 85719, USA*

⁴*Harvard-Smithsonian Center for Astrophysics, Cambridge, MA 02138, USA*

⁵*Department of Astronomy, University of California, Berkeley, CA 94720, USA*

⁶*Centre for Star and Planet Formation, Natural History Museum of Denmark, University of Copenhagen, DK-1350 Copenhagen, Denmark*

⁷*Division of Geological and Planetary Sciences, California Institute of Technology, Pasadena, CA 91125, USA*

⁸*Jet Propulsion Laboratory/California Institute of Technology, Pasadena, CA 91109, USA*

⁹*Institute for Astronomy, University of Hawaii, Honolulu, HI 96822, USA*

¹⁰*Sydney Institute for Astronomy, School of Physics, University of Sydney, NSW 2006, Australia*

¹¹*SETI Institute, Mountain View, CA 94043, USA*

¹²*Stellar Astrophysics Centre, Department of Physics and Astronomy, Aarhus University, DK-8000 Aarhus C, Denmark*

¹³*NASA Ames Research Center, Moffett Field, CA 94035, USA*

¹⁴*Department of Astronomy, California Institute of Technology, Pasadena, CA 91125, USA*

¹⁵*Department of Astronomy, The Ohio State University, Columbus, OH 43210 USA*

¹⁶*Department of Astronomy and Astrophysics, and Center for Exoplanets & Habitable Worlds, The Pennsylvania State University, University Park, PA 16801, USA*

¹⁷*Space Science Institute, Boulder, CO 80301, USA*

¹⁸*Instituto de Astrofísica de Canarias (IAC), La Laguna, Tenerife, Spain*

¹⁹*Universidad de La Laguna, Departamento de Astrofísica, La Laguna, Tenerife, Spain*

ABSTRACT

We present results from spectroscopic follow-up observations of stars identified in the *Kepler* field and carried out by teams of the *Kepler* Follow-Up Observation Program. Two samples of stars were observed over six years (2009–2015): 614 standard stars (divided into “platinum” and “gold” categories) selected based on their asteroseismic detections and 2667 host stars of *Kepler* Objects of Interest (KOIs), most of them planet candidates. Four data analysis pipelines were used to derive stellar parameters for the observed stars. We compare the T_{eff} , $\log(g)$, and $[\text{Fe}/\text{H}]$ values derived for the same stars by different pipelines; from the average of the standard deviations of the differences in these parameter values, we derive error floors of ~ 100 K, 0.2 dex, and 0.1 dex for T_{eff} , $\log(g)$, and $[\text{Fe}/\text{H}]$, respectively. Noticeable disagreements are seen mostly at the largest and smallest parameter values (e.g., in the giant star regime). Most of the $\log(g)$ values derived from spectra for the platinum stars agree on average within 0.025 dex (but with a spread of 0.1–0.2 dex) with the asteroseismic $\log(g)$ values. Compared to the *Kepler* Input Catalog (KIC), the spectroscopically derived stellar parameters agree within the uncertainties of the KIC, but are more precise and are thus an important contribution towards deriving more reliable planetary radii.

Keywords: planets and satellites: fundamental parameters — stars: fundamental parameters — surveys
— techniques: spectroscopic

1. INTRODUCTION

The majority of extrasolar planets known to date were discovered by the *Kepler* mission (Borucki 2016). It has yielded several thousand planet candidates during its operation from March 2009 to May 2013, observing over 150,000 stars in the constellation Cygnus-Lyra (Borucki et al. 2011a,b; Batalha et al. 2014; Burke et al. 2014; Rowe et al. 2015; Seader et al. 2015; Mullally et al. 2015; Coughlin et al. 2016; Thompson et al. 2018). These candidates were discovered via the transit method, which detects a planet as it passes in front of its star, periodically dimming the stellar light. Transit events identified in *Kepler* data that pass a certain threshold and a vetting process are given a *Kepler* Object of Interest (KOI) number, and they are categorized as either planet candidates or false positives. The latter group includes eclipsing binary stars, which can mimic the signal of a transiting planet. For planet candidates found with the transit method, the planet radius is directly derived from the transit depth; however, it is only known with respect to the stellar radius (the decrease in brightness due to a transit event is equal to the ratio of the square of the planet radius and the stellar radius). Therefore, it is important to know stellar parameters as accurately as possible in order to derive reliable planet parameters.

The Kepler Input Catalog (KIC; Brown et al. 2011) provides stellar parameters for most of the stars in the *Kepler* field, but they were derived using broad-band colors. This results in estimates of stellar properties that are sufficient for target selection, which was the main objective of the KIC; since the priority of the *Kepler* mission was to find small planets in the habitable zones of Sun-like stars, the main goal of the KIC was to distinguish dwarf stars from giant stars. However, the stellar parameters from the KIC are significantly affected by systematic errors (Huber et al. 2014). In some cases, red giant stars were misclassified in the KIC as dwarf stars (Mathur et al. 2016) or subgiants (Yu et al. 2016). Using stellar properties from the KIC to derive other parameters, e.g., planetary radii, could introduce significant systematic errors in the estimation of these parameters.

Spectroscopic observations yield more precise stellar parameters than those inferred from photometry (e.g.,

Torres et al. 2012; Mortier et al. 2013, 2014; Huber et al. 2014). By modeling spectral lines from the star’s atmosphere, the stellar effective temperature (T_{eff}), surface gravity ($\log(g)$, in cgs units), and metallicity ($[\text{Fe}/\text{H}]$) can be derived, and in turn these parameters, combined with stellar evolutionary models, yield the stellar mass and radius. An important quantity that enters the calculation of the stellar luminosity and thus the stellar radius is the surface gravity. By comparing constrained and unconstrained derivations of $\log(g)$, Torres et al. (2012) and Mortier et al. (2013) showed that uncertainties in $\log(g)$ of about 0.2 dex translate to fractional uncertainties of $\sim 20\%$ – 30% in the stellar radius. Moreover, uncertainties in $\log(g)$ also affect T_{eff} and $[\text{Fe}/\text{H}]$, since there are degeneracies between these parameters (Torres et al. 2012). Any uncertainties in the stellar properties will propagate to the planet properties; for the planet radius, the uncertainty in the stellar radius linearly increases the uncertainty in the planet radius (since $R_p \propto R_*$).

As part of the *Kepler* Follow-Up Observation Program (KFOP), spectroscopic observations of KOI host stars were carried out from June 2009 to October 2015 to derive more precise and accurate stellar effective temperatures, surface gravities, and metallicities. Other, independent groups have carried out spectroscopic follow-up observations of *Kepler* stars, with the goal of improving stellar parameters (e.g., De Cat et al. 2015; Fleming et al. 2015; Petigura et al. 2017). The spectra are also important for vetting the KOIs to identify false positives. Some of the observations were done using high-resolution spectrographs to measure radial velocity signals as a confirmation of planetary candidates. Spectra may also reveal whether a close companion is present (Marcy et al. 2014; Kolbl et al. 2015). Besides spectroscopic observations, high-resolution imaging observations were carried out as part of KFOP to detect close companions to KOI host stars, which would dilute the transit depth and thus lead to underestimated planet radii. Results from that program are presented in Furlan et al. (2017). Both the imaging and spectroscopic data and results have been posted on the *Kepler* Community Follow-Up Observation Program (CFOP) website¹.

To revise the stellar parameters from the KIC, Huber et al. (2014) compiled stellar properties for the en-

* Hubble Fellow

† NASA Sagan Fellow

¹ <https://exofop.ipac.caltech.edu/cfop.php>

tire sample of stars observed by *Kepler* (almost 200,000 stars). They used published literature values as well as asteroseismology and broadband photometry to derive atmospheric parameters (T_{eff} , $\log(g)$, $[\text{Fe}/\text{H}]$), which were then fit to a grid of Dartmouth isochrones (Dotter et al. 2008). The stellar parameters from an updated version of this catalog (Huber 2014) were used for the Q1-Q17 Data Release 24 (DR24) transit detection run; the KOI table² resulting from this run (Coughlin et al. 2016) was the most recent one used for KFOP observation planning. The latest update to the stellar properties catalog (Mathur & Huber 2016; Mathur et al. 2017), which also included data from the KFOP program, was used for the Q1-Q17 DR25 run (Thompson et al. 2018). For the KOI host stars in the DR25 catalog, 27% of the T_{eff} and $[\text{Fe}/\text{H}]$ values and 24% of the $\log(g)$ values are derived from spectra, while in the DR24 catalog, just 4%-6% of stellar parameters of KOI host stars were determined spectroscopically (78% of T_{eff} values were derived from photometry, and $\sim 85\%$ of $\log(g)$ and $[\text{Fe}/\text{H}]$ values were still adopted from the KIC). Thus, the stellar and therefore planetary parameters are more accurate in the latest KOI table. We note that in all KOI tables, the presence of any stellar companions within $\sim 1''$ - $2''$ of the primary star is not taken into account, so, if follow-up work identified such a companion, the planetary parameters from the KOI tables would have to be revised (see Ciardi et al. 2015; Furlan et al. 2017).

In this work, we present for the first time the results from the KFOP spectroscopic follow-up program that targeted two particular subsets of *Kepler* stars: host stars of KOIs that are planet candidates, and a set of standard stars. In section 2 we introduce these two samples of stars, and in section 3 we briefly describe the observations. In sections 4 and 5 we explain the analysis done for the spectra and give an overview of the results, which we discuss in section 6 and summarize in section 7.

2. THE SAMPLE

For the spectroscopic program, there are two sets of targets: (1) host stars of KOIs (mostly planet candidates), (2) a sample of standard stars. All targets have identifiers from the KIC, so called KIC IDs, but only KOI host stars and a few of the standard stars also have a KOI identifier. The two groups of targets are introduced below.

2.1. KOI Host Stars

As for high-resolution imaging follow-up observations (see Furlan et al. 2017), the targets for the spectroscopic follow-up observations were selected from the latest KOI cumulative table available at the time observations were planned. For the last *Kepler* observing season, the summer-fall 2015, the KOI cumulative table that mainly included objects from the Q1-Q17 DR24 table was used; it contained 7557 stars, of which 3665 were hosts to at least one candidate planet (we refer to these stars as “planet host stars”, even though many of the planets have not yet been confirmed or validated), and 3892 were hosts to only false positive events. The total number of planets from that KOI cumulative table was 4706, since many stars are hosts to more than one planet. Not included in this number are a few dozen additional planets that were confirmed, but not previously identified as KOIs by the *Kepler* pipeline and therefore not found in any KOI table (they have *Kepler* planet numbers and can be found in the NASA Exoplanet Archive). For the follow-up observations, usually only host stars to planet candidates were selected, and priority was given to stars with smaller planets ($\lesssim 4 R_{\oplus}$), planets in the habitable zone, and stars with multiple planet candidates.

Given that many KOI host stars are faint, a first goal of spectroscopic observations was to obtain reconnaissance spectra of the stars to detect if stellar companions are present. These spectra with a lower S/N ratio are sufficient to detect large RV variations due to a companion. Spectra with modest S/N ratios are adequate to derive stellar properties; these derived stellar parameters will be the focus of this work.

2.2. Standard Stars

In addition to the KOI sample selected from the KOI cumulative tables, a set of standard stars selected by the Kepler Asteroseismic Science Consortium was targeted by the spectroscopic follow-up observations. There are two main samples: 523 “gold” and 101 “platinum” standard stars. Of the 523 gold standard stars, 79 are also KOIs; of the 101 platinum stars, just 7 are also KOIs (note that the standard star samples were selected before any KOI identification was done; therefore, they do not include all exoplanet host stars with parameters derived from asteroseismology – see Huber et al. 2013; Lundkvist et al. 2016).

These standard stars were part of a sample of ~ 2000 solar-type main-sequence and subgiant stars observed at the beginning of the *Kepler* mission to measure stellar oscillations (Huber et al. 2011; Verner et al. 2011; Chaplin et al. 2011, 2014). Of the surveyed stars, ~ 500 have detections of solar-like oscillations; these are the

² The KOI tables can be accessed at the NASA Exoplanet Archive at <http://exoplanetarchive.ipac.caltech.edu>.

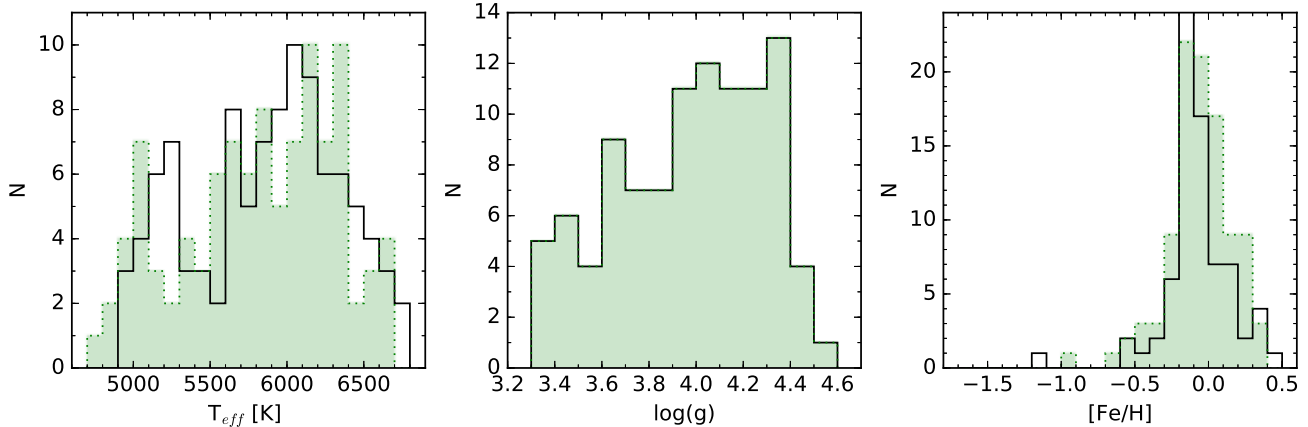


Figure 1. Histograms of the Q1-Q17 DR24 (*black*) and DR25 (*green*) stellar parameters of the platinum standard stars. Note that there are 38 stars in the DR24 table for which an $[\text{Fe}/\text{H}]$ value was not derived, but adopted to be -0.2 .

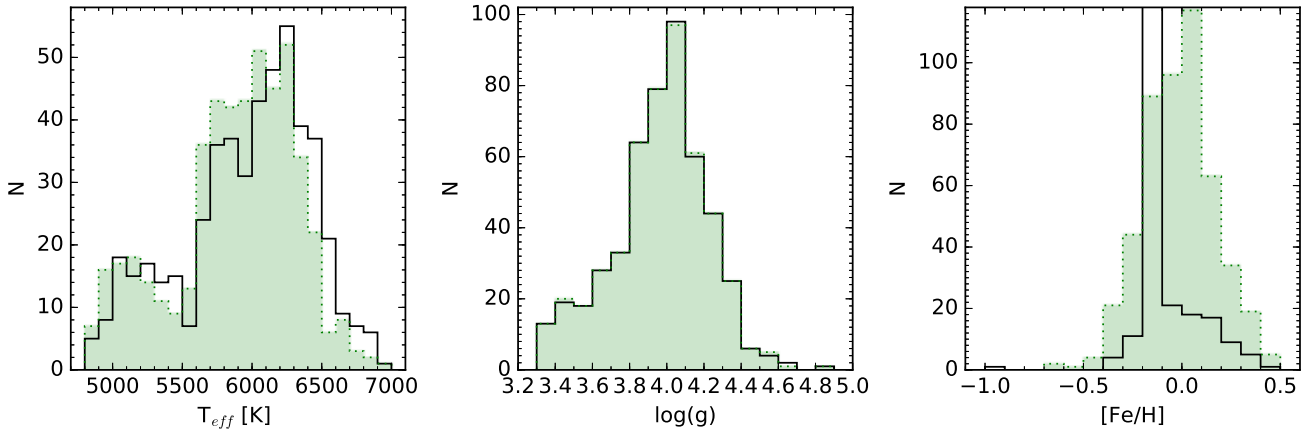


Figure 2. Histograms of the Q1-Q17 DR24 (*black*) and DR25 (*green*) stellar parameters of the gold standard stars. Similar to Figure 1, there are 391 stars in the DR24 table for which the $[\text{Fe}/\text{H}]$ value was adopted to be -0.2 .

“gold” standard stars. The stars with the best asteroseismic detections were observed for several more quarters beyond the first few of the *Kepler* mission; they form the sample of “platinum” standard stars. Asteroseismic parameters allow precise estimates of fundamental stellar properties such as the mass, radius, mean density, and surface gravity. The platinum stars are particularly well-characterized; their $\log(g)$ values have very small uncertainties (~ 0.01 dex). However, in order to derive mass and radius separately from stellar oscillations, effective temperatures have to be known. Moreover, stellar compositions cannot be derived from asteroseismology. Spectroscopy can yield T_{eff} , $\log(g)$, and $[\text{Fe}/\text{H}]$, but there are degeneracies between these parameters (Torres et al. 2012). By using constraints on stellar parameters from both seismic and non-seismic data, a full set of stellar properties can be determined more precisely (see Chaplin et al. 2014). The main purpose of obtaining follow-up spectra of the standard stars was to determine

spectroscopically derived stellar parameters of stars with reliable properties from asteroseismology; this would allow to assess any systematic errors in stellar properties listed in the KIC, as well as to test systematic errors in spectroscopically derived surface gravities.

Figures 1 and 2 display histograms of the stellar parameters for the platinum and gold standard stars, respectively, from the Q1-Q17 DR24 (Huber 2014; Huber et al. 2014) and DR25 (Mathur & Huber 2016; Mathur et al. 2017) stellar catalogs (using the input values). While there are stellar parameters for all platinum standard stars, these catalogs do not have any parameters listed for 28 gold standard stars. One more star, KIC 8566020, has stellar parameters in the DR25 catalog, but not in the DR24 catalog. We note that there is a large fraction of stars with DR24 $[\text{Fe}/\text{H}]$ values of -0.2 ± 0.3 (38 out of the 101 platinum stars and 391 out of the 523 gold standard stars). These are stars for which the effective temperatures were derived from photometry by

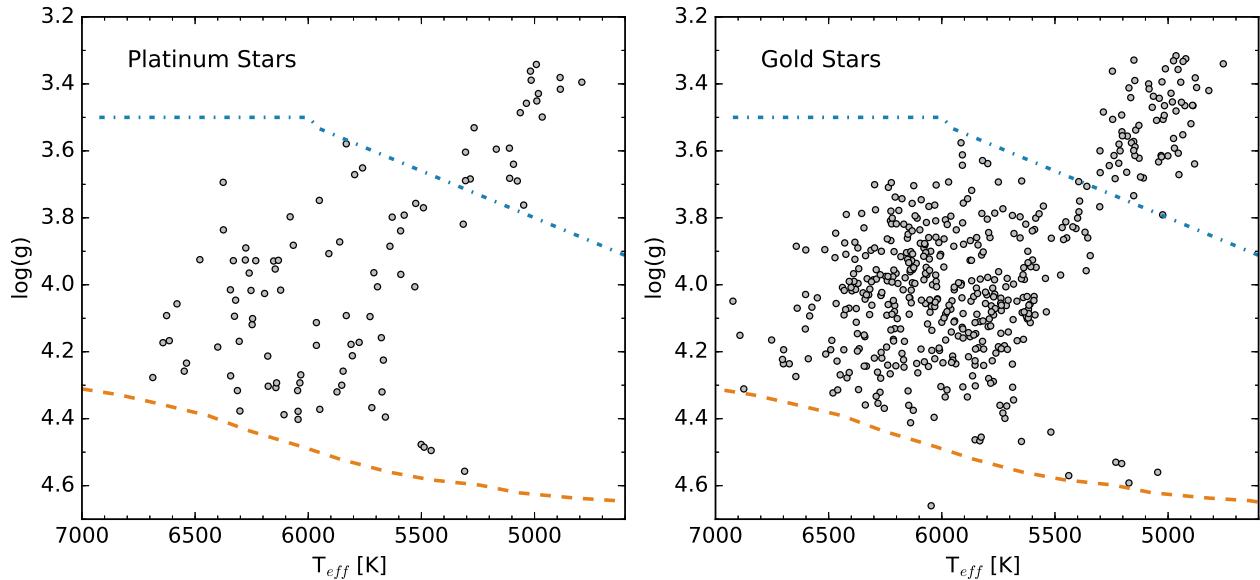


Figure 3. Surface gravities versus effective temperatures (input values of the Q1-Q17 DR25 catalog) for the platinum (*left*) and gold (*right*) standard stars. The orange dashed is the zero-age main sequence for solar-metallicity stars from Dartmouth models. The blue dash-dotted line represents the empirical boundary between giant and dwarf stars from Ciardi et al. (2011).

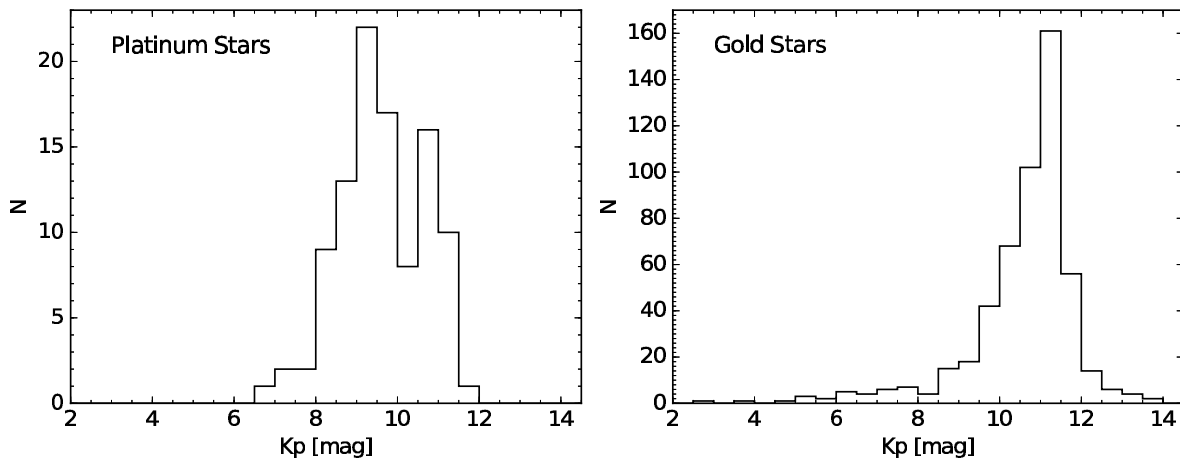


Figure 4. Histogram of the K_p magnitudes of the platinum (*left*) and gold (*right*) standard stars.

Pinsonneault et al. (2012) by adopting an $[\text{Fe}/\text{H}]$ value of -0.2 ± 0.3 , which is the mean metallicity of the *Kepler* field as reported by the KIC (Chaplin et al. 2014). In the DR25 stellar table, these stars have $[\text{Fe}/\text{H}]$ values mostly derived from spectroscopy (Buchhave & Latham 2015). Thus, the distributions of the metallicities, as well as effective temperatures, for the standard stars are somewhat different for the DR24 and DR25 versions of the catalog. On the other hand, the seismic surface gravities did not change significantly since they only depend weakly on temperature ($T_{\text{eff}}^{-0.5}$, Brown et al. 1991).

For the platinum standard stars, the T_{eff} values range from ~ 4800 to 6700 K, $\log(g)$ from 3.3 to 4.6 , and $[\text{Fe}/\text{H}]$ from -1.1 (DR24) or -1.75 (DR25) to $+0.4$. For the gold

standard stars, the parameter ranges are similar; just a few stars have $T_{\text{eff}} < 4900$ K or $T_{\text{eff}} > 6700$ K. Both groups of standard stars contain a substantial fraction of subgiants ($\log(g) \lesssim 3.8$): $\sim 31\%$ of platinum stars and 23% of gold stars have surface gravities indicative of more evolved stars (see also Figure 3). This reflects the fact that amplitudes of asteroseismic oscillations scale with luminosity (Kjeldsen & Bedding 1995), and hence both standard samples are biased towards evolved stars.

Figure 4 shows the distribution of *Kepler* magnitudes (K_p) for the platinum and gold standard stars. The median K_p values for the platinum and gold stars are 9.52 and 10.91 , respectively; for the sample of KOI host stars (see Figure 5), the median K_p value is 14.54 . Thus,

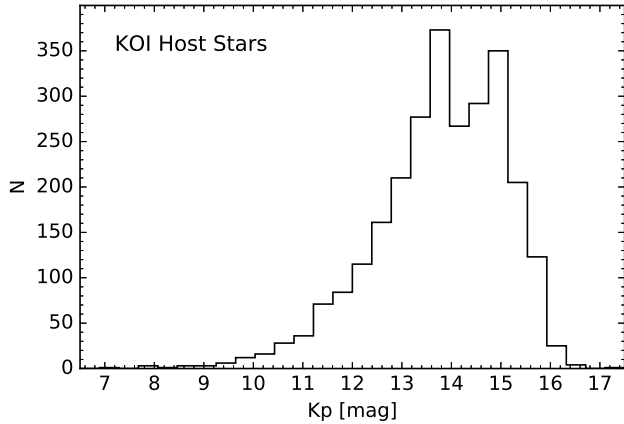


Figure 5. Histogram of the Kp magnitudes of those KOI host stars with spectroscopic observations by the KFOP teams obtained at the Tillinghast 1.5-m, McDonald 2.7-m, KPNO 4-m, Keck I, and the Nordic Optical 2.6-m telescope.

on average, the standard stars are brighter than the KOI host stars, therefore yielding higher S/N spectra.

3. OBSERVATIONS

Four main facilities were used to carry out the KFOP spectroscopic follow-up observations: the Tillinghast 1.5-m telescope with the Tillinghast Reflector Echelle Spectrograph (TRES; Fűrész 2008), the McDonald 2.7-m telescope with the Tull Coudé Spectrograph (Tull et al. 1995), the Kitt Peak National Observatory (KPNO) Mayall 4-m telescope with the facility Richey-Chretien long-slit spectrograph (RC Spec), and the Keck I 10-m telescope with the High Resolution Echelle Spectrometer (HIRES; Vogt et al. 1994). In addition, a few stars were also observed at the 2.6-m Nordic Optical Telescope (NOT) with the FIBer-fed Echelle Spectrograph (FIES; Djupvik & Andersen 2010). Table 1 gives an overview of the instruments, their resolving power and wavelength coverage, and the number of targets observed at each of the five observing facilities mentioned above. In the summer of 2010 reconnaissance spectra were also obtained for 124 stars at the Lick Observatory 3-m telescope with the Hamilton Spectrometer, but they were not used in the analysis summarized in this work, since they were superseded by the data sets taken later.

The first KFOP observations started in 2009 June and continued through the following observing seasons up to 2015 October. A few more spectra were obtained at the Tillinghast 1.5-m telescope up to 2016 September, but they are not included in this work. All spectra cover the optical wavelength region, and most of them have high resolving power ($R \sim 45,000$ -65,000), with low to medium S/N ratios (~ 10 -40 per pixel; the median S/N ratio is ~ 50). Only the spectra obtained with RC Spec

at the KPNO 4-m telescope have a medium resolving power of $R \sim 3,000$.

For the KOI targets, in order to avoid duplicate observations at the four main telescope facilities used for the FOP, target lists were divided based on the *Kepler* magnitude (Kp) of the stars: the list for the Tillinghast 1.5-m telescope included stars up to Kp of 13.5, the list for the McDonald 2.7-m telescope stars with $13.5 < Kp \leq 15.0$, and the list for the KPNO 4-m telescope stars with $Kp > 15.0$. The Keck observations focused on stars with $Kp \leq 14.5$, as well as stars with planets in the habitable zone ($T_{eq} \leq 320$ K) and stars with multiple planet candidates.

Overall, at these four telescope facilities and at the NOT, 3195 unique *Kepler* stars were observed; of these stars, 2667 are KOI host stars, and 614 are either gold or platinum standard stars (note that some standard stars are also hosts to KOIs; also, here we use KOI properties from the latest KOI table available during the last KFOP observing season, so mostly the Q1-Q17 DR24 table). Of the observed KOI sample, 2326 stars host at least one planet candidate or confirmed planet, while 341 stars only have transit events classified as false positives (see Table 2). Since some stars host more than one planet, a total of 3293 planets were covered by these observations. Of these 3293 planets, 2765 (or 84%) have radii $< 4 R_{\oplus}$; this is somewhat larger than the fraction of all planets with radii $< 4 R_{\oplus}$ (80%), a result of the sample selection.

Given that the platinum standard stars had higher priority than the gold standard stars, all 101 platinum standard stars were observed at least at one facility; the observations at Keck covered all of them, while at the Tillinghast 1.5-m and McDonald 2.7-m telescopes 99 and 100 stars, respectively, were observed. At the KPNO 4-m telescope, only 32 of the 101 platinum stars were targeted with RC Spec. Of the 523 gold standard stars, only 10 were not observed (KIC 8099517, 8566020, 3520395, 9119139, 8379927, 7529180, 8898414, 3393677, 12650049, 11467550). The majority of these standard stars were observed at the Tillinghast 1.5-m telescope (507 of the 523); 34, 79, and 11 were observed at the McDonald 2.7-m, Keck, and KPNO 4-m telescopes, respectively. Of the observed KOI host stars, 7 are also platinum standards, while 79 are also gold standards. Most of the gold standard stars observed at the Tillinghast 1.5-m telescope are not KOI host stars, while only 7 of the gold standards observed at Keck are not host stars to KOIs. At the McDonald 2.7-m and KPNO 4-m telescopes, all of the observed gold standards are also KOI host stars.

Table 1. Spectroscopic Observations of *Kepler* Stars

Telescope	Instrument	Wavelengths	Resolving Power	N
(1)	(2)	(3)	(4)	(5)
Keck I (10 m)	HIRES	364-800 nm	60,000	1653
KPNO (4 m)	RC Spec	380-490 nm	3,000	797
McDonald (2.7 m)	Tull	380-1000 nm	60,000	1033
NOT (2.6 m)	FIES	370-730 nm	46,000 and 67,000	44
Tillinghast (1.5 m)	TRES	385-910 nm	44,000	1341

NOTE—Column (1) lists the telescope and the mirror size (in parentheses), column (2) the instrument used, column (3) the wavelength coverage of the instrument, column (4) the resolving power (i.e., the ratio of wavelength and spectral resolution), and column (5) the number of *Kepler* stars observed at each facility.

The spectroscopic observations of all the *Kepler* stars observed by the FOP teams (standard stars and KOI host stars) are summarized in Table 3. This table lists each observation of each target separately, together with information on the S/N ratio of the spectrum at a certain wavelength as reported on the CFOP website by the observers.

4. ANALYSIS OF THE SPECTRA

Each of the four main KFOP groups (based at the Harvard-Smithsonian Center for Astrophysics, the McDonald Observatory, the National Optical Astronomy Observatory, and the University of California, Berkeley, respectively) developed software tools to analyze the spectra obtained in follow-up observations of KOI host stars and of the set of standard stars in order to derive stellar effective temperatures, surface gravities, and metallicities. These stellar parameters are derived from model fits to the spectra; then, the T_{eff} , $\log(g)$, and $[\text{Fe}/\text{H}]$ values can be compared to evolutionary tracks to yield estimates of stellar radii (Huber et al. 2014; Mathur & Huber 2016; Mathur et al. 2017). Here we briefly summarize the four main codes used to analyze the spectra obtained under the FOP, and then we compare the stellar parameters derived by these codes to identify trends and features.

SPC. The SPC code was developed for TRES spectra (Buchhave et al. 2012). It extracts stellar parameters from spectra with modest S/N ratios by comparing the observed spectrum to a grid of model spectra with the cross-correlation technique. The synthetic spectra are based on the Kurucz (1992) model atmospheres and cover the entire 505 to 536 nm wavelength region and values in T_{eff} , $\log(g)$, and metallicity of 3500–9750 K, 0.0–5.0, and -2.5 to $+0.5$, respectively. Overall, the model grid contains 51359 spectra, but best-fit stellar

parameters are not limited to the values of the model grid (see Buchhave et al. 2012, for details). Since SPC uses the full wavelength region and thus many spectral lines, it can derive reliable stellar parameters even for spectra with S/N ratios as low as 30 per resolution element (Buchhave et al. 2012).

Kea. The Kea code was developed for spectra obtained with the Tull Coudé spectrograph at the 2.7-m telescope at McDonald Observatory (Endl & Cochran 2016). Similar to SPC, it derives stellar parameters from high-resolution spectra that have only moderate S/N ratios. It uses a large grid of synthetic stellar spectra, based on the Kurucz (1993) stellar atmosphere grid that used the “ODFNEW” opacity distribution functions; T_{eff} values range from 3500 to 10,000 K, $\log(g)$ values from 1.0 to 5.0, and $[\text{Fe}/\text{H}]$ from -1.0 to $+0.5$ (see Endl & Cochran 2016, for details). The model spectra cover the wavelength region from 345 to 700 nm, which corresponds to 21 spectral orders of the Tull spectra. Each of the three main stellar parameters are derived from only those spectral orders with lines most sensitive to them.

Newspec. The Newspec code is used primarily on spectra from the RC Spec spectrograph on Kitt Peak’s 4-m telescope (Everett et al. 2013). As SPC and Kea, it fits observed spectra to model spectra to derive T_{eff} , $\log(g)$, and $[\text{Fe}/\text{H}]$. The synthetic spectra used are those from Coelho et al. (2005), who based them on stellar model atmospheres of Castelli & Kurucz (2003). The best-fit values of the stellar parameters are found by interpolation of the values of the best-fitting models from the grid. The models encompass T_{eff} values from 3500 to 7000 K, $\log(g)$ values from 1.0 to 5.0, and $[\text{Fe}/\text{H}]$ values from -2.5 to $+0.5$ (see Everett et al. 2013, for details). The model fits mainly use the spectral lines from 460 to 490 nm.

Table 2. Summary of KOI Host Stars with Spectroscopic Observations

KOI	KICID	CP	PC	FP	$R_{p,min}$	KOI($R_{p,min}$)	$T_{eq,min}$	KOI($T_{eq,min}$)	K_p	V	K_s	Observatories
(1)	(2)	(3)	(4)	(5)	(6)	(7)	(8)	(9)	(10)	(11)	(12)	(13)
1	11446443	1	0	0	12.9	1.01	1344	1.01	11.34	11.46	9.85	Keck,Til
2	10666592	1	0	0	16.4	2.01	2025	2.01	10.46	10.52	9.33	Keck
3	10748390	1	0	0	4.8	3.01	801	3.01	9.17	9.48	7.01	Keck
4	3861595	0	1	0	13.1	4.01	2035	4.01	11.43	11.59	10.19	Keck,NOT,Til
5	8554498	0	2	0	0.7	5.02	1124	5.02	11.66	11.78	10.21	Keck,McD,Til
6	3248033	0	0	1	50.7	6.01	2166	6.01	12.16	12.33	10.99	Keck,McD,Til
7	11853905	1	0	0	4.1	7.01	1507	7.01	12.21	12.39	10.81	Keck,McD,Til
8	5903312	0	0	1	2.0	8.01	1752	8.01	12.45	12.62	11.04	Keck,Til
10	6922244	1	0	0	14.8	10.01	1521	10.01	13.56	13.71	12.29	Keck,NOT
11	11913073	0	0	1	10.5	11.01	1031	11.01	13.50	13.75	11.78	Keck,Til
12	5812701	1	0	0	14.6	12.01	942	12.01	11.35	11.39	10.23	Keck,McD,Til
13	9941662	1	0	0	25.8	13.01	3560	13.01	9.96	9.87	9.43	KP-4,Keck,Til
14	7684873	0	0	1	5.9	14.01	2405	14.01	10.47	10.62	9.84	KP-4,McD,Til
16	9110357	0	0	1	12.6	16.01	4255	16.01	13.57	13.61	12.64	Til
17	10874614	1	0	0	13.4	17.01	1355	17.01	13.30	13.41	11.63	Keck,McD,NOT
18	8191672	1	0	0	15.3	18.01	1640	18.01	13.37	13.47	11.77	Keck,NOT
19	7255336	0	1	0	33.1	19.01	2124	19.01	11.37	11.84	10.26	Til
20	11804465	1	0	0	18.2	20.01	1338	20.01	13.44	13.58	12.07	Keck,NOT
22	9631995	1	0	0	12.2	22.01	1000	22.01	13.44	13.64	12.04	Keck,NOT
23	9071386	0	0	1	18.0	23.01	1398	23.01	12.29	12.42	11.07	Til
24	4743513	0	0	1	7.7	24.01	1502	24.01	12.96	13.19	11.60	Til
25	10593759	0	1	0	22.4	25.01	1444	25.01	13.50	13.82	12.15	Til
28	4247791	0	0	1	83.1	28.01	1412	28.01	11.26	11.79	10.29	Til
31	6956014	0	0	1	45.3	31.01	6642	31.01	10.80	11.92	7.94	Til
41	6521045	3	0	0	1.3	41.02	674	41.03	11.20	11.36	9.77	Keck,McD,Til
42	8866102	1	0	0	2.5	42.01	859	42.01	9.36	9.60	8.14	Keck,McD,Til
44	8845026	0	0	1	11.9	44.01	462	44.01	13.48	13.71	11.66	Keck,McD,Til
46	10905239	2	0	0	0.9	46.02	1075	46.02	13.77	13.80	12.01	Keck,McD
49	9527334	1	0	0	2.7	49.01	886	49.01	13.70	13.56	11.92	Keck,McD
51	6056992	0	1	0	49.8	51.01	833	51.01	13.76	14.02	14.31	Til
63	11554435	1	0	0	5.6	63.01	789	63.01	11.58	11.81	10.00	Keck,Til
64	7051180	0	1	0	10.3	64.01	2007	64.01	13.14	13.45	11.23	Keck,Til
69	3544595	1	0	0	1.6	69.01	1039	69.01	9.93	10.20	8.37	Keck,McD,NOT,Til
70	6850504	5	0	0	0.8	70.04	397	70.03	12.50	12.70	10.87	KP-4,Keck,McD,NOT
72	11904151	2	0	0	1.5	72.01	521	72.02	10.96	11.16	9.50	Keck,Til
74	6889235	0	0	1	4.5	74.01	2118	74.01	10.96	10.93	10.70	KP-4,McD,NOT,Til
75	7199397	0	1	0	10.5	75.01	596	75.01	10.77	10.94	9.39	Keck,McD,Til
76	9955262	0	1	0	8.2	76.01	695	76.01	10.14	10.40	9.11	Keck,NOT,Til
80	9552608	0	0	1	864.5	80.01	1966	80.01	11.31	11.35	10.59	McD,Til

NOTE—The full table is available in a machine-readable form in the online journal. A portion is shown here for guidance regarding content and form.

Column (1) lists the KOI number of the star, column (2) its identifier from the Kepler Input Catalog (KIC), columns (3) to (5) the number of confirmed planets (CP), planet candidates (PC), and false positives (FP), respectively, in the system, column (6) the radius of the smallest planet in the system (in R_{\oplus}) and column (7) its KOI number, column (8) the equilibrium temperature of the coolest planet in the system (in K) and column (9) its KOI number, columns (10) to (11) the *Kepler*, V , and K_s magnitudes of the KOI host stars, and column (13) the observatories where data were taken. Note that if a system contains both planets and false positives, only the planets are used to determine the smallest planet radius and lowest equilibrium temperature. The abbreviations in column (13) identify the following telescopes: KP-4 – Kitt Peak 4-m, Keck – Keck I, McD – McDonald 2.7-m, NOT – Nordic Optical Telescope, Til – Tillinghast.

Table 3. Summary of KFOP Spectroscopic Observations of *Kepler* Stars (Standard Stars, KOI Host Stars)

KOI	KICID	Group	Telescope	Instrument	R	Wavelengths	SNR	λ_{SNR}	Obs. Date
(1)	(2)	(3)	(4)	(5)	(6)	(7)	(8)	(9)	(10)
0	1255848	2	Til	TRES	44000	385-910	154.8	511	2014-06-12
0	1430163	2	Til	TRES	44000	385-910	57.3	511	2014-06-07
0	1435467	1	Keck	HIRES	60000	320-800	87.0	550	2014-08-22
0	1435467	1	McD	Tull	60000	376-1020	71.4	565	2014-07-22
0	1435467	1	Til	TRES	48000	505-535	58.6	511	2011-07-14
0	1725815	2	Til	TRES	44000	385-910	41.7	511	2014-06-15
0	2309595	2	Til	TRES	44000	385-910	38.4	511	2014-06-15
0	2450729	2	Til	TRES	44000	385-910	43.1	511	2014-06-16
0	2685626	2	Til	TRES	44000	385-910	68.6	511	2014-04-22
0	2837475	1	Til	TRES	48000	505-535	54.9	511	2011-07-09
0	2837475	1	KP-4	RC Spec	3000	380-490	40.0	440	2014-06-08
0	2837475	1	McD	Tull	60000	376-1020	73.4	565	2014-07-03
0	2837475	1	Keck	HIRES	60000	320-800	85.0	550	2014-08-22
0	2849125	2	Til	TRES	44000	385-910	45.7	511	2014-06-13
0	2852862	1	McD	Tull	60000	376-1020	72.0	565	2014-07-25
0	2852862	1	Til	TRES	44000	385-910	22.9	511	2014-07-14
0	2852862	1	Keck	HIRES	60000	364-800	85.0	520	2011-07-26
0	2852862	1	Til	TRES	44000	385-910	46.8	511	2014-06-04
0	2865774	2	Til	TRES	44000	385-910	38.6	511	2014-06-23
0	2991448	2	Til	TRES	44000	385-910	36.4	511	2014-06-15
0	2998253	2	Til	TRES	44000	385-910	43.6	511	2014-06-16
0	3112152	2	Til	TRES	44000	385-910	42.3	511	2014-06-13
0	3112889	2	Til	TRES	44000	385-910	44.1	511	2014-06-13
0	3115178	2	Til	TRES	44000	385-910	41.0	511	2014-06-14
0	3123191	2	Til	TRES	44000	385-910	45.8	511	2014-06-04
0	3207108	2	Til	TRES	44000	385-910	72.9	511	2014-04-21
0	3212440	2	Til	TRES	44000	385-910	38.1	511	2014-04-25
0	3223000	2	Til	TRES	44000	385-910	64.1	511	2014-05-21
0	3236382	2	Til	TRES	44000	385-910	45.5	511	2014-06-15
0	3241581	2	Til	TRES	44000	385-910	46.6	511	2014-06-16
0	3329196	2	Til	TRES	44000	385-910	43.2	511	2014-05-18
0	3344897	2	Til	TRES	44000	385-910	44.0	511	2014-06-15
0	3424541	1	McD	Tull	60000	376-1020	74.0	565	2014-07-03
0	3424541	1	Til	TRES	44000	385-910	51.8	511	2014-05-15
0	3424541	1	Keck	HIRES	60000	320-800	83.0	550	2014-08-22
0	3427720	1	Til	TRES	48000	505-535	65.7	511	2011-07-14
0	3427720	1	KP-4	RC Spec	3000	380-490	41.1	440	2014-06-10
0	3427720	1	McD	Tull	60000	376-1020	74.3	565	2014-07-03
0	3427720	1	Keck	HIRES	60000	364-800	85.0	520	2011-07-26

NOTE—The full table is available in a machine-readable form in the online journal. A portion is shown here for guidance regarding content and form.

Column (1) lists the KOI number of the star (if 0, the star is in the *Kepler* field, but was not identified as a KOI), column (2) its identifier from the Kepler Input Catalog (KIC), column (3) identifies whether the target is a platinum standard (1), gold standard (2), or just a KOI host star (0), column (4) the telescope where the images were taken (see the notes of Table 2 for an explanation of the abbreviations), column (5) the instrument used, column (6) the resolving power, column (7) the wavelengths covered by the spectrograph in nm, column (8) the signal-to-noise ratio of the spectrum at the wavelength (in nm) specified in column (9), and column (11) the date of the observation (in year-month-day format).

SpecMatch. The `SpecMatch` code was developed for Keck/HIRES spectra (Petigura 2015). `SpecMatch` fits an observed stellar spectrum by interpolating between a grid of model spectra from Coelho et al. (2005), spanning 3500–7500 K in T_{eff} , 1.0–5.0 in $\log(g)$, and -2.0 to $+0.5$ dex in $[\text{Fe}/\text{H}]$. `SpecMatch` also accounts for instrumental and rotational-macroturbulent broadening by convolution with appropriate broadening kernels. As with the Tull spectra, only certain wavelength regions of the high-resolution spectra are used to determine best-fit stellar parameters.

Recently, Petigura et al. (2017) presented results of the California-Kepler Survey on 1305 KOI host stars, of which about 300 are also included in this work. They analyzed HIRES spectra of the stars with `SpecMatch` and `SME@XSEDE`, a descendant of `SME` (Valenti & Piskunov 1996), resulting in improved stellar parameters (Johnson et al. 2017). However, the stellar parameters presented in this work are the ones that were incorporated into the latest *Kepler* stellar table (DR25; Mathur et al. 2017), and so we did not update them to the newest version.

5. RESULTS

5.1. Standard Stars

5.1.1. Platinum Standard Stars

The stellar parameters derived for the set of platinum stars using `SPC`, `Kea`, `Newspec`, and `SpecMatch` are listed in Table 4. As mentioned in section 3, all 101 platinum stars were observed at Keck, while at the Tillinghast 1.5-m, McDonald 2.7-m, and KPNO 4-m telescopes 99, 100, and 32 stars, respectively, were observed. However, not all spectra allowed the extraction of stellar parameters; 3 of the Keck spectra, 4 of the Tillinghast spectra, and 3 of the KPNO spectra did not result in stellar parameters.

Figure Set 6 compares the values for T_{eff} , $\log(g)$, and $[\text{Fe}/\text{H}]$ of the platinum standard stars obtained at different observatories and with different analysis pipelines, and Table 5 lists the average values and standard deviations of the differences of these parameter values. These comparisons are done for pairs of parameter sets; therefore, in some cases only somewhat more than 25 values can be compared, while in other cases there are over 90 stars with parameters derived from spectra from two telescopes (e.g., the Tillinghast and McDonald data, Fig. 6.1).

The agreement in the derived effective temperatures can be gauged from the differences of individual values derived from different data sets (see Table 5). The average of these differences ranges from -31 to 36 K, indicating no significant systematic offsets. The standard deviation of the differences is about twice as large

as the $1-\sigma$ uncertainties of ~ 50 -75 K for the individual measurements, so there are some disagreements. Trends can be seen in Figure Set 6: the T_{eff} values below about 5500 K derived with `Kea` or `SpecMatch` are lower by ~ 100 -200 K than those derived with `SPC`, but there is a close match at higher temperatures. Furthermore, the T_{eff} values derived with `Newspec` are ~ 75 -150 K larger than those derived with the other pipelines for the few stars found at the highest temperatures ($\gtrsim 6400$ K).

There are larger disagreements in the derived $\log(g)$ and $[\text{Fe}/\text{H}]$ values. The standard deviation of the difference in $\log(g)$ values from different analysis codes ranges from 0.14 to 0.29 dex (with average values for the difference between 0.003 and 0.16 dex), which is larger than most $1-\sigma$ uncertainties of 0.1 dex. The `SpecMatch` and `Kea` $\log(g)$ values are very similar for the majority of stars ($\overline{\Delta \log(g)} = 0.003 \pm 0.14$, which is the best agreement among the different pairs of results); there is just a trend of somewhat larger `SpecMatch` values (by about 0.1 dex) below $\log(g) \sim 4.0$. Comparing `Newspec` and `SPC` values, the former are larger at `SPC`-derived $\log(g) \lesssim 4.2$ (by up to 0.6 dex at $\log(g) \sim 3.6$ -3.8, but with smaller differences as $\log(g)$ increases) and about 0.1 dex smaller at $\log(g) \gtrsim 4.4$. The largest differences overall can be found for the `SPC` and `Kea` results, which is also reflected in their standard deviation of 0.29 dex. When comparing the results from these two sets, the `Kea` values for $\log(g)$ are usually larger, except for a cluster of values with $\log(g)=3.1$ -3.6 that are lower than those found with `SPC` by up to 0.7 dex. This cluster of lower $\log(g)$ values can also be seen in the comparison between `SPC` and `SpecMatch` results; the latter values are lower. There are two outliers that stand out in the comparison of `Newspec`, `Kea`, and `SpecMatch` results: KIC 11968749, for which the `Kea` and `SpecMatch` $\log(g)$ values are 3.42 ± 0.08 and 3.34 ± 0.1 , respectively, compared to 4.07 ± 0.15 for the `Newspec` value, and KIC 8760414, for which the `Kea` and `SpecMatch` values are 4.33 ± 0.25 and 3.83 ± 0.1 , respectively. The latter star also has discrepant T_{eff} values.

For the $[\text{Fe}/\text{H}]$ values, the average differences in values from different analysis codes lie between -0.03 to 0.13, with the standard deviation of the differences ranging from 0.05 to 0.09 dex, which is comparable to the mean $1-\sigma$ uncertainties of 0.04-0.10 dex. The values from `SPC` and `SpecMatch` agree broadly over the whole range of metallicities. There is also overall good agreement among the metallicities derived with `SPC` and `Kea`; however, at the largest $[\text{Fe}/\text{H}]$ values ($\gtrsim 0.2$ from `SPC`), the `Kea` values are lower than the `SPC` values by about 0.1-0.2 dex. Compared to the `Kea` values, those from `SpecMatch` are on average larger by ~ 0.05 -0.1 dex.

Table 4. Stellar Parameters of the Platinum Standard Stars

KICID	KOI	Tillinghast (SPC)				McDonald 2.7-m (kea)				Keck (Spectrograph)				Kitt Peak 4-m (newspec)			
		T_{eff}	$\log(g)$	[Fe/H]	T_{eff}	$\log(g)$	[Fe/H]	T_{eff}	$\log(g)$	[Fe/H]	T_{eff}	$\log(g)$	[Fe/H]	T_{eff}	$\log(g)$	[Fe/H]	
(1)	(2)	(3)	(4)	(5)	(6)	(7)	(8)	(9)	(10)	(11)	(12)	(13)	(14)				
1435467	...	6332 ± 50	4.13 ± 0.1	0.03 ± 0.08	6325 ± 80	4.33 ± 0.11	0.04 ± 0.04	6278 ± 60	4.1 ± 0.07	0.05 ± 0.04				
2837475	...	6478 ± 50	3.95 ± 0.1	-0.07 ± 0.08	6488 ± 91	4.29 ± 0.19	-0.14 ± 0.07	6632 ± 75	4.38 ± 0.15	0.11 ± 0.1				
2852862	...	6104 ± 50	3.66 ± 0.1	-0.2 ± 0.08	6250 ± 78	4.08 ± 0.12	-0.16 ± 0.05	6230 ± 60	4.05 ± 0.07	-0.1 ± 0.04				
3424541	6338 ± 89	4.33 ± 0.12	0.16 ± 0.07				
3427720	...	6002 ± 50	4.28 ± 0.1	-0.09 ± 0.08	6000 ± 96	4.38 ± 0.09	-0.04 ± 0.07	6025 ± 60	4.28 ± 0.09	-0.05 ± 0.04	6039 ± 75	4.34 ± 0.15	0.11 ± 0.1				
3429205	...	5239 ± 50	3.82 ± 0.1	0.01 ± 0.08	5050 ± 42	3.42 ± 0.08	-0.14 ± 0.07	5078 ± 60	3.47 ± 0.1	0.02 ± 0.04				
3632418	975	6086 ± 50	3.81 ± 0.1	-0.19 ± 0.08	6112 ± 109	4.08 ± 0.14	-0.16 ± 0.04	6207 ± 60	4.07 ± 0.07	-0.09 ± 0.04				
3656476	...	5702 ± 50	4.29 ± 0.1	0.28 ± 0.08	5625 ± 86	4.21 ± 0.08	0.2 ± 0.05	5730 ± 60	4.24 ± 0.07	0.29 ± 0.04	5608 ± 75	4.21 ± 0.15	0.28 ± 0.1				
3733735	...	6604 ± 50	4.17 ± 0.1	-0.05 ± 0.08	6538 ± 84	4.42 ± 0.11	-0.12 ± 0.05	6562 ± 60	4.39 ± 0.1	-0.05 ± 0.04				
3735871	...	6062 ± 50	4.31 ± 0.1	-0.07 ± 0.08	6062 ± 98	4.46 ± 0.08	-0.08 ± 0.04	6065 ± 60	4.29 ± 0.07	-0.06 ± 0.04	6066 ± 75	4.32 ± 0.15	0.02 ± 0.1				
4351319	...	5060 ± 50	3.71 ± 0.1	0.3 ± 0.08	4862 ± 32	3.42 ± 0.08	0.1 ± 0.06	4992 ± 60	3.5 ± 0.1	0.32 ± 0.04				
4914923	...	5757 ± 50	4.1 ± 0.1	0.04 ± 0.08	5775 ± 73	4.21 ± 0.1	0.1 ± 0.04	5871 ± 60	4.17 ± 0.07	0.14 ± 0.04	5873 ± 75	4.32 ± 0.15	0.17 ± 0.1				
5184732	...	5971 ± 50	4.5 ± 0.1	0.44 ± 0.08	5812 ± 81	4.38 ± 0.09	0.36 ± 0.07	5874 ± 60	4.21 ± 0.07	0.41 ± 0.04				
5596656	...	5188 ± 50	3.67 ± 0.1	-0.43 ± 0.08	5088 ± 67	3.33 ± 0.11	-0.56 ± 0.09	5044 ± 60	3.19 ± 0.1	-0.48 ± 0.04				
5607242	...	5538 ± 50	3.86 ± 0.1	-0.03 ± 0.08	5462 ± 92	3.75 ± 0.17	-0.18 ± 0.07	5526 ± 60	3.88 ± 0.07	-0.07 ± 0.04				
5689820	...	5182 ± 50	4.04 ± 0.1	0.3 ± 0.08	4962 ± 46	3.58 ± 0.15	0.04 ± 0.05	5063 ± 60	3.75 ± 0.1	0.24 ± 0.04				
5723165	...	5337 ± 50	3.79 ± 0.1	-0.03 ± 0.08	5225 ± 82	3.58 ± 0.15	-0.12 ± 0.08	5291 ± 60	3.66 ± 0.1	0.0 ± 0.04				
5955122	...	5845 ± 50	3.83 ± 0.1	-0.2 ± 0.08	5950 ± 96	3.92 ± 0.08	-0.16 ± 0.06	5887 ± 60	3.96 ± 0.07	-0.13 ± 0.04				

NOTE.—The full table is available in a machine-readable form in the online journal. A portion is shown here for guidance regarding content and form.

Column (1) lists the identifier of the star from the Kepler Input Catalog (KIC), column (2) the KOI number of the star (if available), columns (3)-(5) the stellar parameters derived from spectra from the Tillinghast telescope, columns (6)-(8) the stellar parameters derived from spectra from the McDonald 2.7-m telescope, columns (9)-(11) the stellar parameters derived from spectra from the Keck I telescope, and columns (12)-(14) the stellar parameters derived from spectra from the Kitt Peak 4-m telescope.

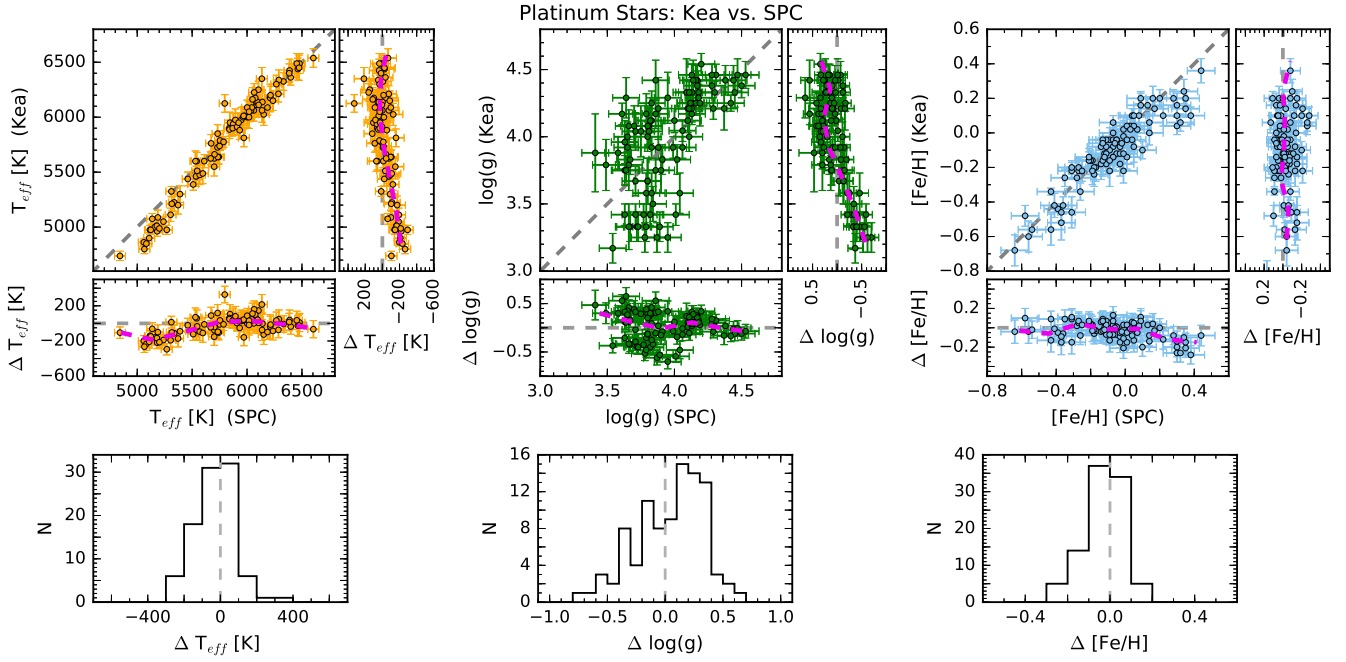


Figure 6. Comparison of T_{eff} (*left*), $\log(g)$ (*middle*), and $[\text{Fe}/\text{H}]$ (*right*) determined for the platinum standard stars observed at the Tillinghast 1.5-m and the McDonald 2.7-m telescopes and analyzed with SPC and Kea, respectively (95 stars in common). The top row shows the parameter values of the two sets plotted versus each other (large panels) and the differences in parameter values vs. the values determined with SPC and Kea (smaller panels). The magenta line in the smaller panels represents a running median. The bottom row shows the histograms of the differences in parameter values. Only the first comparison plot is shown here; the complete figure set (6 plots) is shown in Appendix B.

Table 5. Average and Standard Deviation of the Differences in Stellar Parameters for the Platinum Standard Stars Derived by Different Groups and also Compared to the KIC

	SPC	Kea	SpecMatch	Newspec
SPC	...	$\overline{\Delta T_{\text{eff}}} = -31 \pm 106$ K $\overline{\Delta \log(g)} = 0.04 \pm 0.29$ $\overline{\Delta [\text{Fe}/\text{H}]} = -0.03 \pm 0.09$	$\overline{\Delta T_{\text{eff}}} = 1 \pm 84$ K $\overline{\Delta \log(g)} = 0.03 \pm 0.23$ $\overline{\Delta [\text{Fe}/\text{H}]} = 0.04 \pm 0.05$	$\overline{\Delta T_{\text{eff}}} = 11 \pm 106$ K $\overline{\Delta \log(g)} = 0.16 \pm 0.24$ $\overline{\Delta [\text{Fe}/\text{H}]} = 0.12 \pm 0.08$
Kea	see first row	...	$\overline{\Delta T_{\text{eff}}} = 36 \pm 84$ K $\overline{\Delta \log(g)} = 0.003 \pm 0.14$ $\overline{\Delta [\text{Fe}/\text{H}]} = 0.07 \pm 0.09$	$\overline{\Delta T_{\text{eff}}} = 18 \pm 69$ K $\overline{\Delta \log(g)} = 0.03 \pm 0.18$ $\overline{\Delta [\text{Fe}/\text{H}]} = 0.13 \pm 0.09$
SpecMatch	see first row	see second row	...	$\overline{\Delta T_{\text{eff}}} = -9 \pm 74$ K $\overline{\Delta \log(g)} = 0.11 \pm 0.19$ $\overline{\Delta [\text{Fe}/\text{H}]} = 0.08 \pm 0.08$
KIC	$\overline{\Delta T_{\text{eff}}} = -117 \pm 138$ K $\overline{\Delta \log(g)} = 0.06 \pm 0.37$ $\overline{\Delta [\text{Fe}/\text{H}]} = -0.19 \pm 0.25$	$\overline{\Delta T_{\text{eff}}} = -84 \pm 111$ K $\overline{\Delta \log(g)} = 0.01 \pm 0.32$ $\overline{\Delta [\text{Fe}/\text{H}]} = -0.15 \pm 0.25$	$\overline{\Delta T_{\text{eff}}} = -127 \pm 123$ K $\overline{\Delta \log(g)} = 0.02 \pm 0.31$ $\overline{\Delta [\text{Fe}/\text{H}]} = -0.23 \pm 0.25$	$\overline{\Delta T_{\text{eff}}} = -131 \pm 115$ K $\overline{\Delta \log(g)} = -0.16 \pm 0.26$ $\overline{\Delta [\text{Fe}/\text{H}]} = -0.26 \pm 0.19$

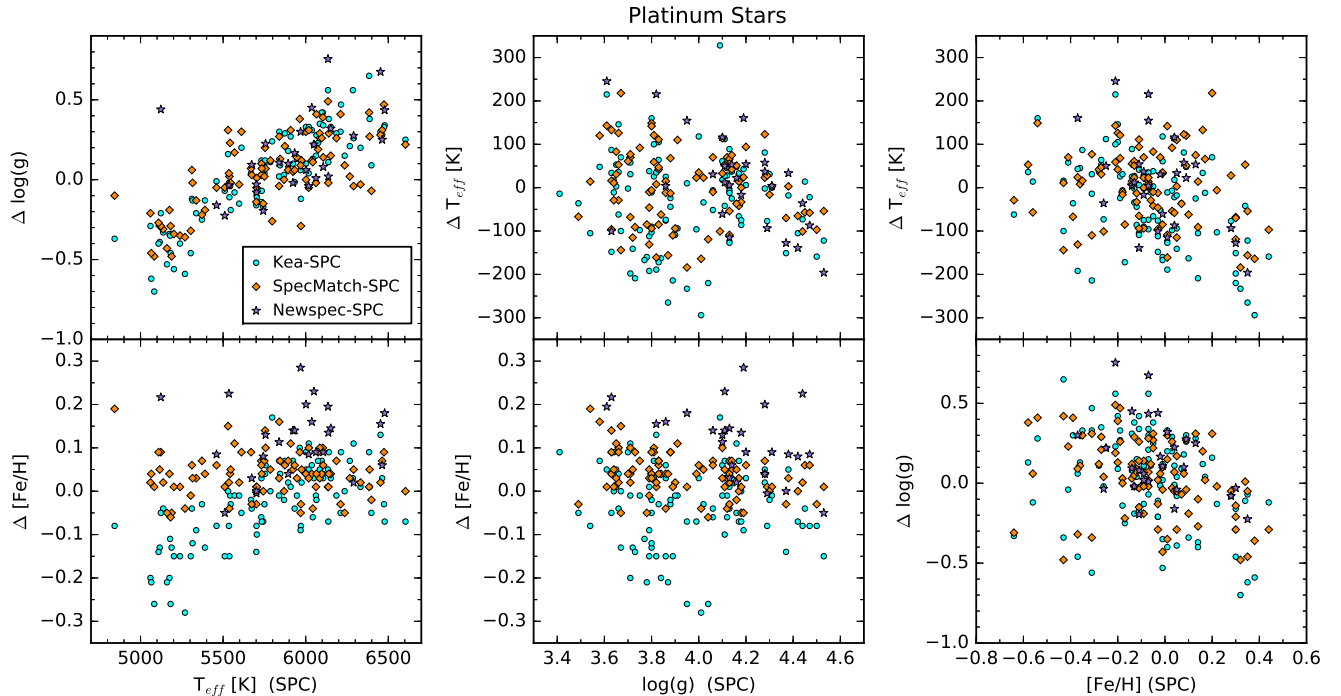


Figure 7. Comparison of the differences of T_{eff} , $\log(g)$, and $[\text{Fe}/\text{H}]$ values determined for the platinum standard stars with different analysis codes (see label) versus the values obtained with SPC.

When comparing the metallicities derived with *Newspec* to those derived with SPC, *Kea*, or *SpecMatch*, the *Newspec* values are, with just a few exceptions, larger (on average by 0.08–0.13; see Table 5), with much larger discrepancies (> 0.25 dex) at lower metallicities.

To see whether the differences in derived parameter values for the platinum stars are correlated with the other stellar parameters, these differences are shown as a function of parameter values derived with SPC and *Kea* in Figures 7 and 8, respectively. The clearest trend can be seen for the $\log(g)$ values: for lower stellar effective temperatures ($\lesssim 5500$ K), the SPC values and, to a lesser extent, the *SpecMatch* values are larger than those derived with *Kea*; the opposite trend can be observed at $T_{\text{eff}} \gtrsim 5800$ K. The stars for which $\Delta \log(g)$ is most negative ($\lesssim -0.3$) in Figure 7 (or $\gtrsim 0.3$ in Figure 8) have temperatures below 5300 K, placing them into the giant regime (see Figure 3). These are also the stars for which *Kea* derived $\log(g)$ values of 3.1–3.6 (and *SpecMatch* values just 0.1–0.2 dex larger than these), while SPC found values of 3.5–4.1. It is likely that for these giant stars the $\log(g)$ values derived with SPC are too high. Stars for which the $[\text{Fe}/\text{H}]$ values from SPC are larger than those from *Kea* have $T_{\text{eff}} \lesssim 5700$ K and $\log(g) \lesssim 3.8$ –4.0. Also, stars for which the temperatures derived with *Kea* are smaller than those derived with SPC have $\log(g) \lesssim 3.8$ –4.0.

In Figure Set 9 we show how the differences in stellar parameters derived for the platinum stars with different analysis codes correlate with each other. In particular when comparing the SPC and *Kea* values, it is clear that changes in one parameter set are strongly correlated with changes in another parameter set (Pearson correlation coefficient of 0.7–0.8). So, if *Kea* yielded a larger surface gravity, it also resulted in higher effective temperatures and higher metallicities. The strong positive correlation between ΔT_{eff} and $\Delta \log(g)$ is also found when comparing SPC and *SpecMatch* results. The other plots show overall weaker, but still positive, correlations.

We also compared the stellar parameters of the platinum standard stars derived from KFOP observations to those in the KIC. The uncertainties in the KIC are fairly large: 0.4 dex for $\log(g)$, 0.3 dex for $[\text{Fe}/\text{H}]$, and about 3.5% (or about 200 K) for T_{eff} (Huber et al. 2014). In Table 5, we list the average and standard deviation of the difference in values derived from the FOP spectra and those from the KIC. The standard deviations amount to ~ 110 –140 K for T_{eff} , 0.26–0.37 dex for $\log(g)$, and 0.19–0.25 dex for $[\text{Fe}/\text{H}]$. On average, the effective temperatures and metallicities derived from spectroscopic follow-up observations are higher than those listed in the KIC by 115 K and 0.21 dex, respectively. Thus, overall the KIC values and those derived from follow-up spectra agree within the uncertainties of the KIC values, but there seem to be systematic differences.

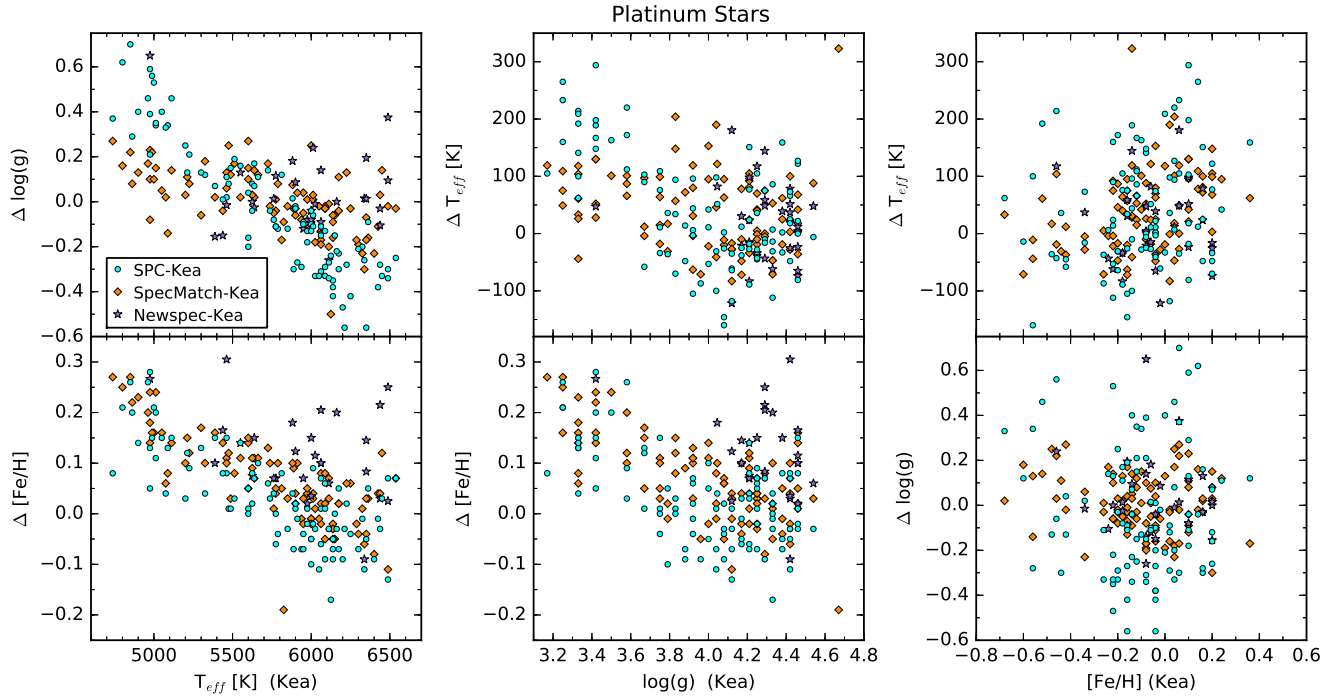


Figure 8. Similar to Figure 7, but with the differences of parameter values plotted versus the values obtained with Kea.

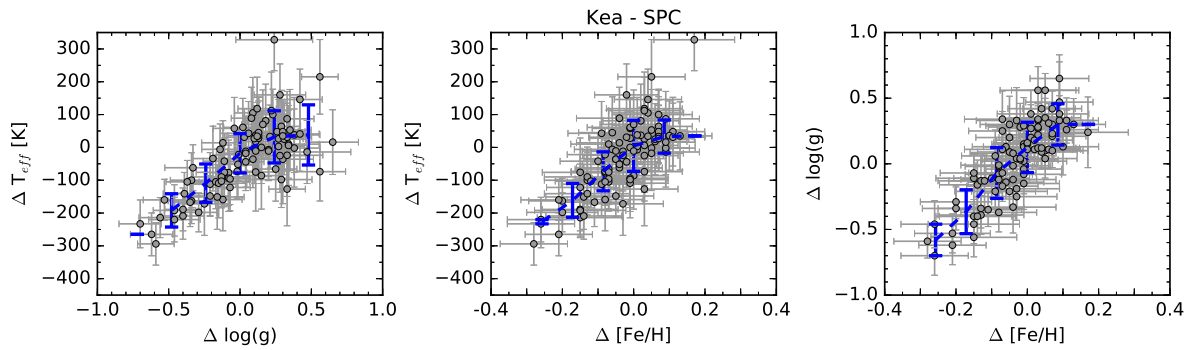


Figure 9. Comparison of the differences of stellar parameters derived for the platinum stars with SPC and Kea. The blue dashed line represents a running median. The Pearson correlation coefficients are 0.74 (*left*), 0.76 (*middle*), and 0.82 (*right*). Only the first comparison plot is shown here; the complete figure set (6 plots) is shown in Appendix B.

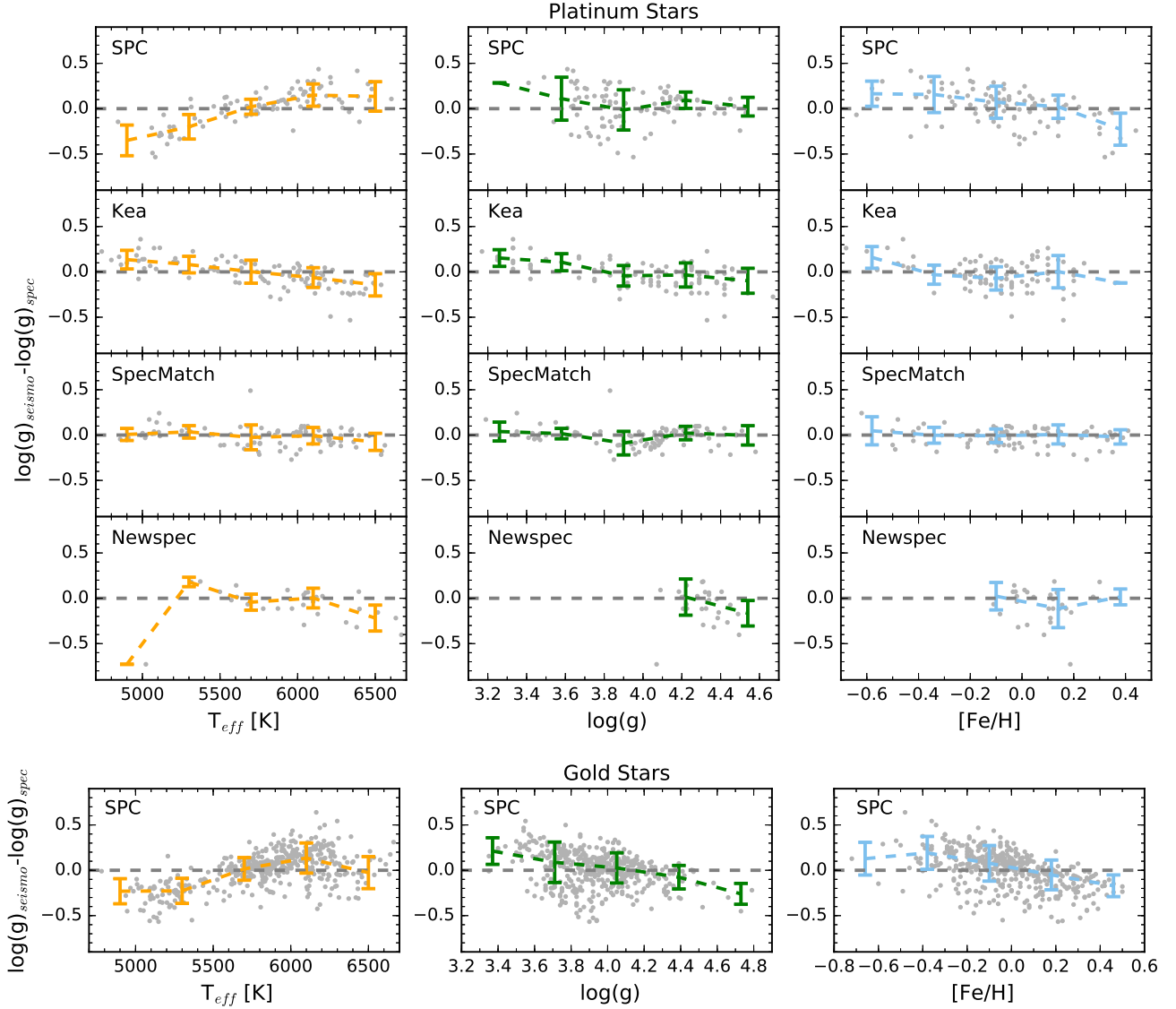


Figure 10. Comparison of the difference in $\log(g)$ values of the platinum standard stars (*top four rows*) and gold standard stars (*bottom row*) determined with asteroseismology (DR25 input values) and determined from spectra versus their T_{eff} (*left*), $\log(g)$ (*middle*), and $[Fe/H]$ (*right*) values determined from spectra. The label inside each panel identifies the analysis code used to derive the spectroscopic stellar parameters. The colored dashed lines and error bars represent median bins.

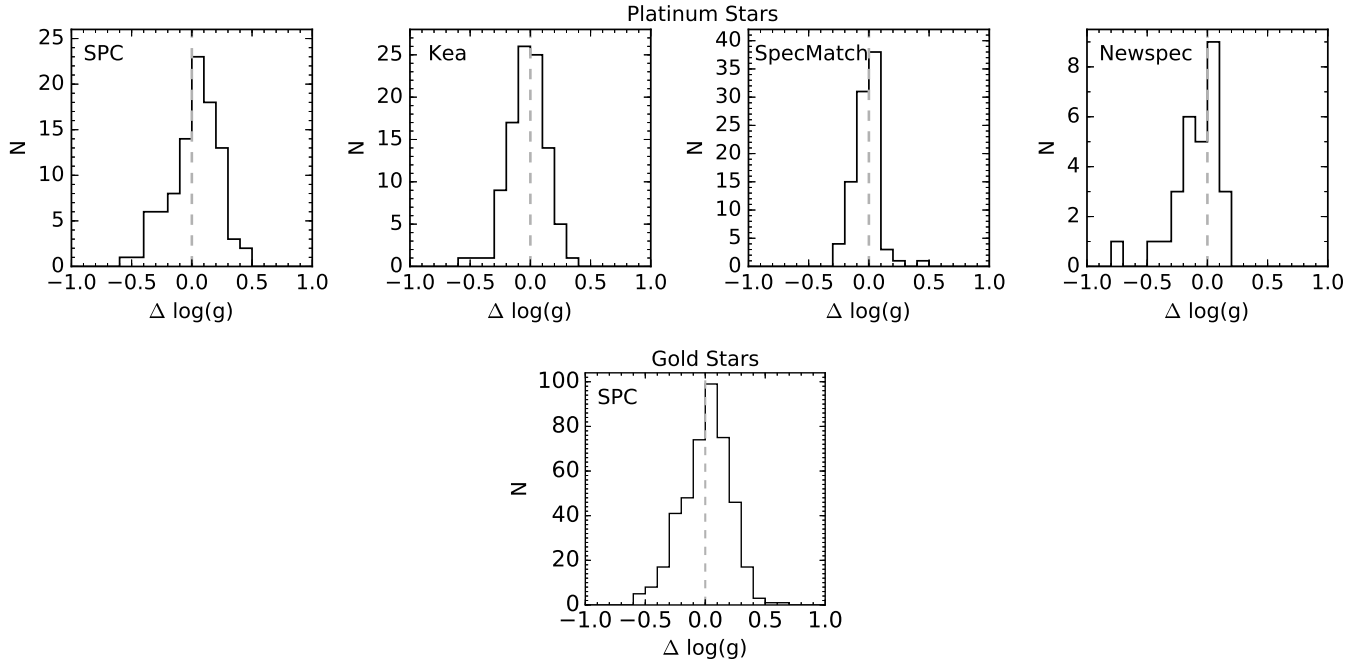


Figure 11. Histogram of the differences in $\log(g)$ values of the platinum standard stars (*top row*) and gold standard stars (*bottom row*) determined with asteroseismology (DR25 input values) and determined from spectra.

Given the selection criteria of the platinum stars, the $\log(g)$ values used as input for the DR24 and DR25 stellar catalogs are very reliable, since they were derived using asteroseismology. Using the input values for the DR25 catalog, we find the average and median $\log(g)$ uncertainties of the platinum stars to be both 0.01 dex (compared to 0.3 and 0.4 dex, respectively, for all stars in the *Kepler* Stellar Properties Catalog). On the other hand, the T_{eff} and $[\text{Fe}/\text{H}]$ input values of the platinum stars in the DR25 catalog were adopted from photometry or spectroscopy, which in some cases were more uncertain. In Figure 10 we compare the difference in $\log(g)$ values determined from asteroseismology and those determined from spectroscopy as a function of stellar parameters derived from spectroscopy. There are some trends for different data sets: the surface gravities derived with SPC are overestimated by up to ~ 0.5 dex below ~ 5500 K and underestimated by an average of 0.15 dex above ~ 6000 K. The opposite trend is seen with metallicities: at subsolar metallicities, the SPC $\log(g)$ values are underestimated by 0.1–0.2 dex, while at $[\text{Fe}/\text{H}] \sim 0.4$ they are overestimated by an average of 0.14 dex. The $\log(g)$ values derived with Kea show a similar behavior with metallicities at $[\text{Fe}/\text{H}]$ values $\lesssim -0.4$. On the other hand, the surface gravities derived with Kea are underestimated by about 0.1 dex below ~ 5300 K and overestimated by a similar amount at $\gtrsim 6200$ K. Kea $\log(g)$ values in the 3.2–3.6 range are also underestimated by 0.1–0.15 dex. This trend can also

be seen in the SPC values, but the scatter is larger. The SpecMatch $\log(g)$ values closely match the asteroseismic values; they represent the best agreement of the four different analysis methods and data sets. Compared to the other three data sets, there are relatively few stars with parameters from Newspec. There are noticeable offsets (~ 0.2 dex) compared to the asteroseismic $\log(g)$ values at $T_{\text{eff}} \gtrsim 6300$ K and $\log(g) \gtrsim 4.4$.

A histogram of the $\log(g)$ differences from Figure 10 is shown in Figure 11. The standard deviation of the differences amounts to 0.1–0.2 dex, with the average difference between -0.024 and 0.025 for the SPC, Kea, and SpecMatch results and -0.078 for the Newspec results. As seen in the previous figure, the closest agreement between asteroseismic and spectroscopic $\log(g)$ values is found for the SpecMatch values, for which the average $\Delta \log(g)$ is -0.014 ± 0.106 .

5.1.2. Gold Standard Stars

Of the 507 gold standard stars observed at the Tillinghast 1.5-m telescope, 436 have stellar parameters derived with SPC; they are listed in Table 6. Even though the other three KFOP groups also observed some of the gold standard stars, almost all of them are also KOI host stars (see section 3), and therefore their stellar parameters will be presented in section 5.2.

When comparing the stellar parameters for the gold standard stars from SPC to those from the KIC, we find similar results as for the platinum stars: the T_{eff} and

Table 6. Stellar Parameters of the Gold Standard Stars Derived from Tillinghast Spectra With SPC

KICID	KOI	T_{eff}	$\log(g)$	[Fe/H]
(1)	(2)	(3)	(4)	(5)
1430163	...	6388 ± 50	3.85 ± 0.1	-0.19 ± 0.08
1725815	...	6133 ± 50	3.63 ± 0.1	-0.19 ± 0.08
2010607	4929	6132 ± 50	3.65 ± 0.1	-0.07 ± 0.08
2306756	113	5616 ± 50	4.23 ± 0.1	0.46 ± 0.08
2309595	...	5212 ± 50	3.86 ± 0.1	-0.06 ± 0.08
2450729	...	5861 ± 50	3.96 ± 0.1	-0.25 ± 0.08
2849125	...	6114 ± 50	3.88 ± 0.1	0.23 ± 0.08
2865774	...	5793 ± 50	4.02 ± 0.1	-0.07 ± 0.08
2991448	...	5640 ± 50	3.98 ± 0.1	-0.11 ± 0.08
2998253	...	6215 ± 50	4.09 ± 0.1	0.04 ± 0.08
3102384	273	5697 ± 50	4.41 ± 0.1	0.33 ± 0.08
3112152	...	5973 ± 50	3.95 ± 0.1	-0.02 ± 0.08
3112889	...	6018 ± 50	3.74 ± 0.1	-0.27 ± 0.08
3115178	...	5020 ± 50	3.75 ± 0.1	0.11 ± 0.08
3123191	...	6266 ± 50	4.14 ± 0.1	-0.12 ± 0.08
3223000	...	6234 ± 50	4.32 ± 0.1	-0.15 ± 0.08
3236382	...	6641 ± 50	3.99 ± 0.1	-0.11 ± 0.08
3241581	...	5750 ± 50	4.42 ± 0.1	0.28 ± 0.08
3329196	...	5156 ± 50	3.91 ± 0.1	-0.14 ± 0.08
3344897	...	6271 ± 50	3.71 ± 0.1	-0.1 ± 0.08
3430893	...	6105 ± 50	4.04 ± 0.1	0.04 ± 0.08
3437637	...	5468 ± 49	3.88 ± 0.1	-0.18 ± 0.08
3438633	...	6002 ± 50	3.57 ± 0.1	-0.3 ± 0.08
3456181	...	6214 ± 50	3.6 ± 0.1	-0.26 ± 0.08
3531558	118	5711 ± 50	4.13 ± 0.1	0.01 ± 0.08
3534307	...	5699 ± 49	4.11 ± 0.1	-0.23 ± 0.08
3544595	69	5660 ± 50	4.47 ± 0.1	-0.2 ± 0.08
3545753	...	5907 ± 50	3.67 ± 0.1	-0.26 ± 0.08
3547794	...	6299 ± 50	3.55 ± 0.1	-0.36 ± 0.08
3630240	...	5245 ± 50	3.56 ± 0.1	-0.49 ± 0.08
3633847	...	6096 ± 50	4.09 ± 0.1	0.12 ± 0.08
3633889	...	6364 ± 50	4.19 ± 0.1	-0.12 ± 0.08
3640905	1221	5090 ± 50	3.83 ± 0.1	0.28 ± 0.08
3642422	...	5295 ± 50	3.78 ± 0.1	0.04 ± 0.08
3643774	...	5955 ± 50	4.13 ± 0.1	0.15 ± 0.08
3657002	...	5883 ± 50	4.08 ± 0.1	0.02 ± 0.08
3661135	...	5611 ± 50	3.93 ± 0.1	-0.02 ± 0.08
3730801	...	5934 ± 50	4.25 ± 0.1	0.28 ± 0.08
3854781	...	5722 ± 50	4.08 ± 0.1	0.36 ± 0.08
3942719	...	5561 ± 50	3.76 ± 0.1	-0.41 ± 0.08
3952307	...	6077 ± 50	3.77 ± 0.1	-0.05 ± 0.08
3952580	...	6074 ± 50	3.59 ± 0.1	-0.07 ± 0.08
3967430	...	6612 ± 50	4.17 ± 0.1	-0.04 ± 0.08
3967859	...	5896 ± 50	4.18 ± 0.1	-0.33 ± 0.08
4038445	...	5195 ± 50	3.77 ± 0.1	-0.6 ± 0.08

NOTE—The full table is available in a machine-readable form in the online journal. A portion is shown here for guidance regarding content and form.

Column (1) lists the identifier of the star from the Kepler Input Catalog (KIC), column (2) the KOI number of the star (if available), and columns (3)-(5) the stellar parameters derived from spectra from the Tillinghast telescope.

Table 7. Stellar Parameters of KOI Host Stars

KOI	KICID	SPC			Kea			SpecMatch			Newspec		
		T_{eff}	$\log(g)$	[Fe/H]	T_{eff}	$\log(g)$	[Fe/H]	T_{eff}	$\log(g)$	[Fe/H]	T_{eff}	$\log(g)$	[Fe/H]
(1)	(2)	(3)	(4)	(5)	(6)	(7)	(8)	(9)	(10)	(11)	(12)	(13)	(14)
1	11446443	5870 ± 50	4.47 ± 0.1	-0.05 ± 0.08
2	10666592
3	10748390	4876 ± 50	4.63 ± 0.1	0.21 ± 0.08
4	3861595
5	8554498	5810 ± 50	4.08 ± 0.1	0.12 ± 0.08	5881 ± 102	4.295 ± 0.11	0.03 ± 0.08
6	3248033	6175 ± 94	4.33 ± 0.15	-0.26 ± 0.04	6278 ± 64	4.227 ± 0.1	-0.027 ± 0.1
7	11853905	5887 ± 50	4.26 ± 0.1	0.29 ± 0.08	5856 ± 90	4.105 ± 0.14	0.08 ± 0.06	5813 ± 64	4.093 ± 0.1	0.144 ± 0.1
8	5903312	5910 ± 64	4.54 ± 0.1	-0.1 ± 0.1
10	6922244	6243 ± 64	4.141 ± 0.1	-0.11 ± 0.1
11	11913073
12	5812701	6625 ± 387	4.67 ± 0.17	-1.0 ± 0.11
13	9941662
14	7684873	7062 ± 346	3.5 ± 0.5	-0.3 ± 0.25
16	9110357
17	10874614	5775 ± 50	4.41 ± 0.1	0.48 ± 0.08	5625 ± 108	3.96 ± 0.15	0.06 ± 0.07	5732 ± 64	4.286 ± 0.1	0.357 ± 0.1
18	8191672	6278 ± 64	4.059 ± 0.1	-0.037 ± 0.1
19	7255336
20	11804465	5987 ± 64	4.121 ± 0.1	0.02 ± 0.1
22	9631995	5850 ± 50	4.29 ± 0.1	0.16 ± 0.08	5918 ± 64	4.239 ± 0.1	0.187 ± 0.1
23	9071386
24	4743513
25	10593759
28	4247791
31	6956014
41	6521045	5824 ± 49	4.13 ± 0.1	0.07 ± 0.08	5988 ± 74	4.25 ± 0.09	0.0 ± 0.08	5855 ± 64	4.096 ± 0.1	0.068 ± 0.1
42	8866102	6344 ± 50	4.17 ± 0.1	-0.07 ± 0.08	6212 ± 104	4.38 ± 0.09	-0.12 ± 0.05	6279 ± 64	4.198 ± 0.1	-0.065 ± 0.1
44	8845026	5388 ± 316	2.17 ± 0.48	0.2 ± 0.2
46	10905239	5594 ± 176	3.875 ± 0.27	0.4 ± 0.1
49	9527334	5782 ± 129	4.165 ± 0.179	-0.05 ± 0.11
51	6056992
63	11554435	5583 ± 50	4.51 ± 0.1	0.01 ± 0.08
64	7051180	5362 ± 64	3.831 ± 0.1	0.031 ± 0.1
69	3544595	5718 ± 50	4.52 ± 0.1	-0.18 ± 0.08	5675 ± 65	4.418 ± 0.10	-0.235 ± 0.056	5580 ± 64	4.418 ± 0.1	-0.167 ± 0.1
70	6850504	5547 ± 50	4.55 ± 0.1	0.04 ± 0.08	5525 ± 77	4.54 ± 0.14	-0.06 ± 0.07	5496 ± 64	4.491 ± 0.1	0.071 ± 0.1	5563 ± 75	4.32 ± 0.15	0.12 ± 0.1

NOTE—The full table is available in a machine-readable form in the online journal. A portion is shown here for guidance regarding content and form.

Column (1) lists KOI number of the star, column (2) the identifier of the star from the Kepler Input Catalog (KIC), columns (3)-(5) the stellar parameters derived with SPC, columns (6)-(8) the stellar parameters derived with Kea, columns (9)-(11) the stellar parameters derived with SpecMatch, and columns (12)-(14) the stellar parameters derived with Newspec.

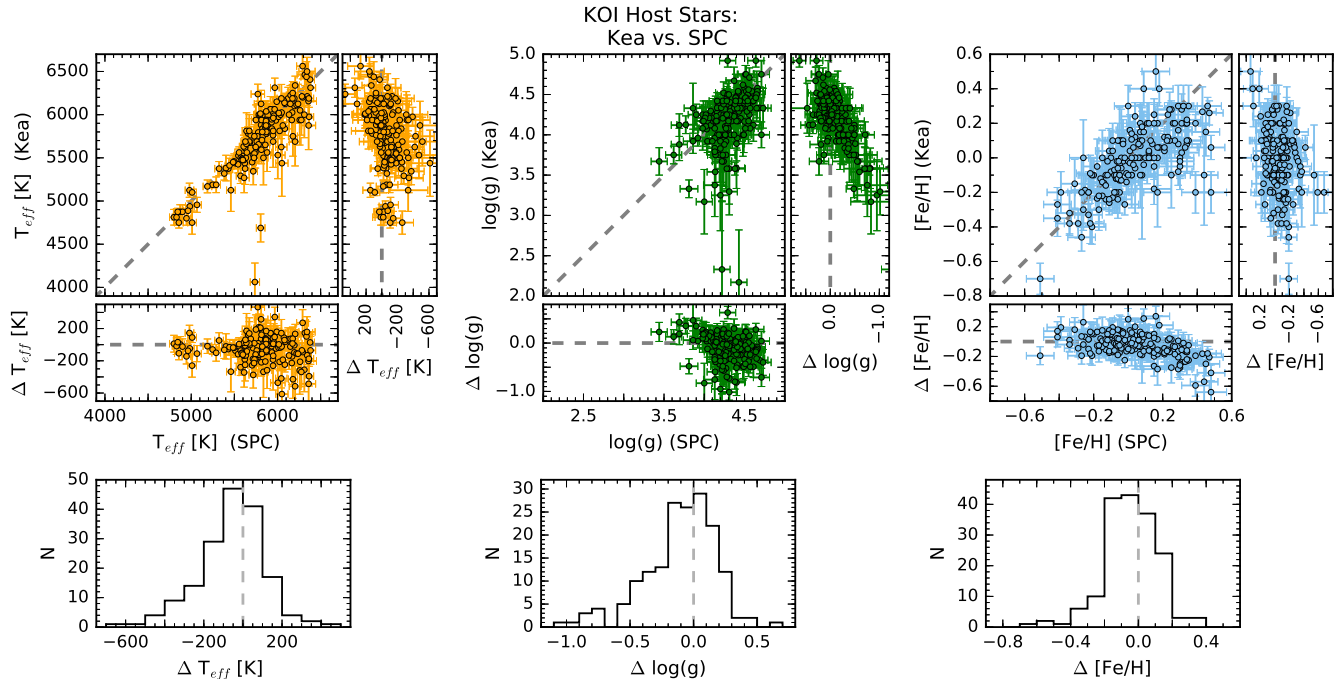


Figure 12. Comparison of T_{eff} (left), $\log(g)$ (middle), and $[\text{Fe}/\text{H}]$ (right) determined for the KOI host stars with SPC and Kea. The top row shows the parameter values of the two sets plotted versus each other (large panels) and the differences in parameter values vs. the values determined with SPC and Kea (smaller panels). The bottom row shows the histograms of the differences in parameter values (172 stars in common). Only the first comparison plot is shown here; the complete figure set (6 plots) is shown in Appendix B.

$[\text{Fe}/\text{H}]$ values derived with SPC are typically larger (on average by 105 K and 0.25 dex, respectively) than those listed in the KIC. The average difference in $\log(g)$ values amounts to -0.15 dex, which implies that KIC $\log(g)$ values tend to be larger for the majority of the gold standard stars. For all three stellar parameters there is a trend of largest differences between SPC and KIC values at the lowest parameter values and decreasing differences as the parameter values increase. This can also be seen for the smaller sample of platinum stars.

In Figure 10 (bottom row) we compare the difference in $\log(g)$ values from asteroseismology (i.e., the input values of the DR25 stellar catalog) and those derived with SPC (Figure 11, bottom row, shows the histogram of $\log(g)$ differences). As we found for the surface gravities derived with SPC for the platinum stars, they are overestimated below about 5600 K and underestimated at subsolar metallicities. In addition, the spectroscopic $\log(g)$ are also underestimated for surface gravities below about 4.0 and are overestimated at the highest values measured for surface gravities and metallicities. The average difference between the asteroseismic and spectroscopic $\log(g)$ values amounts to 0.010 dex with a standard deviation of 0.207.

5.2. KOI Host Stars

The stellar parameters T_{eff} , $\log(g)$, and $[\text{Fe}/\text{H}]$ of KOI host stars derived from spectra obtained and analyzed by the KFOP teams are listed in Table 7. Not all 2667 unique KOI host stars observed at the Tillinghast 1.5-m, NOT 2.6-m, McDonald 2.7-m, KPNO 4-m, and Keck 10-m telescope have derived stellar parameters; spectra from these five facilities yielded stellar parameters for 1816 unique KOI host stars. Moreover, SPC was mostly used on combined data sets from the Tillinghast, NOT, McDonald, and Keck telescope. Overall, SPC yielded parameters for 469, Kea for 944, SpecMatch for 262, and Newspec for 591 KOI host stars. Similar to Figure Set 6, Figure Set 12 compares these parameters for those stars observed by more than one team. There is not much overlap in targets in the results from SPC, Kea, Newspec, and SpecMatch (at most 172, as little as 47), since, as mentioned in section 3, in general duplicate observations at different facilities were avoided.

From Figure Set 12, there is generally broad agreement in derived stellar parameters (see also Table 8). The closest match is seen for the SPC and SpecMatch results, which have the smallest dispersion in parameter differences; there is also no significant offset. The largest differences are found for the Kea and Newspec results; besides a large dispersion, on average there is

Table 8. Average and Standard Deviation of the Differences in Stellar Parameters for the KOI Host Stars Derived by Different Groups and also Compared to the KIC

SPC		Kea	SpecMatch	Newspec
SPC	...	$\overline{\Delta T_{\text{eff}}} = -70 \pm 220$ K (-40 ± 155 K)	$\overline{\Delta T_{\text{eff}}} = -19 \pm 69$ K (-19 ± 69 K)	$\overline{\Delta T_{\text{eff}}} = -40 \pm 96$ K (-40 ± 96 K)
		$\overline{\Delta \log(g)} = -0.12 \pm 0.35$ (-0.08 ± 0.28)	$\overline{\Delta \log(g)} = -0.01 \pm 0.11$ (-0.01 ± 0.11)	$\overline{\Delta \log(g)} = -0.06 \pm 0.18$ (-0.06 ± 0.18)
		$\overline{\Delta[\text{Fe}/\text{H}]} = -0.05 \pm 0.16$ (-0.05 ± 0.15)	$\overline{\Delta[\text{Fe}/\text{H}]} = -0.03 \pm 0.08$ (-0.03 ± 0.08)	$\overline{\Delta[\text{Fe}/\text{H}]} = -0.03 \pm 0.14$ (-0.03 ± 0.14)
Kea	see first row	...	$\overline{\Delta T_{\text{eff}}} = 100 \pm 304$ K (17 ± 98 K)	$\overline{\Delta T_{\text{eff}}} = 127 \pm 307$ K (-33 ± 162 K)
			$\overline{\Delta \log(g)} = 0.18 \pm 0.51$ (0.04 ± 0.19)	$\overline{\Delta \log(g)} = 0.22 \pm 0.60$ (-0.03 ± 0.22)
			$\overline{\Delta[\text{Fe}/\text{H}]} = 0.003 \pm 0.13$ (0.03 ± 0.11)	$\overline{\Delta[\text{Fe}/\text{H}]} = -0.04 \pm 0.15$ (-0.01 ± 0.14)
SpecMatch	see first row	see second row	...	$\overline{\Delta T_{\text{eff}}} = -26 \pm 118$ K (-25 ± 112 K)
				$\overline{\Delta \log(g)} = -0.07 \pm 0.27$ (-0.06 ± 0.27)
				$\overline{\Delta[\text{Fe}/\text{H}]} = 0.11 \pm 0.13$ (0.11 ± 0.13)
KIC				$\overline{\Delta T_{\text{eff}}} = -58 \pm 173$ K
				$\overline{\Delta \log(g)} = 0.01 \pm 0.29$
				$\overline{\Delta[\text{Fe}/\text{H}]} = -0.27 \pm 0.27$
				$\overline{\Delta T_{\text{eff}}} = 89 \pm 360$ K
				$\overline{\Delta \log(g)} = 0.38 \pm 0.59$
				$\overline{\Delta[\text{Fe}/\text{H}]} = -0.21 \pm 0.29$
				$\overline{\Delta T_{\text{eff}}} = -41 \pm 373$ K
				$\overline{\Delta \log(g)} = 0.20 \pm 0.37$
				$\overline{\Delta[\text{Fe}/\text{H}]} = -0.10 \pm 0.30$
				$\overline{\Delta T_{\text{eff}}} = -23 \pm 165$ K
				$\overline{\Delta \log(g)} = 0.22 \pm 0.21$
				$\overline{\Delta[\text{Fe}/\text{H}]} = -0.20 \pm 0.20$

NOTE—The values in parentheses are the averages and standard deviations calculated when only results from spectra with a signal-to-noise ratio larger than 20 are included.

an offset of 127 K and 0.22 dex in T_{eff} and $\log(g)$ values, respectively. To a lesser extent, this also applies to the parameters derived with **Kea** and **SpecMatch**. As will be discussed later (section 6), the observed discrepancies are mostly due to spectra with low signal-to-noise ratios; if the results from these spectra are excluded, the stellar parameters are in better agreement. For the metallicities, the standard deviation of the differences in parameters values is narrower than for the surface gravities. There is also no systematic offset except for an average difference of 0.11 between the **SpecMatch** and **Newspec** results.

When looking at the plots in Figure Set 12, there are some trends and discrepancies. For a few stars, the $\log(g)$ values derived with **Kea** are lower ($\lesssim 3.5$) than those derived with **SPC** and **Newspec**, which both yield $\log(g)$ of ~ 4.0 – 4.5 for these stars (the **SpecMatch** results include only three such stars). Compared to the **Kea** and **Newspec** results, the metallicities in the $[\text{Fe}/\text{H}] > 0.0$ range derived with **SPC** are somewhat larger. The **SpecMatch** metallicities are typically lower than the **Newspec** metallicities, especially for stars with $[\text{Fe}/\text{H}] < -0.2$. The fewest and smallest discrepancies in stellar parameters are found in the results from **SPC** and **SpecMatch**, as well as **SPC** and **Newspec** (Figs. 12.2 and 12.3).

Figure Set 13 compares the stellar parameters derived with **SPC**, **Kea**, **SpecMatch**, and **Newspec** with those from the KIC. As we found for the platinum stars, the spreads in the differences of parameter values are fairly broad, amounting on average to ~ 270 K, 0.37, and 0.27 for T_{eff} , $\log(g)$, and $[\text{Fe}/\text{H}]$, respectively. Systematic offsets are typically smaller than these values. There are also trends in each result set. The **Newspec** $\log(g)$ values are almost all smaller and the $[\text{Fe}/\text{H}]$ values are almost all larger (both by up to 0.8 dex) than the KIC values; a comparable trend in $\log(g)$ values can also be seen for the **SpecMatch** and **Kea** results, while a similar trend in the $[\text{Fe}/\text{H}]$ values is apparent in the **SPC** and **Kea** results.

As a final comparison, in Figure Set 14 we compare the stellar parameters derived by the KFOP teams with the input values of the DR25 stellar catalog (Mathur et al. 2017). These input values have various origins, such as spectroscopy³, photometry, and asteroseismology. For the KOI host stars, 73% of T_{eff} and $[\text{Fe}/\text{H}]$ input values were not determined from spectroscopy; the average uncertainties of these stellar parameters are about a factor of two larger than those of T_{eff} and $[\text{Fe}/\text{H}]$ values de-

³ The original input tables of Mathur et al. (2017) had erroneous metallicities for 779 KOIs, where the wrong values from KFOP-delivered results were adopted. For this comparison we used the corrected input values.

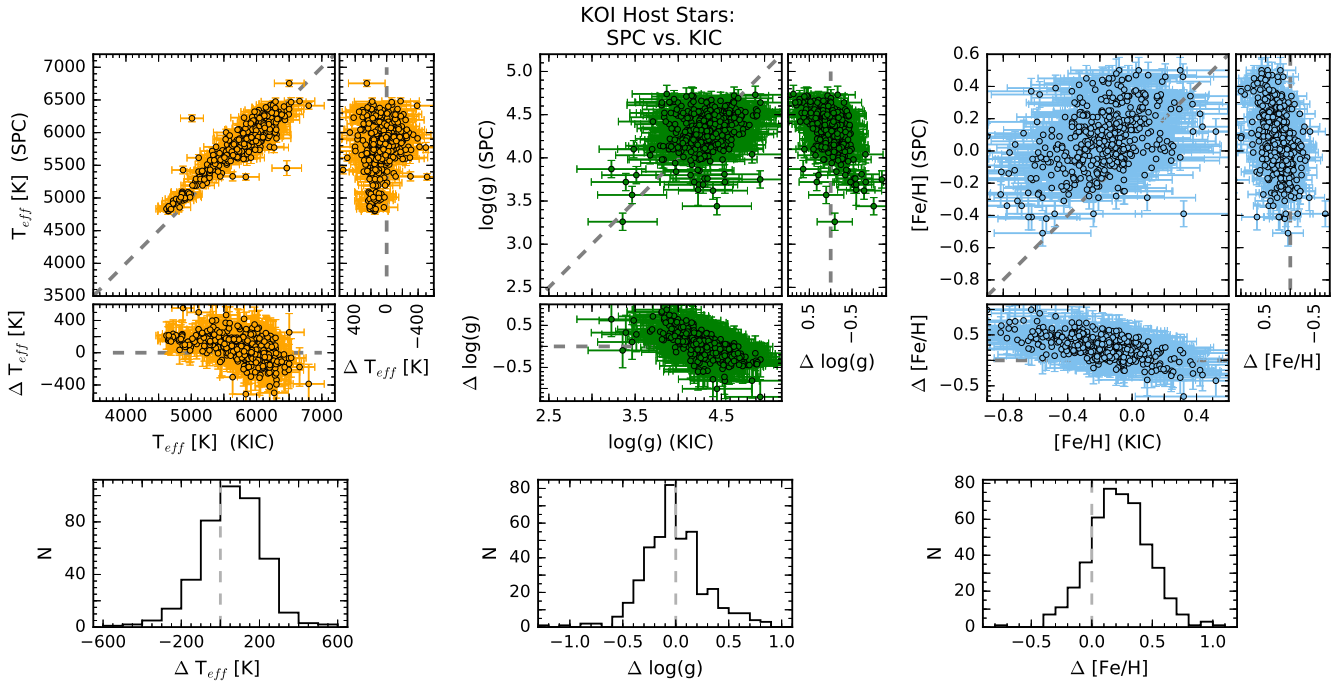


Figure 13. Comparison of T_{eff} (left), $\log(g)$ (middle), and $[\text{Fe}/\text{H}]$ (right) determined for the KOI host stars with SPC and the values from the KIC. The top row shows the parameter values of the two sets plotted versus each other (large panels) and the differences in parameter values vs. the values determined with SPC and the values from the KIC (smaller panels). The bottom row shows the histograms of the differences in parameter values. Only the first comparison plot is shown here; the complete figure set (4 plots) is shown in Appendix B.

terminated from spectra (180 vs. 93 K and 0.29 vs. 0.15 dex, respectively). Just 3% of the DR25 input $\log(g)$ values of KOI host stars were determined from asteroseismology; they are the most accurate values, with mean uncertainties less than a tenth those of the other $\log(g)$ values (0.026 vs. 0.313 dex).

When comparing the stellar parameters derived with SPC for the KOI host stars with the DR25 input values (Fig. 14.1), about three-quarters of parameters values are the same. Except for four $[\text{Fe}/\text{H}]$ values, these matching parameter values in the DR25 catalog were derived from spectroscopy; moreover, many of the stellar parameters from spectroscopy that were adopted as DR25 input values were derived with SPC. In the comparison of *Kea* DR25 input values (see Fig. 14.2), only about one-quarter of T_{eff} , $\log(g)$, and $[\text{Fe}/\text{H}]$ values are the same. *Kea* effective temperatures and surface gravities tend to be lower than the DR25 values, while metallicities tend to be larger. In addition, about 25% of the DR25 T_{eff} and $[\text{Fe}/\text{H}]$ values shown in this figure were not derived from spectroscopy; the former tend to be higher, while the latter tend to be lower than the *Kea* values. A similar trend can be seen in the comparison of *SpecMatch* and DR25 input values (Fig. 14.3), where also about 23% of T_{eff} and $[\text{Fe}/\text{H}]$ values were not derived from spectroscopy. For the *Newspec* sample (see

Fig. 14.4), only $\sim 6\%$ of stars have non-spectroscopically derived DR25 T_{eff} and $[\text{Fe}/\text{H}]$ values; about 75% of stars have the same effective temperatures and surface gravities derived with *Newspec* and as DR25 input values. Of the KOI host stars with $\log(g)$ values derived with SPC, *Kea*, *SpecMatch*, and *Newspec*, 14%, 4%, 13%, and 2%, respectively, of the corresponding DR25 input values were derived from asteroseismology. On average, the spectroscopically derived $\log(g)$ values match those from asteroseismology well (average differences are within 0.05 dex), but there are individual values that are more discrepant.

5.2.1. KOI Host Stars with Companions

In the work summarizing the *Kepler* imaging follow-up observations, Furlan et al. (2017) compiled a catalog of 2297 companions within $4''$ around 1903 KOI host stars; not all of these stars are likely bound, but they nonetheless contaminate the flux measured from the “primary” star, especially if the projected separation is $\lesssim 2''$.

In Figures 15 to 17 we compare the cumulative distributions of stellar parameters derived with SPC, *Kea*, *SpecMatch*, and *Newspec* between KOI host stars with a detected companion within $2''$ and those without (note that even apparently single stars could have companions, since not all KOI host stars were targeted by high-

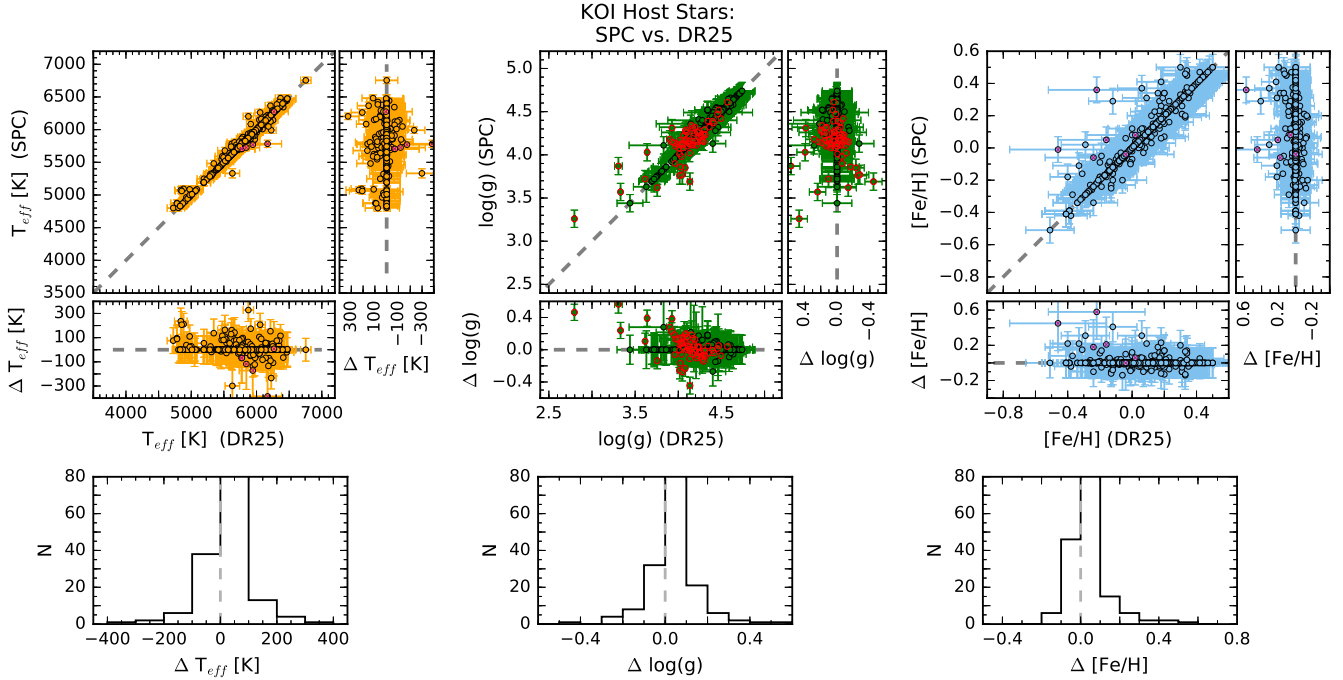


Figure 14. Comparison of T_{eff} (left), $\log(g)$ (middle), and $[\text{Fe}/\text{H}]$ (right) determined for the KOI host stars with SPC and the DR25 input values from Mathur et al. (2017). The top row shows the parameter values of the two sets plotted versus each other (large panels) and the differences in parameter values vs. the values determined with SPC and the DR25 input values (smaller panels). The bottom row shows the histograms of the differences in parameter values. The purple crosses identify those DR25 input values for T_{eff} and $[\text{Fe}/\text{H}]$ that were not determined from spectroscopy, while the red circles identify DR25 input values for $\log(g)$ from asteroseismology. Only the first comparison plot is shown here; the complete figure set (4 plots) is shown in Appendix B.

resolution follow-up observations, and very close and faint companions could have been missed in follow-up images). Two-sample Kolmogorov-Smirnov (K-S) tests yield that the distributions of stellar parameters of single and of multiple stars are typically consistent with being drawn from the same distribution. In particular, the p -values for the distributions of stellar parameters derived with SPC and Newspec range from 0.19 to 0.88. For stellar parameters derived with Kea, there is also no statistically significant difference except for the distribution of $[\text{Fe}/\text{H}]$ values, which have $p = 0.012$. For T_{eff} and $[\text{Fe}/\text{H}]$ values from SpecMatch, the K-S test yields $p = 0.02$, while for $\log(g)$ values $p = 0.11$. If we restrict the sample of multiple stars to those with at least one companion star within $2''$ with a magnitude difference of at most 0.75 (corresponding to a primary-over-secondary flux ratio of at most 2), the p -values of the resulting K-S tests are all larger than 0.2 with the exception of the distributions of T_{eff} and $[\text{Fe}/\text{H}]$ values from Kea ($p = 0.03$ and 0.06 , respectively). We conclude that the sample of KOI host stars with companions does not have a significantly different distribution of stellar parameters compared to apparently single KOI host stars. Also, the presence of a companion within $2''$ does not

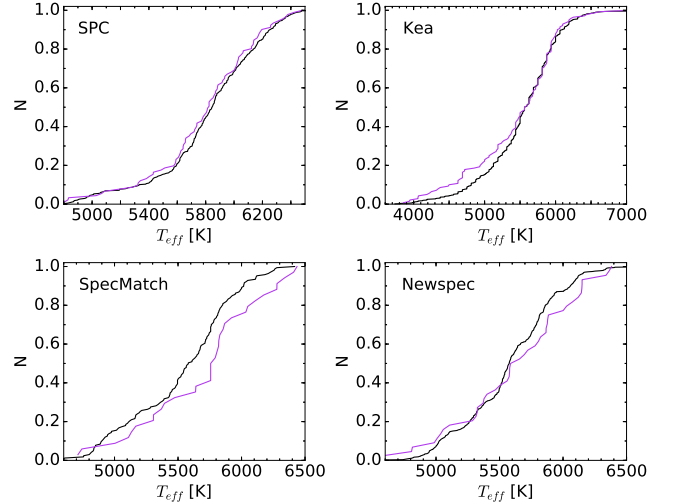


Figure 15. Cumulative distributions of effective temperatures determined with SPC (top left), Kea (top right), SpecMatch (bottom left), and Newspec (bottom right) for KOI host stars that are single or have companions $> 2''$ (black) and those KOI host stars found to have companions within $2''$ (purple).

bias the values of stellar parameters derived from spectroscopy.

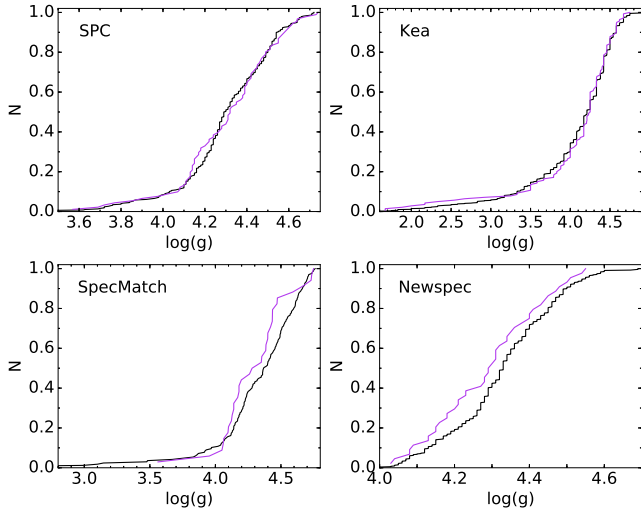


Figure 16. Similar to Figure 15, but for the surface gravities.

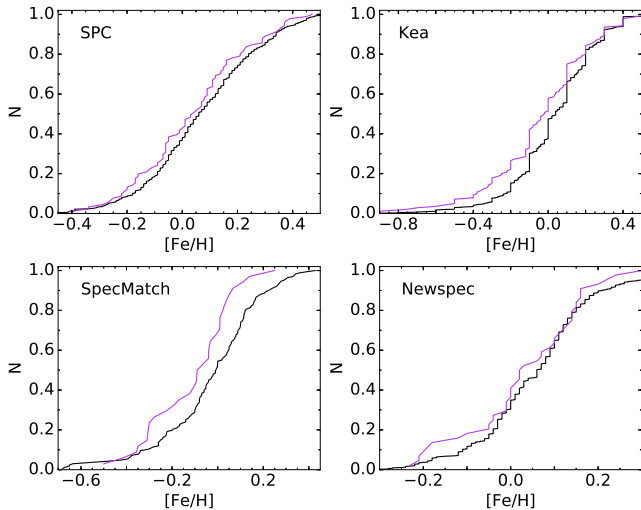


Figure 17. Similar to Figure 15, but for the metallicities.

6. DISCUSSION

We have presented stellar parameters of *Kepler* stars derived with four different analysis pipelines using data from different telescopes and instruments and found that, where overlap exists, the results broadly agree, with some discrepancies in certain regimes of parameter space. One apparent factor is the diversity of the data sets. The resolving power of the spectra plays a role in the accuracy of the derived stellar parameters. The spectra obtained at Keck, McDonald, NOT, and Tillinghast all have a resolving power of $\sim 50,000$, while the spectra from the KPNO 4-m telescope only have $R \sim 3,000$. These latter, medium-resolution spectra seem to yield more uncertain results at lower $\log(g)$ values and lower metallicities, where discrepancies with the stel-

lar parameters derived using the higher-resolution spectra are largest. Furthermore, the signal-to-noise ratio (SNR) of the spectra varies; in general, fainter stars have lower SNR, but it also depends on the observing conditions and the adopted integration time. In Figure Set 18 we show the differences in stellar parameters derived from different data sets as a function of SNR. Large discrepancies are evident at the lowest SNR ($\lesssim 20$) – they can explain the clear outliers seen in the comparison plots of sections 5.1 and 5.2 – but there is still a spread among values derived from spectra with higher SNR. This points to additional uncertainties in the derived stellar parameters due to the use of stellar templates based on different stellar models and different fitting methods. One limitation is also given by the discrete parameter values in the spectral grid and the uncertainties in the model spectra.

For the platinum standard stars, the standard deviation of the difference in parameter values derived with the different analysis tools (SPC, Kea, SpecMatch, and Newspec) is comparable to the $1\text{-}\sigma$ uncertainties of most parameter values except for the surface gravities, where there is a larger spread. The averages of these standard deviations (see Table 5) are ~ 90 K for T_{eff} , 0.2 dex for $\log(g)$, and 0.1 dex for $[\text{Fe}/\text{H}]$, which are indicative of the precision of these spectroscopically derived stellar parameters for brighter stars such as the gold and platinum standard stars, for which the median signal-to-noise ratio in the observed spectra is about 85. For the KOI host stars, which are overall fainter than the standard stars studied in this work, the median signal-to-noise ratio in the spectra is just ~ 40 . Spectra from Keck have on average the highest SNR, while spectra from the McDonald Observatory have relatively low SNR, with a median of 23. As a result, the stellar parameters for the KOI host stars from Kea are on average more uncertain than those from the other analysis codes. The averages of the standard deviations from Table 8 amount to ~ 185 K for T_{eff} , 0.3 dex for $\log(g)$, and 0.13 dex for $[\text{Fe}/\text{H}]$. If we only include results from spectra with $\text{SNR} > 20$, these averages decrease to 115 K, 0.2 dex, and 0.125 dex, respectively. These values are just a bit higher than the results for the platinum stars. Therefore, we suggest a systematic error floor for spectroscopically derived stellar parameters of ~ 100 K for T_{eff} , 0.2 dex for $\log(g)$, and 0.1 dex for $[\text{Fe}/\text{H}]$.

When analyzing the platinum star sample, we usually found the largest differences in derived stellar parameters at the largest or smallest values. In particular, for cooler stars ($T_{\text{eff}} \lesssim 5500$ K) the effective temperatures and surface gravities derived with Kea and SpecMatch are typically lower than those derived with SPC, while

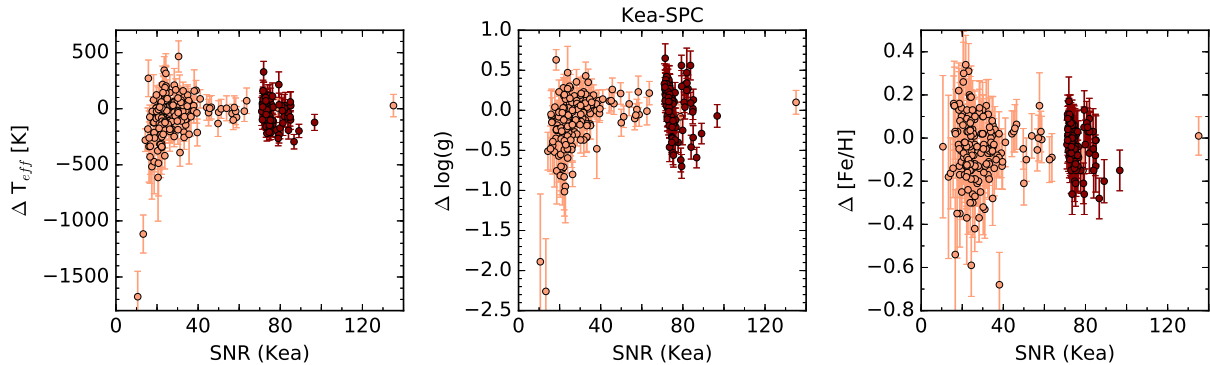


Figure 18. Difference of T_{eff} (left) $\log(g)$ (middle), and $[\text{Fe}/\text{H}]$ (right) values determined with SPC and Kea vs. the signal-to-noise of the spectra used as an input for Kea. Stellar parameter differences for KOI host stars are shown in a lighter color, while those for the standard stars are shown in a darker color. Only the first comparison plot is shown here; the complete figure set (6 plots) is shown in Appendix B.

the metallicities derived with Kea are also smaller than those derived with SPC. These cooler stars are almost exclusively giant stars (see Figure 3), suggesting that their stellar parameters are more uncertain.

We also found that the differences in parameter values for T_{eff} , $\log(g)$, and $[\text{Fe}/\text{H}]$ are positively correlated. Given that all four analysis codes used in this work, SPC, Kea, Newspec, and SpecMatch, rely on fitting observed spectra to a grid of model spectra, the resulting stellar parameters are affected by degeneracies between them. As noted by Torres et al. (2012), when using the spectral synthesis technique, the surface gravity is usually correlated with the effective temperature and metallicity; therefore, when a different analysis yields larger $\log(g)$ values, the T_{eff} and $[\text{Fe}/\text{H}]$ values are typically larger, too. This effect varies depending on the stellar models and spectral lines used to derive stellar parameters (Torres et al. 2012). Spectral line analysis, in which the equivalent widths of certain lines are analyzed, are less affected by parameter degeneracies (Torres et al. 2012; Mortier et al. 2013, 2014). Another method commonly used to constrain surface gravities of transiting planet host stars is to derive stellar densities directly from the transit light curve, which then yields the surface gravity through isochrone fits (Sozzetti et al. 2007). Thus, different methods and constraints can reduce uncertainties in derived stellar parameters.

The results from the KFOP and other teams’ spectroscopy were incorporated in the Q1-Q17 DR25 stellar table (Mathur & Huber 2016; Mathur et al. 2017). Of the KOI host stars in that table, $\sim 25\text{--}30\%$ have spectroscopically determined T_{eff} , $\log(g)$, and $[\text{Fe}/\text{H}]$ input values. The majority of the $\log(g)$ and $[\text{Fe}/\text{H}]$ values of KOI host stars in the DR25 table were adopted from the KIC (59% and 66%, respectively), while most of the T_{eff} values (58%) were determined from photometry. While

spectroscopy is necessary to derive more reliable T_{eff} and $[\text{Fe}/\text{H}]$ for stars, asteroseismology is more precise in deriving $\log(g)$ values (Huber et al. 2013; Mortier et al. 2014; Pinsonneault et al. 2014). All the platinum stars have asteroseismic $\log(g)$ values (only 3% of KOI host stars do); their main uncertainty in the DR25 stellar table is just 0.01 dex. When comparing their spectroscopically derived $\log(g)$ values to their asteroseismic ones, the differences in values seem to be correlated with the stellar parameters, with the largest deviations at the lower and higher end of values. On average, most values agree within 0.025 dex, but the spread is about 0.1–0.2 dex. The SpecMatch results are in closest agreement with the asteroseismic $\log(g)$ values.

As shown in our figures for the gold and platinum stars and mentioned in other work (Verner et al. 2011; Pinsonneault et al. 2012; Everett et al. 2013; Chaplin et al. 2014; Huber et al. 2014), the stellar parameters from the KIC are often very uncertain and have systematic offsets; obtaining spectra for KOI host stars, especially hosts to planet candidates, is crucial. In the latest stellar parameters table for KOI host stars (Mathur & Huber 2016; Mathur et al. 2017), still the majority of $\log(g)$ and $[\text{Fe}/\text{H}]$ values, and 14% of T_{eff} values, are adopted from the KIC. Surface gravities are of particular interest, since they are related to the stellar radius and therefore, in the case of transiting planets, to the planetary radius. The $\log(g)$ values from the KIC are based on photometry and therefore have much larger errors than those derived from spectroscopy. Among the standard star sample, there are more evolved stars (e.g., Chaplin et al. 2014; Huber et al. 2014), given that the standard stars have well-determined surface gravities from asteroseismology, and oscillations are easier to detect in subgiants and giants. Many standard stars have higher effective temperatures and lower surface gravities (depending on

the $\log(g)$ range) derived from spectra than listed in the KIC. Even among the KOI sample, results from follow-up spectroscopy suggest that the surface gravities in the KIC are often overestimated (Everett et al. 2013; Huber et al. 2014; Howell et al. 2016), and thus stellar (and planetary) radii have to be revised upward. This will have an effect on a planet’s bulk density and thus its composition (e.g., Seager et al. 2007; Rogers 2015).

7. SUMMARY

Over six years, the *Kepler* Follow-Up Observation Program has carried out spectroscopic follow-up observations of stars in the *Kepler* field. Two sets of standard stars, labeled as “platinum” and “gold” standard stars, and many KOI host stars were observed mainly at four different facilities: the Tillinghast 1.5-m, the McDonald 2.7-m, the KPNO 4-m, and the Keck I 10-m telescope. A total of 3196 *Kepler* stars were targeted, most of them (2667) KOI host stars. The spectra were analyzed with four different analysis codes, each developed for data from one facility: **SPC** for Tillinghast/TRES spectra, **Kea** for McDonald/Tull spectra, **Newspec** for KPNO/RC Spec spectra, and **SpecMatch** for Keck/HIRES spectra. For the standard stars, the main goal was to obtain spectroscopically derived parameters for stars that have well-measured solar-like oscillations and thus reliable surface gravity (and mass, radius) determinations. For the KOI host stars, targets with small ($\lesssim 4 R_{\oplus}$) planet candidates, planets in the habitable zone, and multi-planet systems were of the highest priority. For transiting planets, determining precise stellar radii is crucial for deriving precise planet radii and thus, in combination with mass measurements, bulk densities and compositions.

The derived stellar parameters from different KFOP teams broadly agree, but there are some differences. In part, they can be attributed to spectra with lower signal-to-noise ratios, which often result in more uncertain stellar parameters that are inconsistent with those derived from other, less noisy data sets. Typically, parameter values are more discrepant in certain, relatively narrow, parameter ranges, in particular at the largest and smallest values. The closest match between different parameter sets is found for the **SPC** and **SpecMatch** results; also, the **SpecMatch** $\log(g)$ values are very similar to the asteroseismic values, which are considered the most accurate. We suggest a systematic error floor of ~ 100 K for T_{eff} , 0.2 dex for $\log(g)$, and 0.1 dex for $[\text{Fe}/\text{H}]$. Spectroscopically derived parameters are an improvement over the KIC, where broad-band colors were used to derive most parameters.

Results from the KFOP observations were included in the latest *Kepler* stellar table, the Q1-Q17 DR25 cata-

log (Mathur & Huber 2016; Mathur et al. 2017). Spectroscopic and other follow-up observations yielded more accurate determinations of stellar parameters for many stars in the *Kepler* field; however, the majority of surface gravities and metallicities are still adopted from the more uncertain estimates of the KIC. Nevertheless, the sample of targets with follow-up data should provide the means to cross-calibrate stellar parameters derived with different methods, and thus result in a more reliable and uniform catalog of *Kepler* stars, including the numerous stars that host planets.

Support for this work was provided by NASA through awards issued by JPL/Caltech. M. Endl acknowledges support by NASA under grant NNX14AB86G issued through the Kepler Participating Scientist Program. A. W. Howard acknowledges NASA grant NNX12AJ23G. D. Huber acknowledges support by the Australian Research Council’s Discovery Projects funding scheme (project number DE140101364). D. Huber and S. Mathur acknowledge support by NASA under grant NNX14AB92G issued through the Kepler Participating Scientist Program. S. Mathur acknowledges support from the Ramon y Cajal fellowship number RYC-2015-17697. We thank Ivan Ramirez for contributing to the observations carried out at the McDonald Observatory. This research has made use of the NASA Exoplanet Archive and the Exoplanet Follow-up Observation Program website, which are operated by the California Institute of Technology, under contract with NASA under the Exoplanet Exploration Program. It has also made use of NASA’s Astrophysics Data System Bibliographic Services. Some of the data presented in this work were obtained at the W.M. Keck Observatory, which is operated as a scientific partnership among the California Institute of Technology, the University of California and the National Aeronautics and Space Administration. The Observatory was made possible by the generous financial support of the W.M. Keck Foundation. The authors wish to recognize and acknowledge the very significant cultural role and reverence that the summit of Mauna Kea has always had within the indigenous Hawaiian community. We are most fortunate to have the opportunity to conduct observations from this mountain. This work is also based in part on observations at Kitt Peak National Observatory, National Optical Astronomy Observatory, which is operated by the Association of Universities for Research in Astronomy (AURA) under a cooperative agreement with the National Science Foundation. It also includes data taken at The McDonald Observatory of The University of Texas at Austin. Some of the data were obtained from

the Mikulski Archive for Space Telescopes (MAST). STScI is operated by the Association of Universities for Research in Astronomy, Inc., under NASA contract

NAS5-26555. Support for MAST for non-HST data is provided by the NASA Office of Space Science via grant NNX09AF08G and by other grants and contracts.

REFERENCES

- Batalha, N. M., Rowe, J. F., Bryson, S. T., et al. 2013, *ApJS*, 204, 24
- Borucki, W. J., Koch, D., Basri, G., et al. 2010, *Science*, 327, 977
- Borucki, W. J., Koch, D. G., Basri, G., et al. 2011, *ApJ*, 728, 117
- Borucki, W. J., Koch, D. G., Basri, G., et al. 2011, *ApJ*, 736, 19
- Borucki, W. J. 2016, *Rep. Prog. Phys.*, 79, 036901
- Brown, T. M., Gilliland, R. L., Noyes, R. W., & Ramsey, L. W. 1991, *ApJ*, 368, 599
- Brown, T. M., Latham, D. W., Everett, M. E., & Esquerdo, G. A. 2011, *AJ*, 142, 112
- Buchhave, L. A., Latham, D. W., Johansen, A., et al. 2012, *Nature*, 486, 375
- Buchhave, L. A., Bizzarro, M., Latham, D. W., et al. 2014, *Nature*, 509, 593
- Buchhave, L. A., & Latham, D. W. 2015, *ApJ*, 808, 187
- Burke, C. J., Bryson, S. T., Mullally, F., et al. 2014, *ApJS*, 210, 19
- Castelli, F., & Kurucz, R. L. 2003, in *IAU Symp. 210, Modelling of Stellar Atmospheres*, ed. N. Piskunov, W. W. Weiss, & D. F. Gray (San Francisco, CA: ASP), A20
- Chaplin, W. J., Kjeldsen, H., Christensen-Dalsgaard, J., et al. 2011, *Science*, 332, 213
- Chaplin, W. J., Basu, S., Huber, D., et al. 2014, *ApJS*, 210, 1
- Ciardi, D. R., von Braun, K., Bryden, G., et al. 2011, *AJ*, 141, 108
- Ciardi, D. R., Beichman, C. A., Horch, E. P., & Howell, S. B. 2015, *ApJ*, 805, 16
- Coelho, P., Barbay, B., Meléndez, J., et al. 2005, *A&A*, 443, 735
- Coughlin, J. L., Thompson, S. E., Bryson, S. T., et al. 2014, *AJ*, 147, 119
- Coughlin, J. L., Mullally, F., Thompson, S. E., et al. 2016, *ApJ*, in press
- De Cat, P., Fu, J. N., Ren, A. B., et al. 2015, *ApJS*, 220, 19
- Désert, J.-M., Charbonneau, D., Torres, G., et al. 2015, *ApJ*, 804, 59
- Djupvik, A. A., & Andersen, J. 2010, in *Highlights of Spanish Astrophysics V*, 211
- Dotter, A., Chaboyer, B., Jevremović, D., et al. 2008, *ApJS*, 178, 89
- Duquennoy, A., & Mayor, M. 1991, *A&A*, 248, 485
- Endl, M., & Cochran, W. D. 2016, *PASP*, 128, 094502
- Everett, M. E., Howell, S. B., Silva, D. R., & Szkody, P. 2013, *ApJ*, 771, 107
- Fleming, S. W., Mahadevan, S., Deshpande, R., et al. 2015, *AJ*, 149, 143
- Fressin, F., Torres, G., Charbonneau, D., et al. 2013, *ApJ*, 766, 81
- Fűrész, G. 2008, PhD thesis, Univ. of Szeged, Hungary
- Furlan, E., Ciardi, D. R., Everett, M. E., et al. 2017, *AJ*, 153, 71
- Horch, E. P., Gomez, S. C., Sherry, W. H., et al. 2011, *AJ*, 141, 45
- Howell, S. B., Rowe, J. F., Bryson, S. T., et al. 2012, *ApJ*, 746, 123
- Howell, S. B., Ciardi, D. R., Giampapa, M. S., et al. 2016, *AJ*, 151, 43
- Huber, D., Bedding, T. R., Stello, D., et al. 2011, *ApJ*, 743, 143
- Huber, D., Chaplin, W. J., Christensen-Dalsgaard, J., et al. 2013, *ApJ*, 767, 127
- Huber, D. 2014, *Kepler Stellar Properties Catalog Update for Q1-Q17 Transit Search (KSCI-19083)*
- Huber, D., Silva Aguirre, V., Matthews, J. M., et al. 2014, *ApJS*, 211, 2
- Johnson, J. A., Petigura, E. A., Fulton, B. J., et al. 2017, *AJ*, 154, 108
- Kjeldsen, H., & Bedding, T. R. 1995, *A&A*, 293, 87
- Kolbl, R., Marcy, G. W., Isaacson, H., & Howard, A. W. 2015, *AJ*, 149, 18
- Kurucz, R. L. 1992, in *IAU Symp. 149, The Stellar Populations of Galaxies*, ed. B. Barbay & A. Renzini (Dordrecht: Kluwer), 225
- Kurucz R. 1993, *ATLAS9 Stellar Atmosphere Programs and 2 km/s grid*, Kurucz CD-ROM No. 13 (Cambridge, MA: Smithsonian Astrophysical Observatory)
- Lundkvist, M. S., Kjeldsen, H., Albrecht, S., et al. 2016, *Nature Comm.*, 7, 11201
- Marcy, G. W., Isaacson, H., Howard, A. W., et al. 2014, *ApJS*, 210, 20
- Mathur, S., & Huber, D. 2016, *Kepler Stellar Properties Catalog Update for Q1-Q17 DR25 Transit Search (KSCI-19097-001)*

- Mathur, S., García, R. A., Huber, D., et al. 2016, *ApJ*, 827, 50
- Mathur, S., Huber, D., Batalha, N. M., et al. 2017, *ApJS*, 229, 30
- McCauliff, S. D., Jenkins, J. M., Catanzarite, J., et al. 2015, *ApJ*, 806, 6
- Mortier, A., Santos, N. C., Sousa, S. G., et al. 2013, *A&A*, 558, A106
- Mortier, A., Sousa, S. G., Adibekyan, V. Zh., et al. 2014, *A&A*, 572, A95
- Morton, T. D., Bryson, S. T., Coughlin, J. L., et al. 2016, *ApJ*, 822, 86
- Mullally, F., Coughlin, J. L., Thompson, S. E., et al. 2015, *ApJS*, 217, 31
- Pecaut, M. J., & Mamajek, E. E. 2013, *ApJS*, 208, 9
- Petigura, E. A., Marcy, G. W., & Howard, A. W. 2013, *ApJ*, 770, 69
- Petigura, E. A. 2015, PhD thesis, Univ. of California
- Petigura, E. A., Howard, A. W., Marcy, G. W., et al. 2017, *AJ*, 154, 107
- Pinsonneault, M. H., An, D., Molenda-Zakowicz, J., et al. 2012, *ApJS*, 199, 30
- Pinsonneault, M. H., Elsworth, Y., Epstein, C., et al. 2014, *ApJS*, 215, 19
- Raghavan, D., McAllister, H. A., Henry, T. J., et al. 2010, *ApJS*, 190, 1
- Rogers, L. A. 2015, *ApJ*, 801, 41
- Rowe, J. F., Bryson, S. T., Marcy, G. W., et al. 2014, *ApJ*, 784, 45
- Rowe, J. F., Coughlin, J. L., Antoci, V., et al. 2015, *ApJS*, 217, 16
- Santerne, A., Moutou, C., Tsantaki, M., et al. 2016, *A&A*, 587, A64
- Seader, S., Jenkins, J. M., Tenenbaum, P., et al. 2015, *ApJS*, 217, 18
- Seager, S., Kuchner, M., Hier-Majumder, C. A., & Militzer, B. 2007, *ApJ*, 669, 1279
- Skrutskie, M. F., Cutri, R. M., Stiening, R., et al. 2006, *AJ*, 131, 1163
- Slawson, R. W., Prša, A., Welsh, W. F., et al. 2011, *AJ*, 142, 160
- Sozzetti, A., Torres, G., Charbonneau, D., et al. 2007, *ApJ*, 664, 1190
- Teske, J. K., Everett, M. E., Hirsch, L., et al. 2015, *AJ*, 150, 144
- Thompson, S. E., Coughlin, J. L., Hoffman, K., et al. 2018, *ApJS*, 235, 38
- Torres, G., Fischer, D. A., Sozzetti, A., et al. 2012, *ApJ*, 757, 161
- Tull, R. G., MacQueen, P. J., Sneden, C., & Lambert, D. L. 1995, *PASP*, 107, 251
- Valenti, J. A., & Piskunov, N. 1996, *A&AS*, 118, 595
- Verner, G. A., Elsworth, Y., Chaplin, W. J., et al. 2011, *MNRAS*, 415, 3539
- Vogt, S. S., Allen, S. L., Bigelow, B. C., et al. 1994, *Proc. SPIE*, 2198, 362
- Yu, J., Huber, D., Bedding, T. R., et al. 2016, *MNRAS*, 463, 1297

APPENDIX

A. STELLAR PARAMETERS FROM THE KEPLER FOLLOW-UP OBSERVATION PROGRAM

In Table 9 we provide combined sets of stellar parameters derived for the standard stars and KOI host stars⁴ using the results from *SPC*, *Kea*, *SpecMatch*, and *Newspec*. When more than one measurement for a given stellar parameter was available, we computed a median value, but only using those parameters derived from spectra with a signal-to-noise ratio larger than 20. If all spectra had $\text{SNR} < 20$, we used the median of all measurements despite their low SNR. If only one measurement was available, we list it in Table 9, irrespective of the SNR of the spectrum used to derive it; in this case the value listed in Table 9 is the same as in Table 4, 6, or 7, depending on whether the star is part of the platinum, gold, or KOI host star sample, respectively. Some of the platinum and gold standard stars are also KOI hosts; given that their stellar parameters were sometimes derived using different data sets obtained at the same telescope, they may differ somewhat, and therefore they are listed twice in Table 9, once among the standard stars and once among the KOI host star sample. For the parameter uncertainties, we used an error floor of 100 K, 0.2 dex, and 0.1 dex for T_{eff} , $\log(g)$, and $[\text{Fe}/\text{H}]$, respectively.

⁴ Note that in Table 9 we list first all the parameters for the platinum standard stars, then the ones for the gold standard stars, and finally the ones for the KOI host stars. Also note that these stellar parameters are often not the same as the input values adopted from the KFOP in the DR25 stellar catalog (Mathur et al. 2017), since in that catalog mostly the *SPC* values were used.

Table 9. Combined Stellar Parameters of the Platinum Standard Stars, Gold Standard Stars, and KOI Host Stars

KOI	KICID	Group	T_{eff}	$\log(g)$	[Fe/H]	N_m
(1)	(2)	(3)	(4)	(5)	(6)	(7)
0	1435467	1	6325 ± 100	4.13 ± 0.20	0.04 ± 0.10	3
0	2837475	1	6488 ± 100	4.29 ± 0.20	-0.07 ± 0.10	3
0	2852862	1	6230 ± 100	4.05 ± 0.20	-0.16 ± 0.10	3
0	3424541	1	6338 ± 100	4.33 ± 0.20	0.16 ± 0.10	1
0	3427720	1	6014 ± 100	4.31 ± 0.20	-0.04 ± 0.10	4
0	3429205	1	5078 ± 100	3.47 ± 0.20	0.01 ± 0.10	3
975	3632418	1	6112 ± 100	4.07 ± 0.20	-0.16 ± 0.10	3
0	3656476	1	5664 ± 100	4.22 ± 0.20	0.28 ± 0.10	4
0	3733735	1	6562 ± 100	4.39 ± 0.20	-0.05 ± 0.10	3
0	3735871	1	6064 ± 100	4.31 ± 0.20	-0.07 ± 0.10	4
			...			
0	1430163	2	6388 ± 100	3.85 ± 0.20	-0.19 ± 0.10	1
0	1725815	2	6133 ± 100	3.63 ± 0.20	-0.19 ± 0.10	1
4929	2010607	2	6132 ± 100	3.65 ± 0.20	-0.07 ± 0.10	1
113	2306756	2	5616 ± 100	4.23 ± 0.20	0.46 ± 0.10	1
0	2309595	2	5212 ± 100	3.86 ± 0.20	-0.06 ± 0.10	1
0	2450729	2	5861 ± 100	3.96 ± 0.20	-0.25 ± 0.10	1
0	2849125	2	6114 ± 100	3.88 ± 0.20	0.23 ± 0.10	1
0	2865774	2	5793 ± 100	4.02 ± 0.20	-0.07 ± 0.10	1
0	2991448	2	5640 ± 100	3.98 ± 0.20	-0.11 ± 0.10	1
0	2998253	2	6215 ± 100	4.09 ± 0.20	0.04 ± 0.10	1
			...			
1	11446443	0	5870 ± 100	4.47 ± 0.20	-0.05 ± 0.10	1
3	10748390	0	4876 ± 100	4.63 ± 0.20	0.21 ± 0.10	1
5	8554498	0	5846 ± 100	4.19 ± 0.20	0.07 ± 0.10	2
6	3248033	0	6226 ± 100	4.28 ± 0.20	-0.14 ± 0.10	2
7	11853905	0	5856 ± 100	4.11 ± 0.20	0.14 ± 0.10	3
8	5903312	0	5910 ± 100	4.54 ± 0.20	-0.10 ± 0.10	1
10	6922244	0	6243 ± 100	4.14 ± 0.20	-0.11 ± 0.10	1
12	5812701	0	6625 ± 387	4.67 ± 0.20	-1.00 ± 0.11	1
14	7684873	0	7062 ± 346	3.50 ± 0.50	-0.30 ± 0.25	1
17	10874614	0	5732 ± 100	4.29 ± 0.20	0.36 ± 0.10	3

NOTE—The full table is available in a machine-readable form in the online journal. A portion is shown here for guidance regarding content and form.

Column (1) lists the KOI number of the star (if 0, the star is in the *Kepler* field, but was not identified as a KOI), column (2) its identifier from the Kepler Input Catalog (KIC), column (3) identifies whether the target is a platinum standard (1), gold standard (2), or only a KOI host star (0), columns (4)-(6) the combined stellar parameters (when more than one measurement was available – see text for details), and column (7) the number of measurements that were combined. The table lists the parameters for the platinum stars (ordered by KICID), then those for the gold stars (also ordered by KICID), and finally those of the KOI host stars (ordered by KOI number).

APPENDIX
B. FIGURE SETS

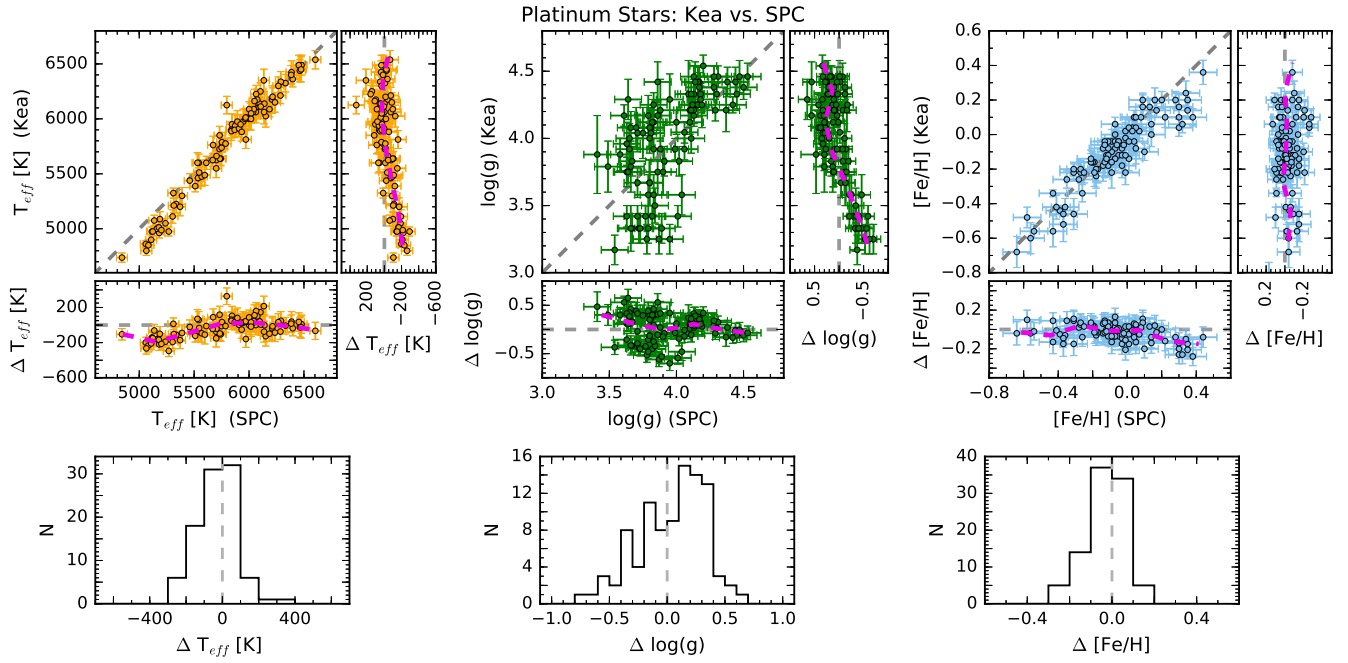


Figure 6.1. Comparison of T_{eff} (*left*), $\log(g)$ (*middle*), and $[\text{Fe}/\text{H}]$ (*right*) determined for the platinum standard stars observed at the Tillinghast 1.5-m and the McDonald 2.7-m telescopes and analyzed with SPC and Kea, respectively (95 stars in common). The top row shows the parameter values of the two sets plotted versus each other (large panels) and the differences in parameter values vs. the values determined with SPC and Kea (smaller panels). The magenta line in the smaller panels represents a running median. The bottom row shows the histograms of the differences in parameter values.

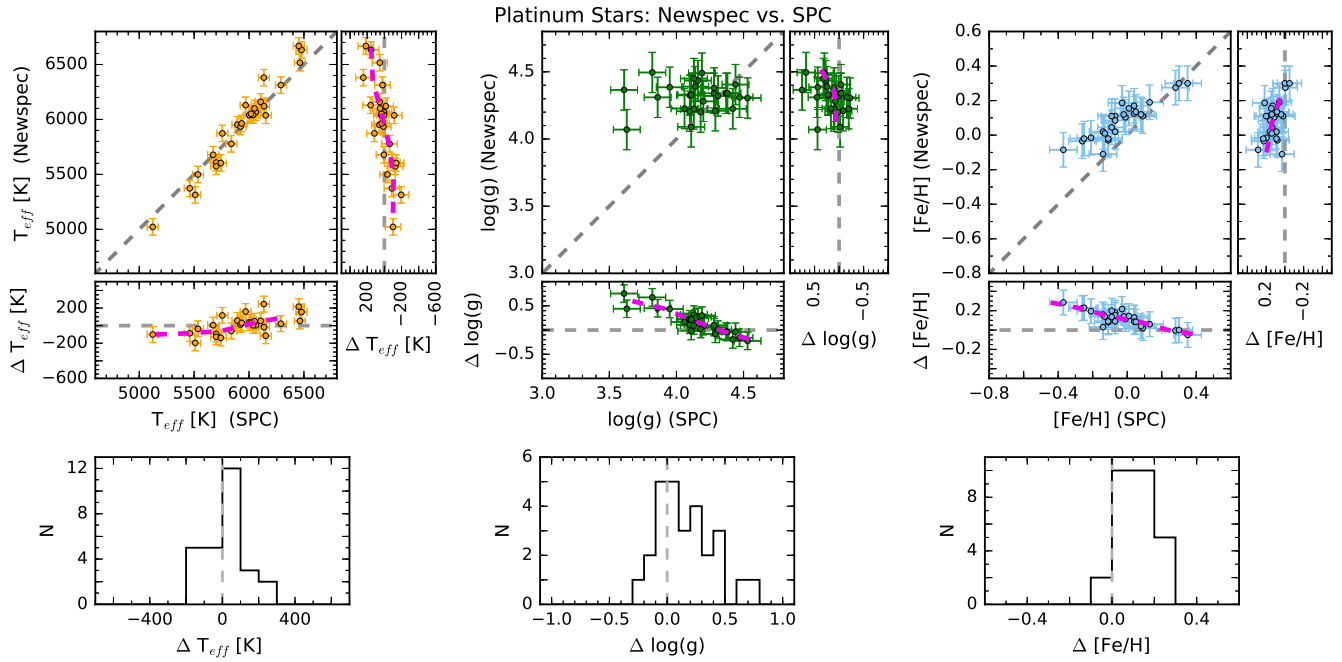


Figure 6.2. Similar to Figure 6.1, but for the platinum standard stars observed at the Tillinghast 1.5-m and the KPNO 4-m telescopes and analyzed with SPC and Newspec, respectively (27 stars in common).

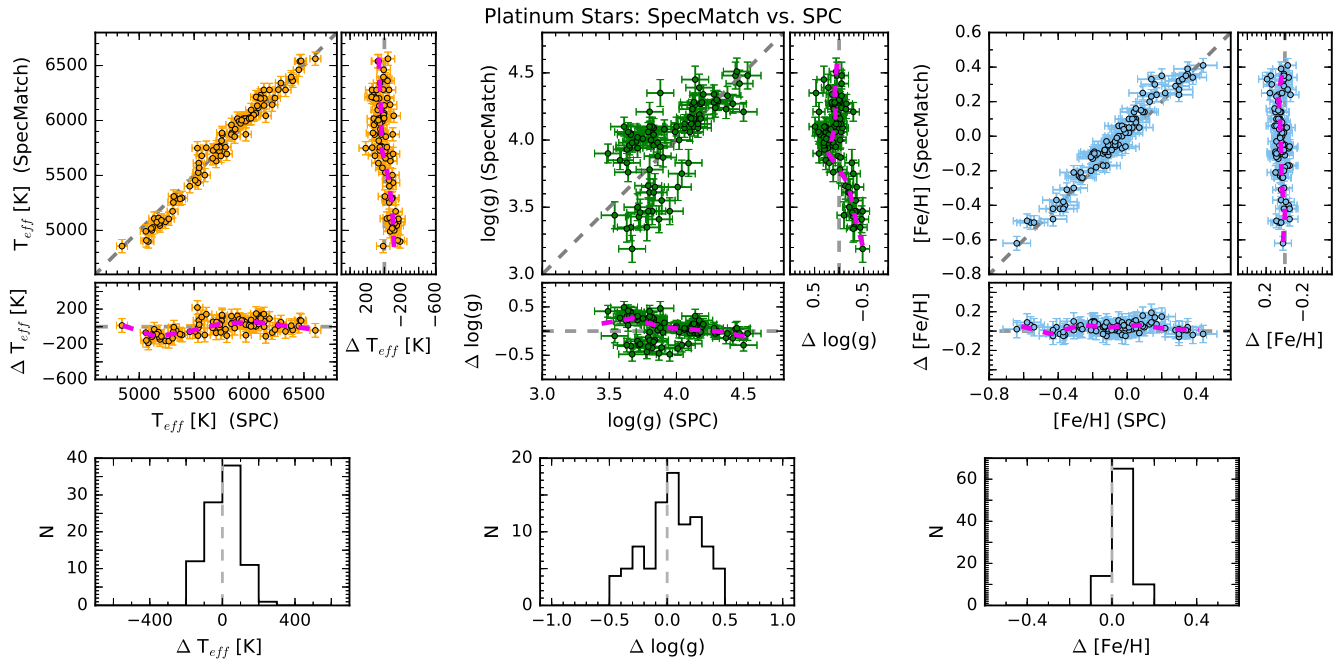


Figure 6.3. Similar to Figure 6.1, but for the platinum standard stars observed at the Tillinghast 1.5-m and the Keck I telescopes and analyzed with SPC and SpecMatch, respectively (93 stars in common).

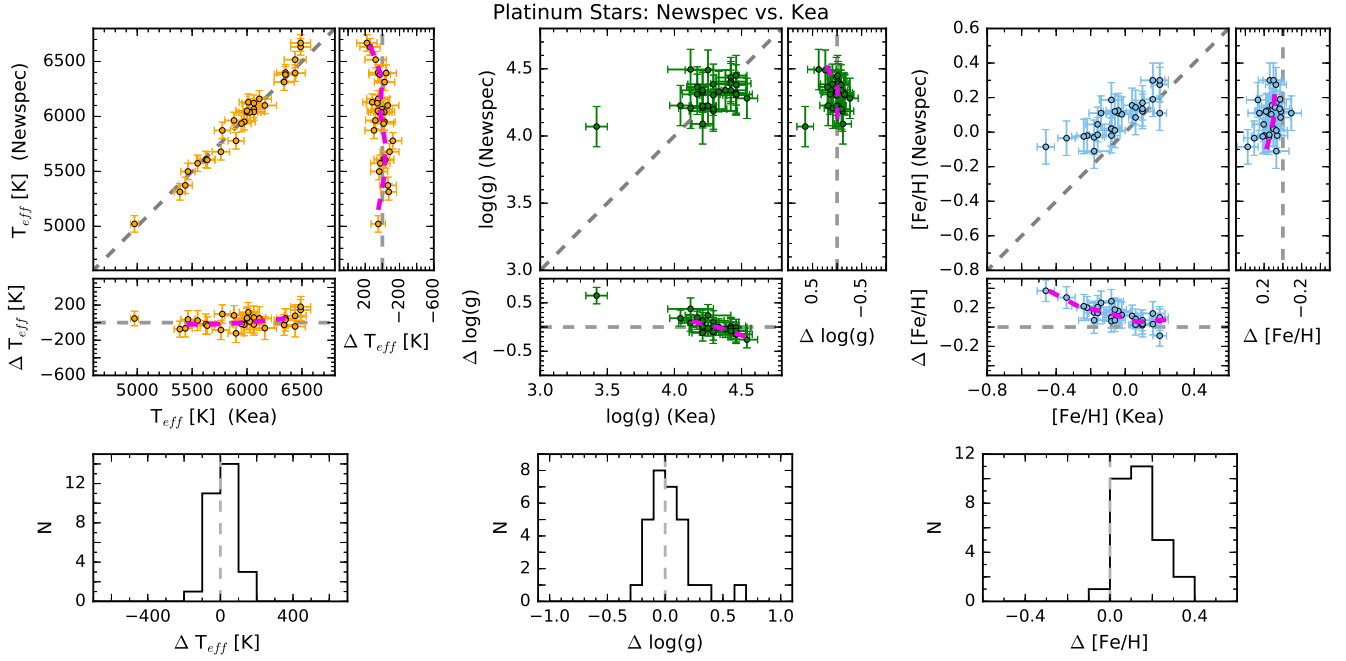


Figure 6.4. Similar to Figure 6.1, but for the platinum standard stars observed at the McDonald 2.7-m and the KPNO 4-m telescopes and analyzed with Kea and Newspec, respectively (29 stars in common).

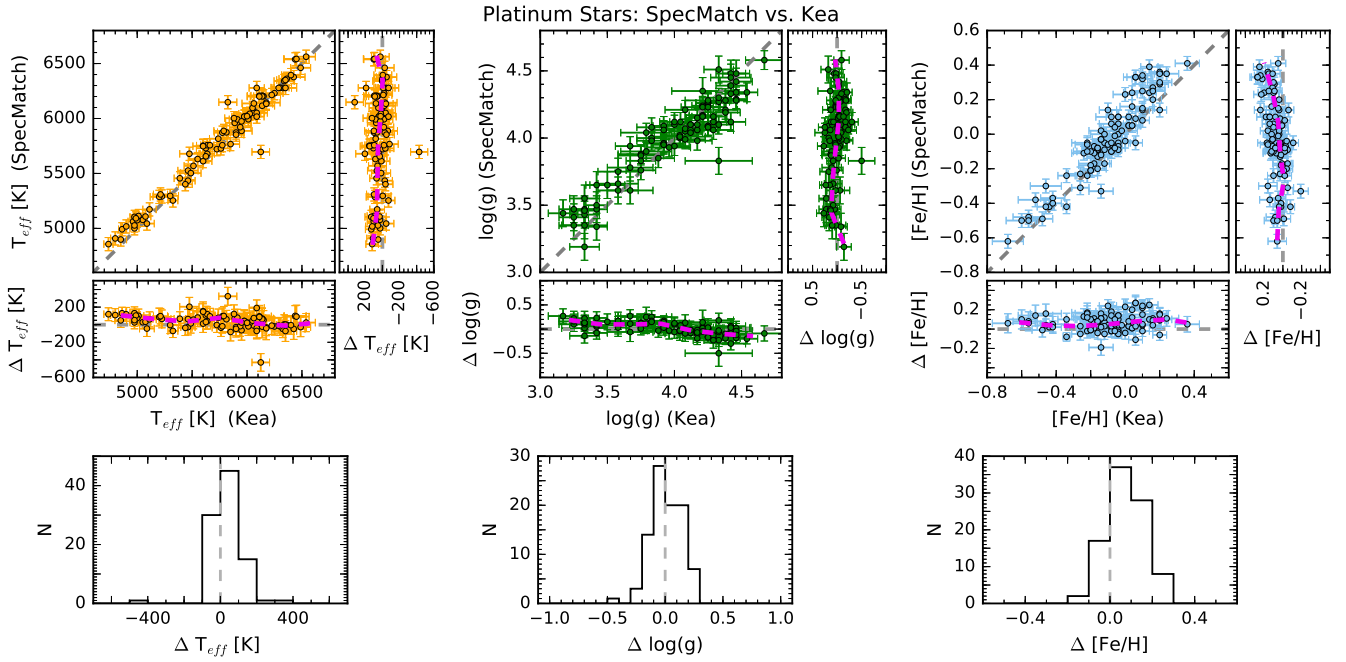


Figure 6.5. Similar to Figure 6.1, but for the platinum standard stars observed at the McDonald 2.7-m and the Keck I telescopes and analyzed with Kea and SpecMatch, respectively (98 stars in common).

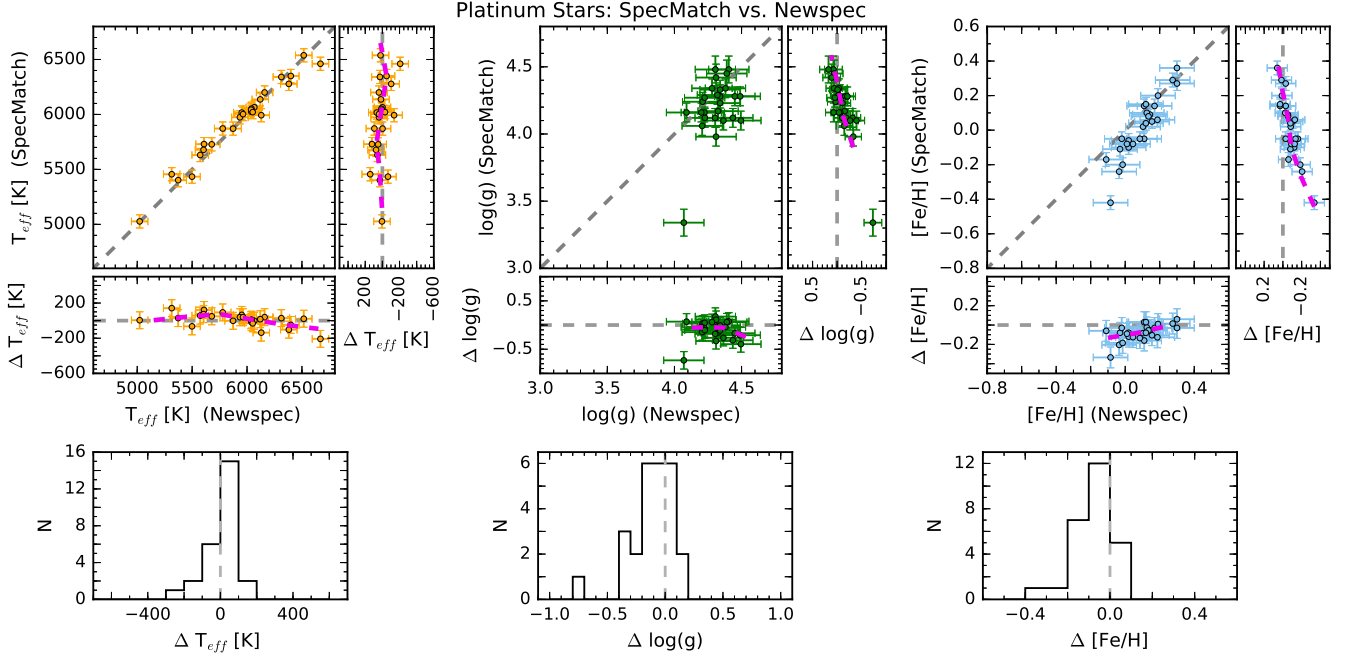


Figure 6.6. Similar to Figure 6.1, but for the platinum standard stars observed at the Keck I and KPNO 4-m telescopes and analyzed with SpecMatch and Newspec, respectively (28 stars in common).

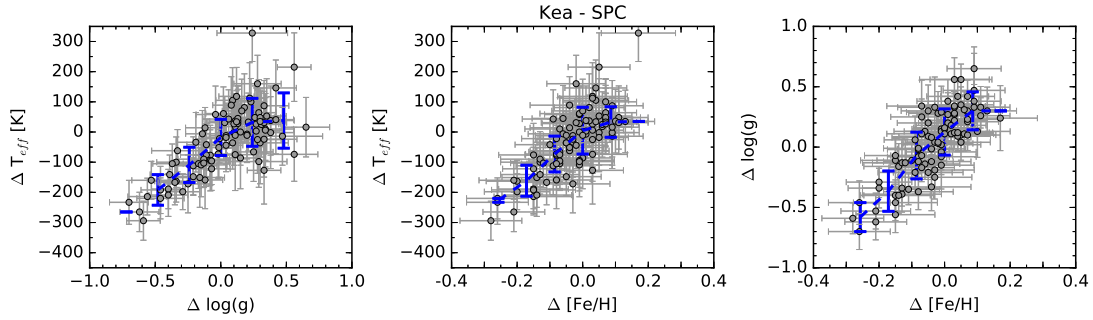


Figure 9.1. Comparison of the differences of stellar parameters derived for the platinum stars with SPC and Kea. The blue dashed line represents a running median. The Pearson correlation coefficients are 0.74 (left), 0.76 (middle), and 0.82 (right).

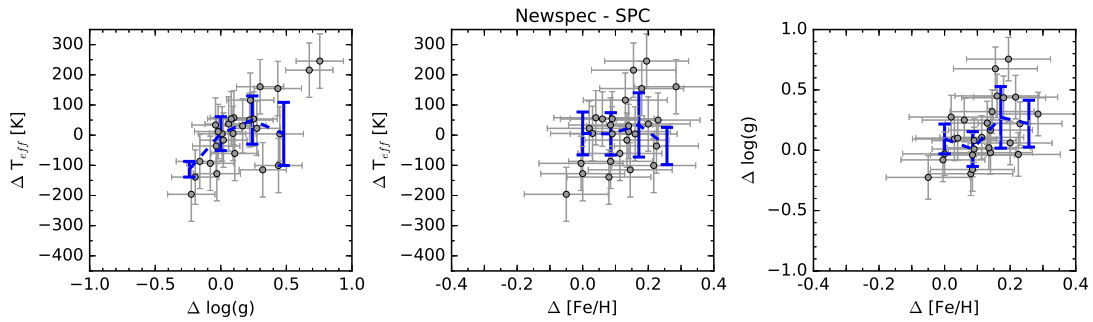


Figure 9.2. Comparison of the differences of stellar parameters derived for the platinum stars with SPC and Newspec. The blue dashed line represents a running median. The Pearson correlation coefficients are 0.57 (left), 0.32 (middle), and 0.45 (right).

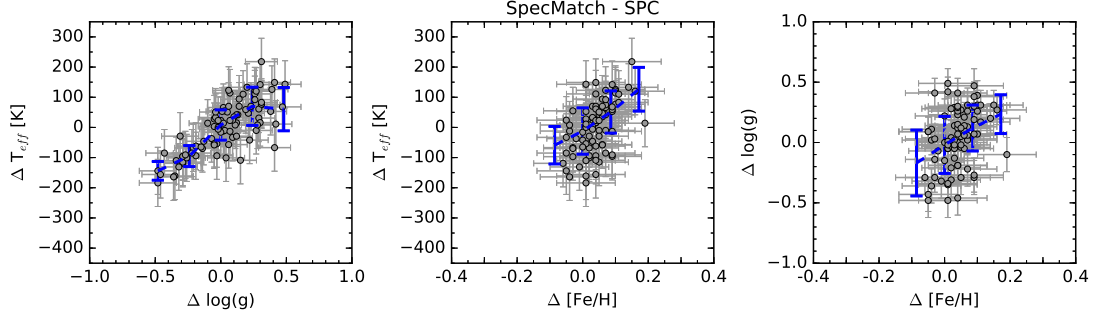


Figure 9.3. Comparison of the differences of stellar parameters derived for the platinum stars with SPC and SpecMatch. The blue dashed line represents a running median. The Pearson correlation coefficients are 0.76 (*left*), 0.53 (*middle*), and 0.36 (*right*).

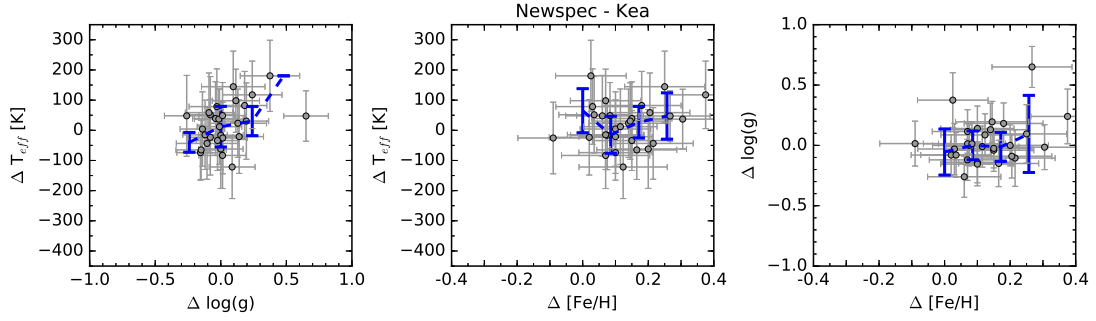


Figure 9.4. Comparison of the differences of stellar parameters derived for the platinum stars with Kea and Newspec. The blue dashed line represents a running median. The Pearson correlation coefficients are 0.56 (*left*), 0.0 (*middle*), and 0.25 (*right*).

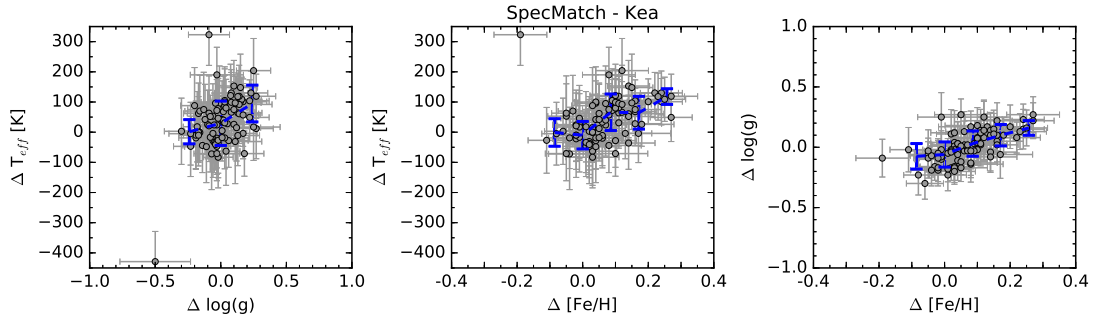


Figure 9.5. Comparison of the differences of stellar parameters derived for the platinum stars with Kea and SpecMatch. The blue dashed line represents a running median. The Pearson correlation coefficients are 0.36 (*left*), 0.55 (*middle*), and 0.66 (*right*).

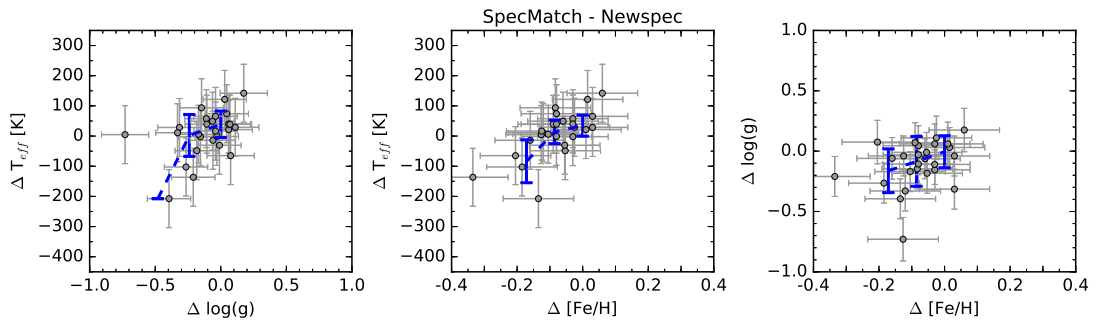


Figure 9.6. Comparison of the differences of stellar parameters derived for the platinum stars with Newspec and SpecMatch. The blue dashed line represents a running median. The Pearson correlation coefficients are 0.51 (*left*), 0.57 (*middle*), and 0.26 (*right*).

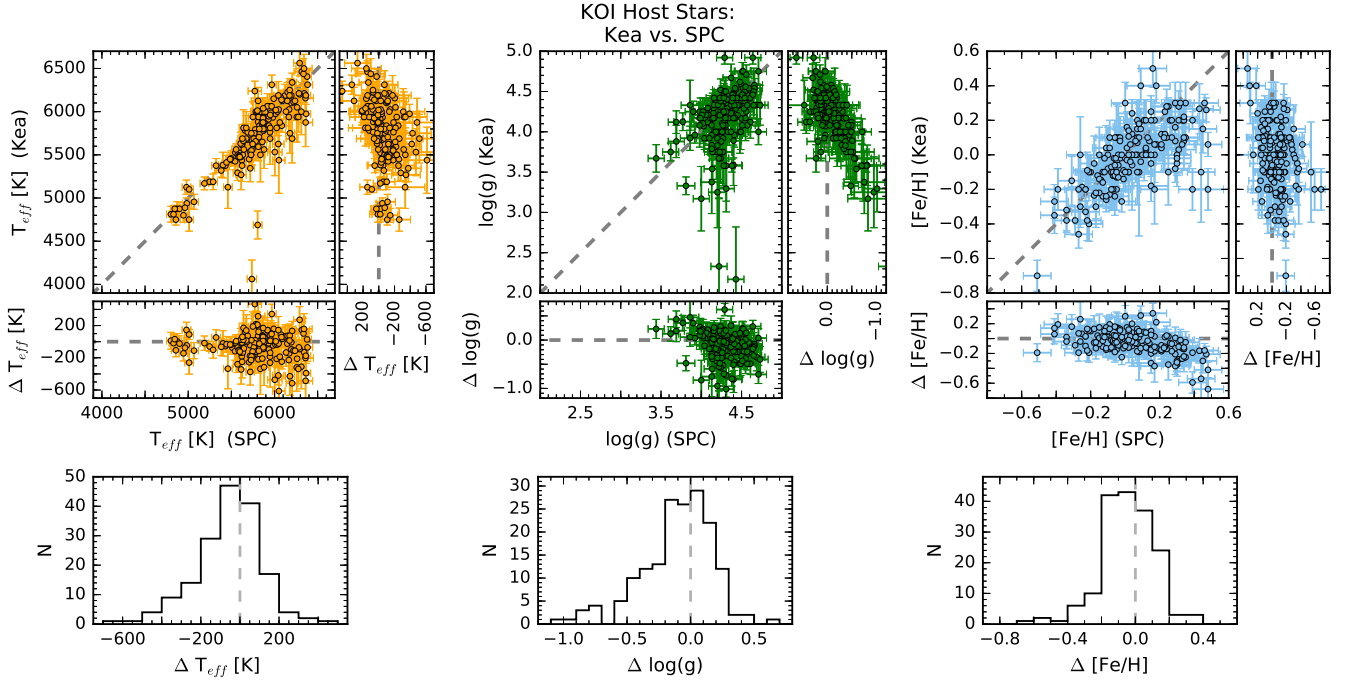


Figure 12.1. Comparison of T_{eff} (left), $\log(g)$ (middle), and $[Fe/H]$ (right) determined for the KOI host stars with SPC and Kea. The top row shows the parameter values of the two sets plotted versus each other (large panels) and the differences in parameter values vs. the values determined with SPC and Kea (smaller panels). The bottom row shows the histograms of the differences in parameter values (172 stars in common).

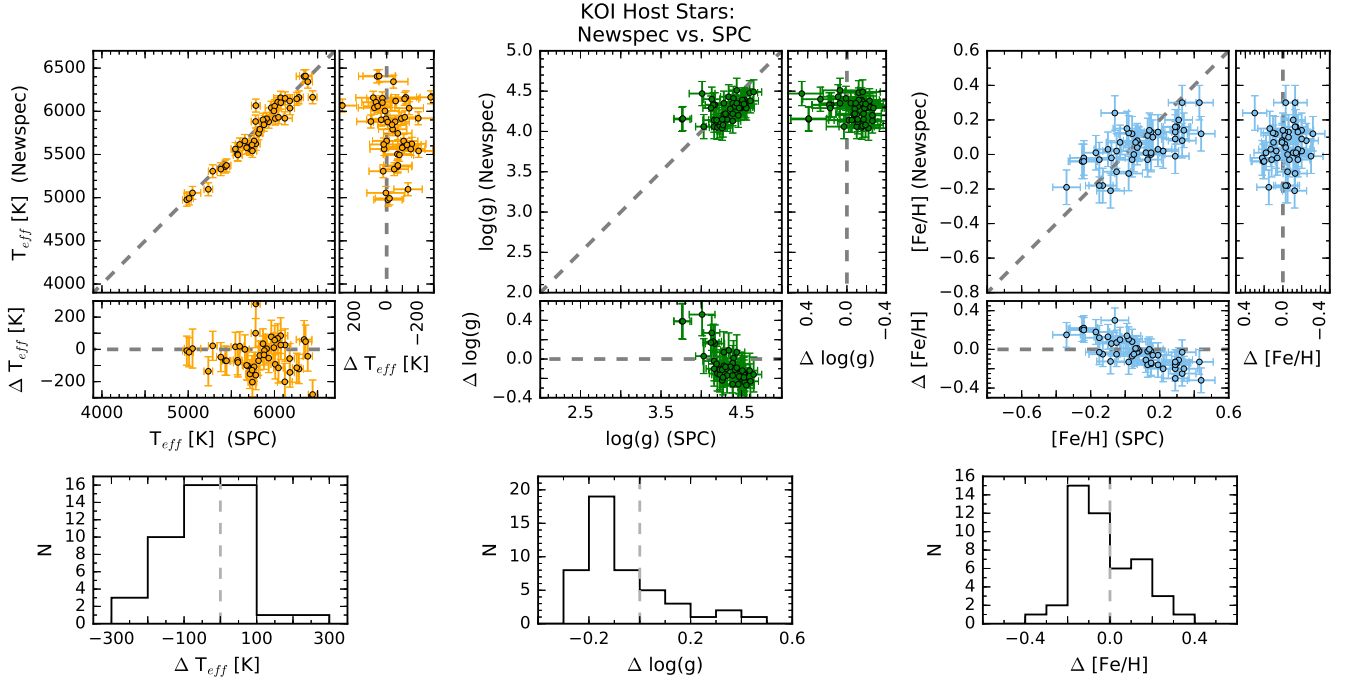


Figure 12.2. Similar to Figure 12.1, but for KOI host star parameters determined with SPC and Newspec (47 stars in common).

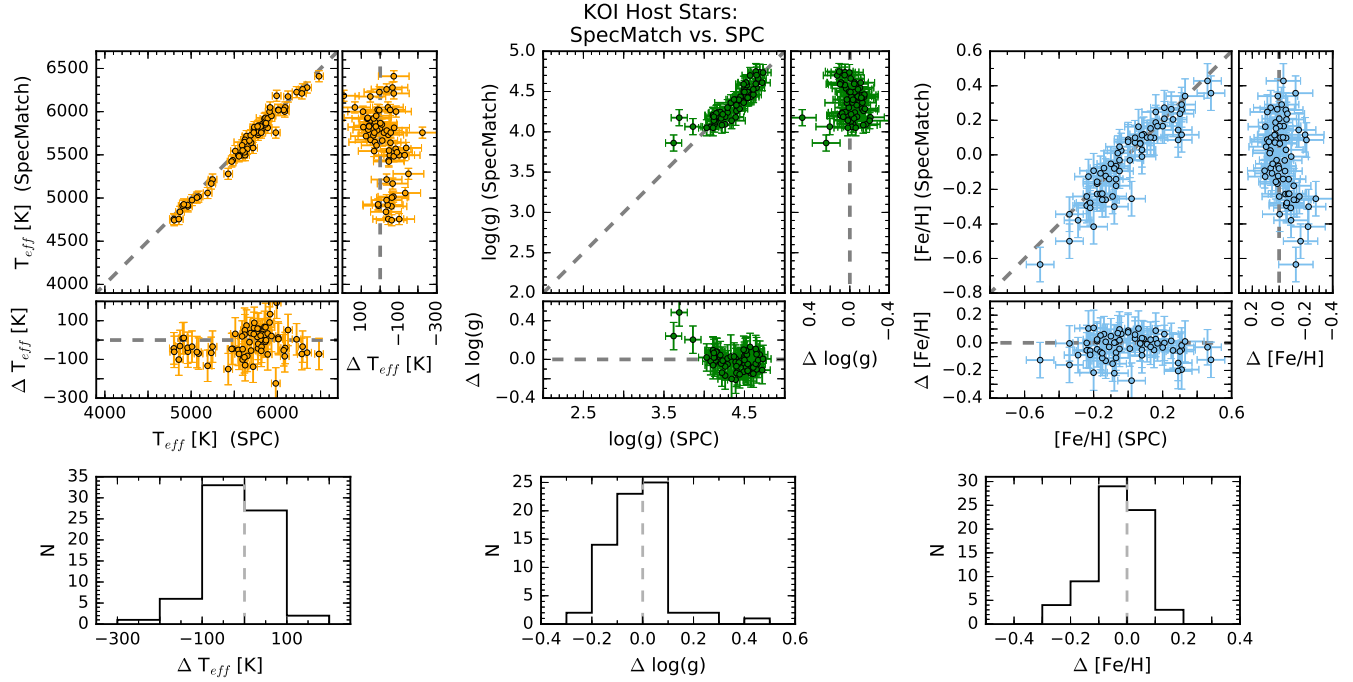


Figure 12.3. Similar to Figure 12.1, but for KOI host star parameters determined with SPC and SpecMatch (70 stars in common).

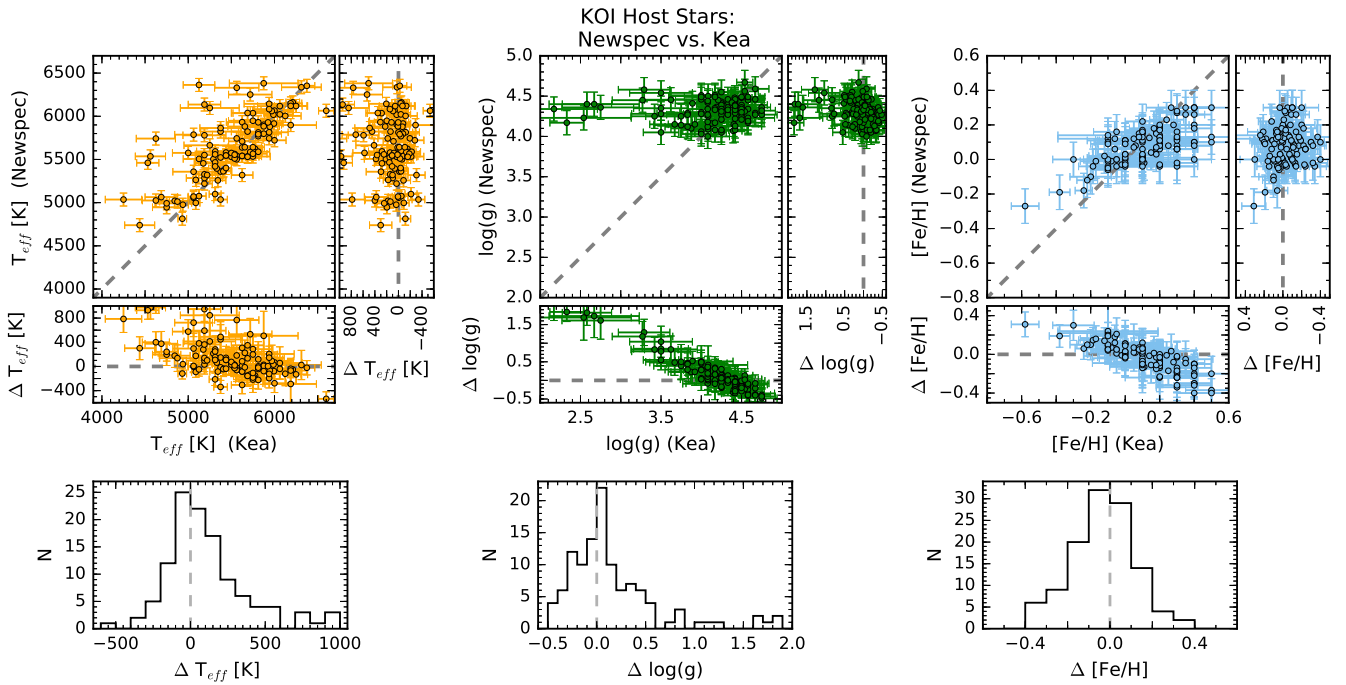


Figure 12.4. Similar to Figure 12.1, but for KOI host star parameters determined with Kea and Newspec (116 stars in common).

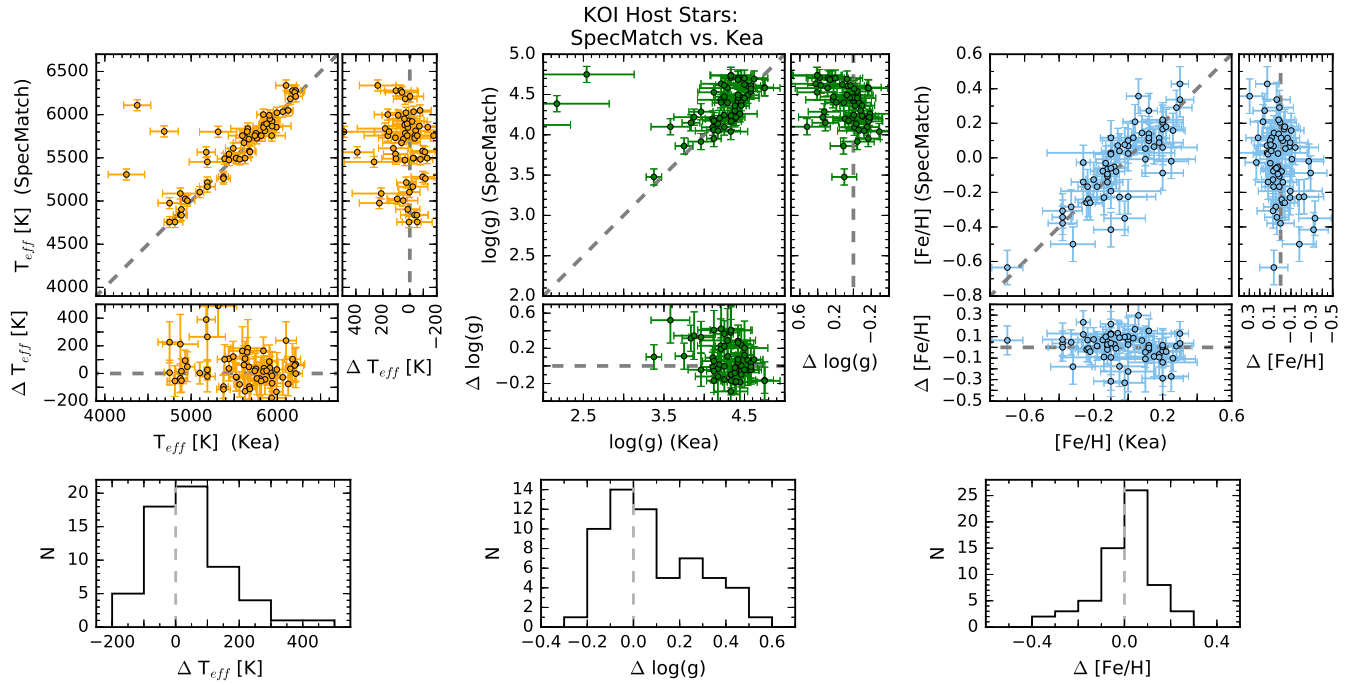


Figure 12.5. Similar to Figure 12.1, but for KOI host star parameters determined with Kea and SpecMatch (74 stars in common).

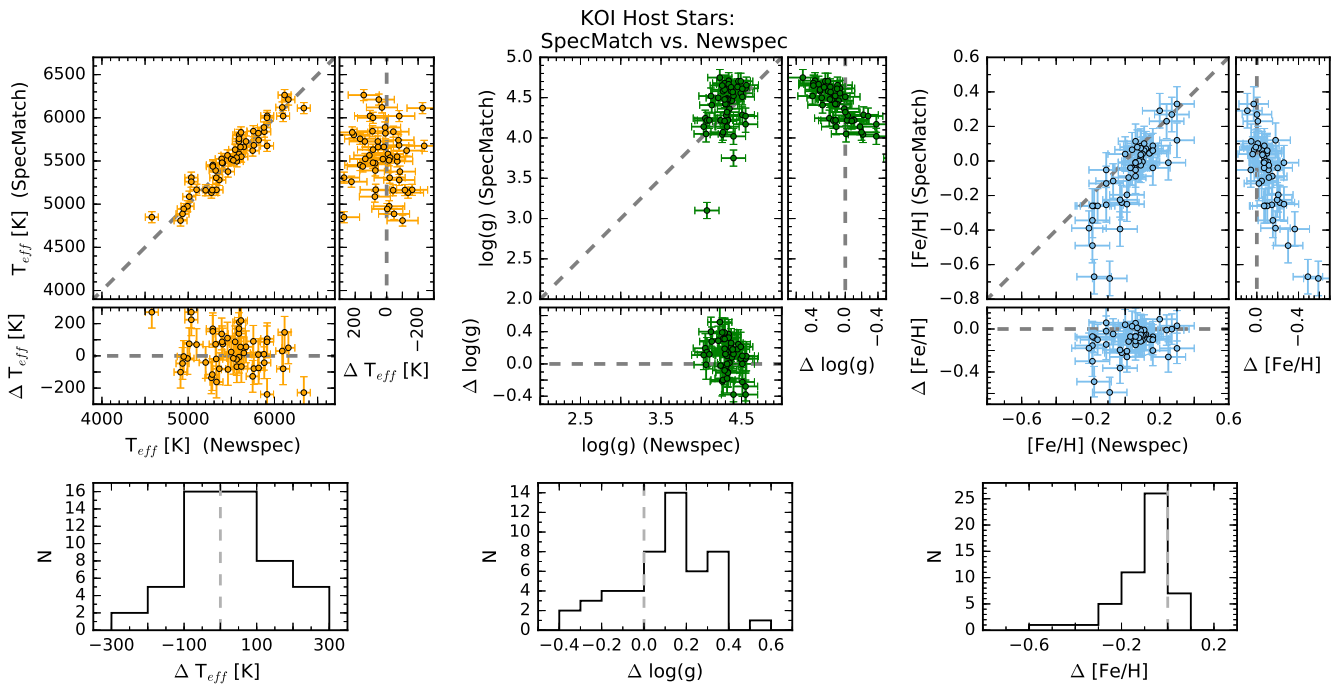


Figure 12.6. Similar to Figure 12.1, but for KOI host star parameters determined with Newspec and SpecMatch (53 stars in common).

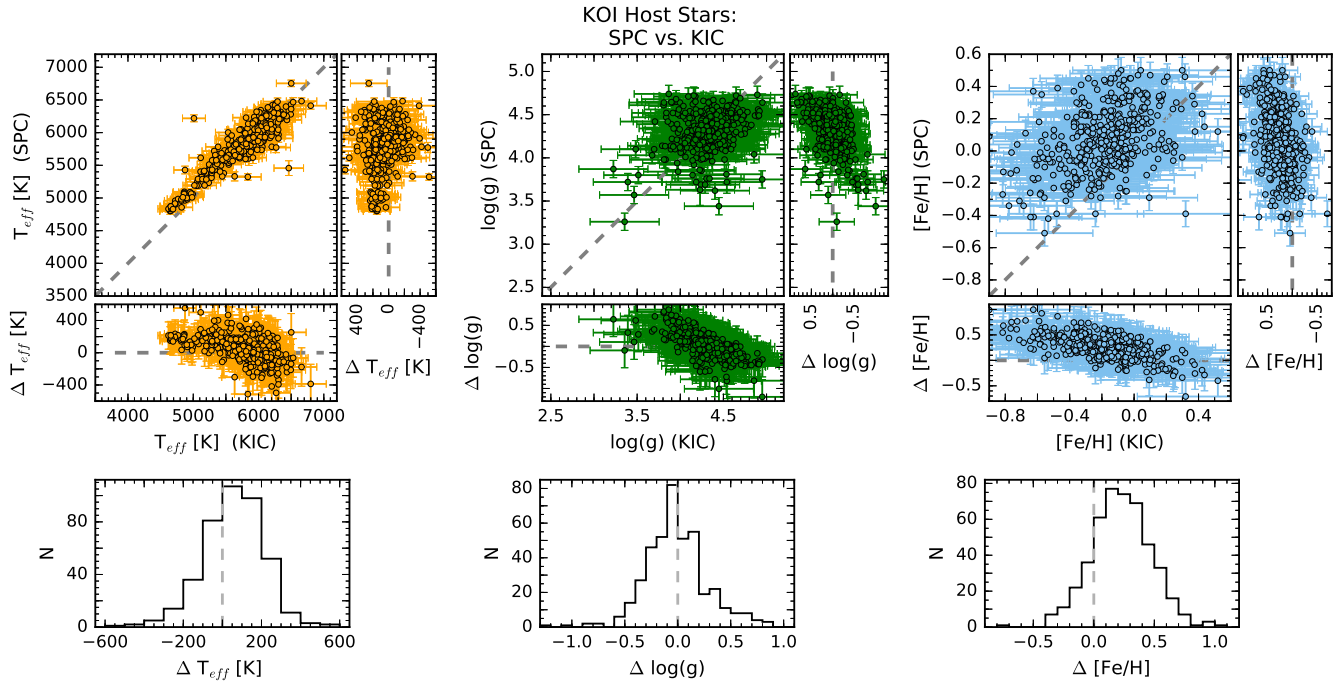


Figure 13.1. Comparison of T_{eff} (left), $\log(g)$ (middle), and $[\text{Fe}/\text{H}]$ (right) determined for the KOI host stars with SPC and the values from the KIC. The top row shows the parameter values of the two sets plotted versus each other (large panels) and the differences in parameter values vs. the values determined with SPC and the values from the KIC (smaller panels). The bottom row shows the histograms of the differences in parameter values.

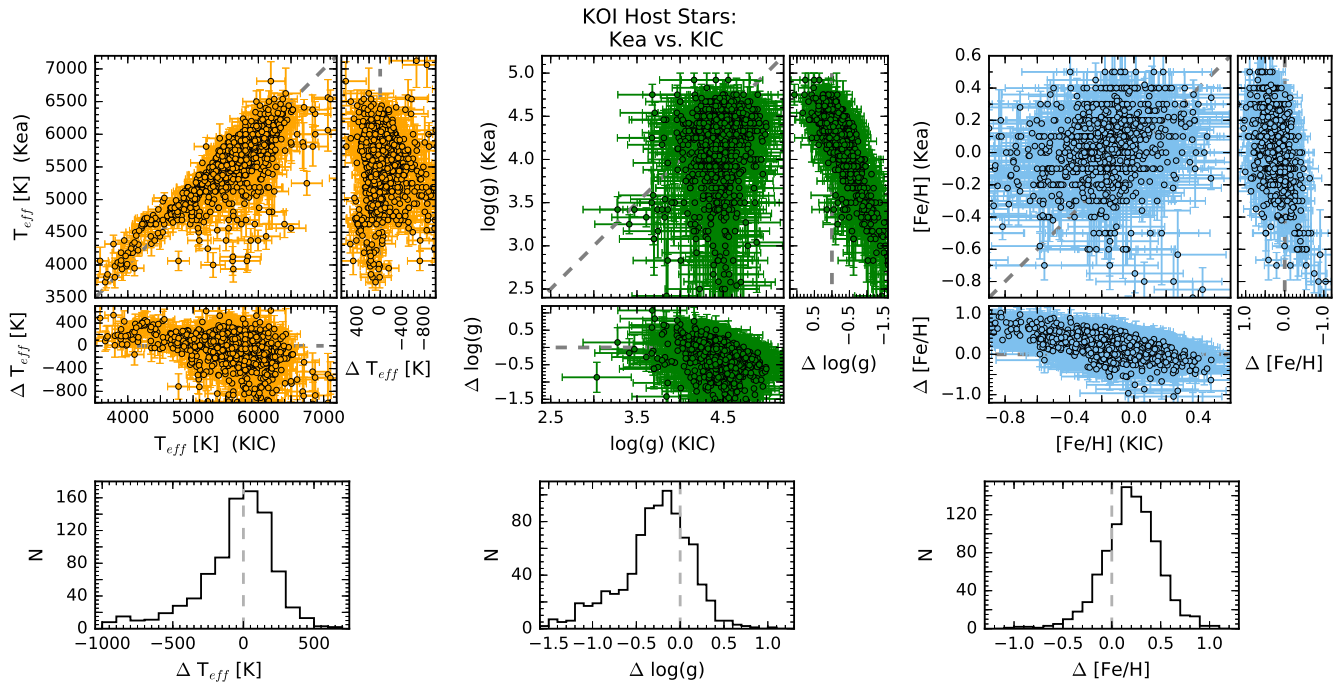


Figure 13.2. Similar to Figure 13.1, but for KOI host star parameters determined with Kea.

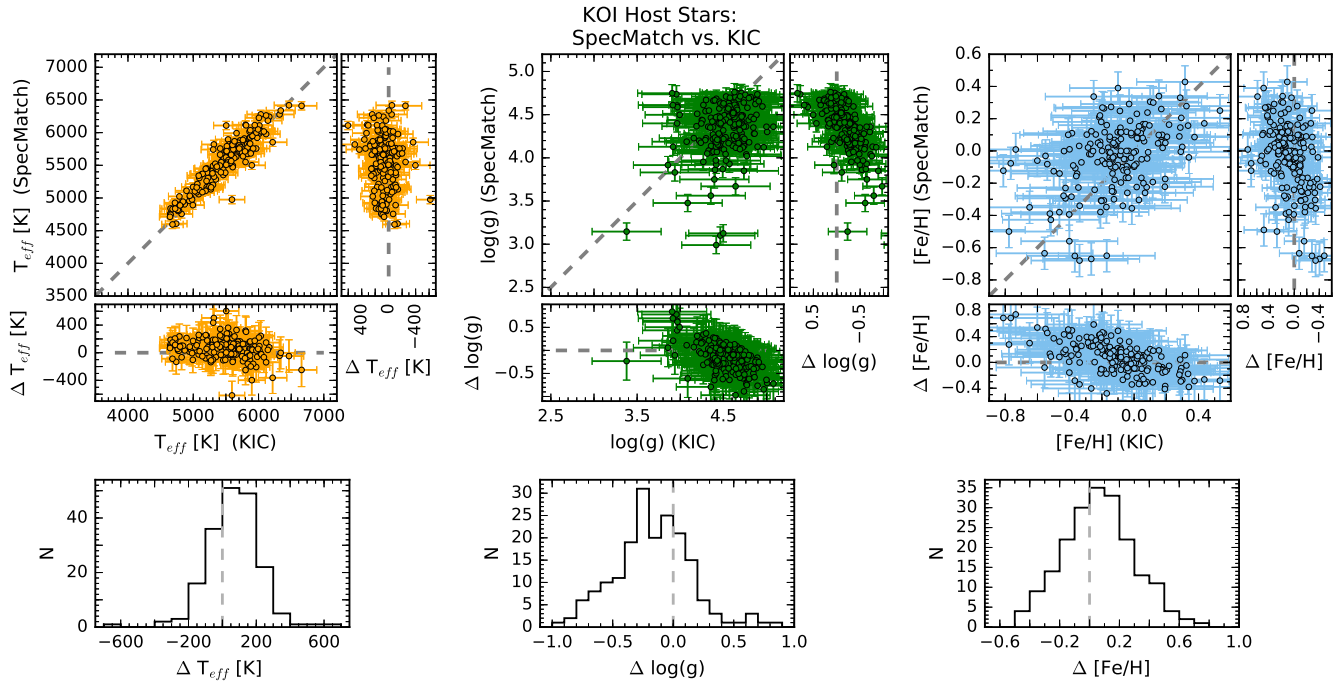


Figure 13.3. Similar to Figure 13.1, but for KOI host star parameters determined with SpecMatch.

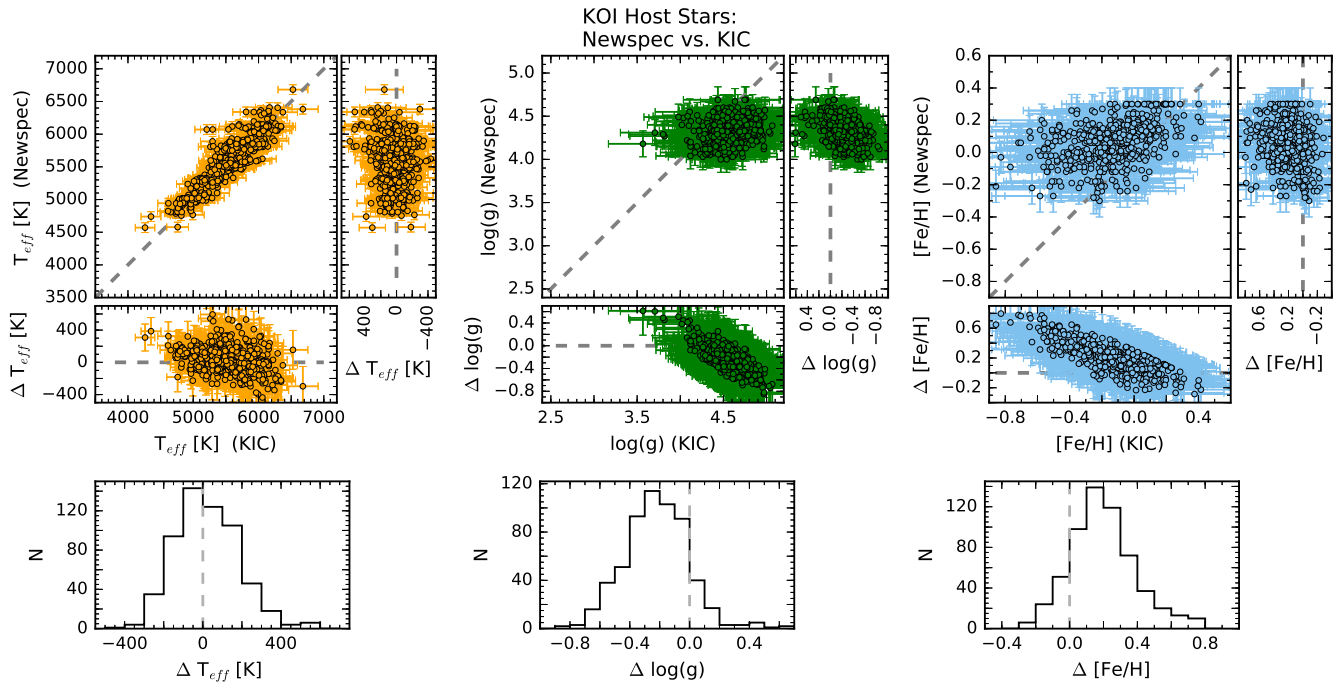


Figure 13.4. Similar to Figure 13.1, but for KOI host star parameters determined with Newspec.

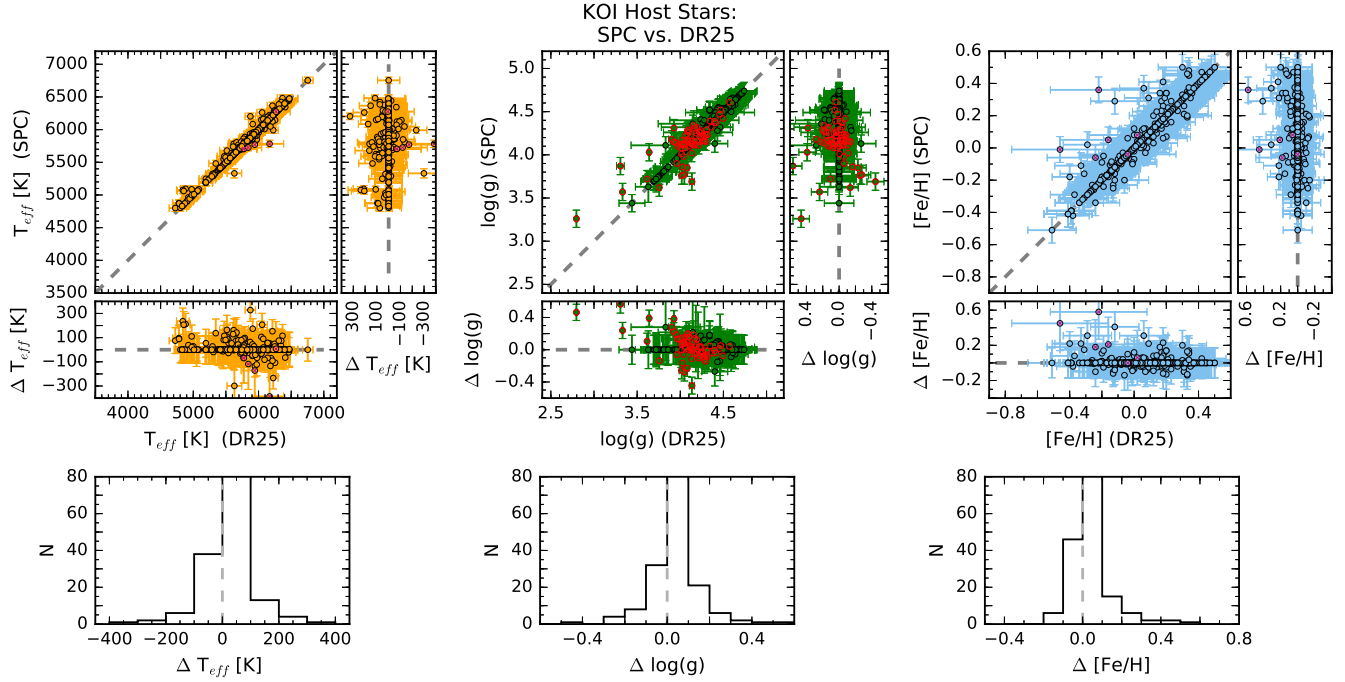


Figure 14.1. Comparison of T_{eff} (left), $\log(g)$ (middle), and $[\text{Fe}/\text{H}]$ (right) determined for the KOI host stars with SPC and the DR25 input values from Mathur et al. (2017). The top row shows the parameter values of the two sets plotted versus each other (large panels) and the differences in parameter values vs. the values determined with SPC and the DR25 input values (smaller panels). The bottom row shows the histograms of the differences in parameter values. The purple crosses identify those DR25 input values for T_{eff} and $[\text{Fe}/\text{H}]$ that were not determined from spectroscopy, while the red circles identify DR25 input values for $\log(g)$ from asteroseismology.

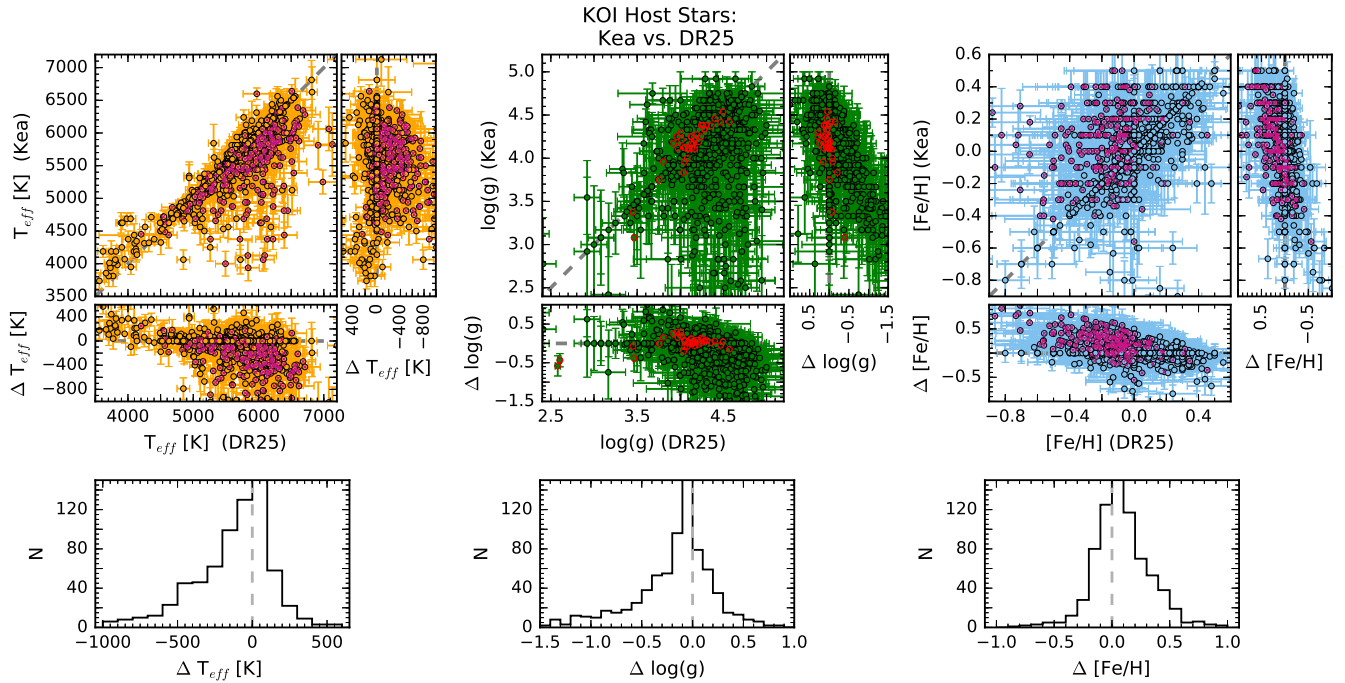


Figure 14.2. Similar to Figure 14.1, but for KOI host star parameters determined with Kea.

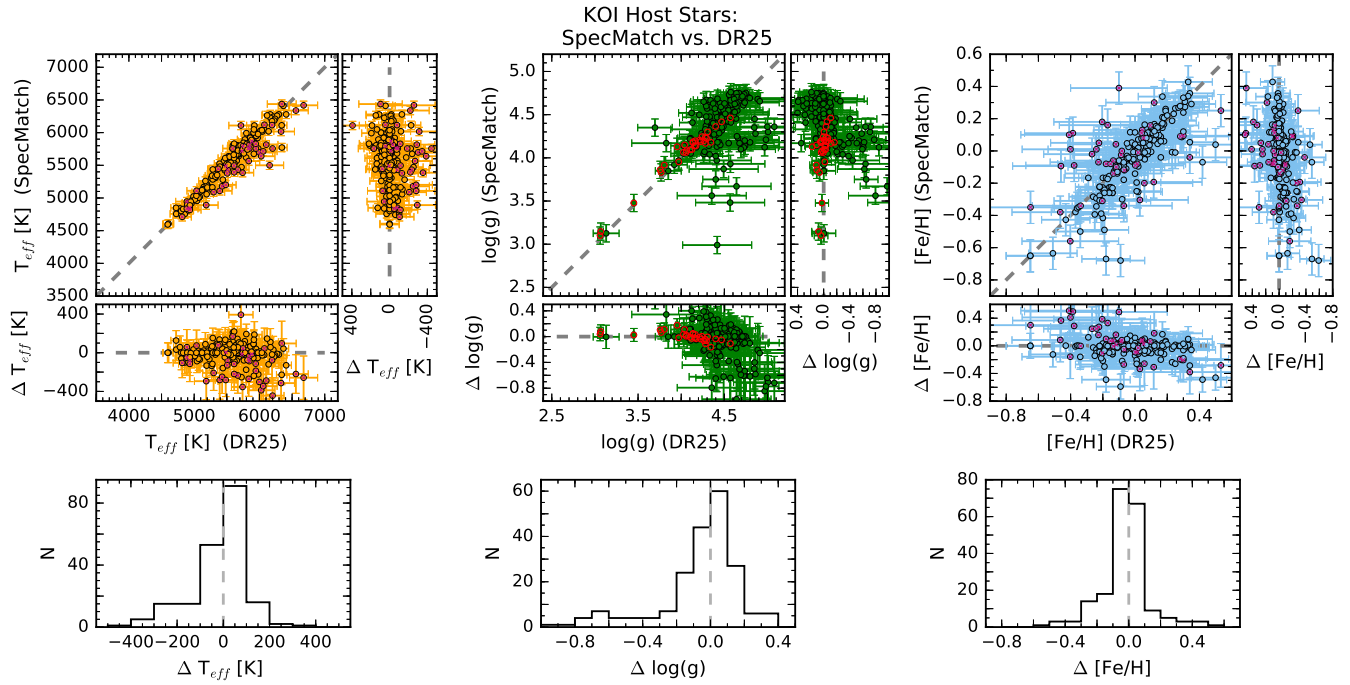


Figure 14.3. Similar to Figure 14.1, but for KOI host star parameters determined with SpecMatch.

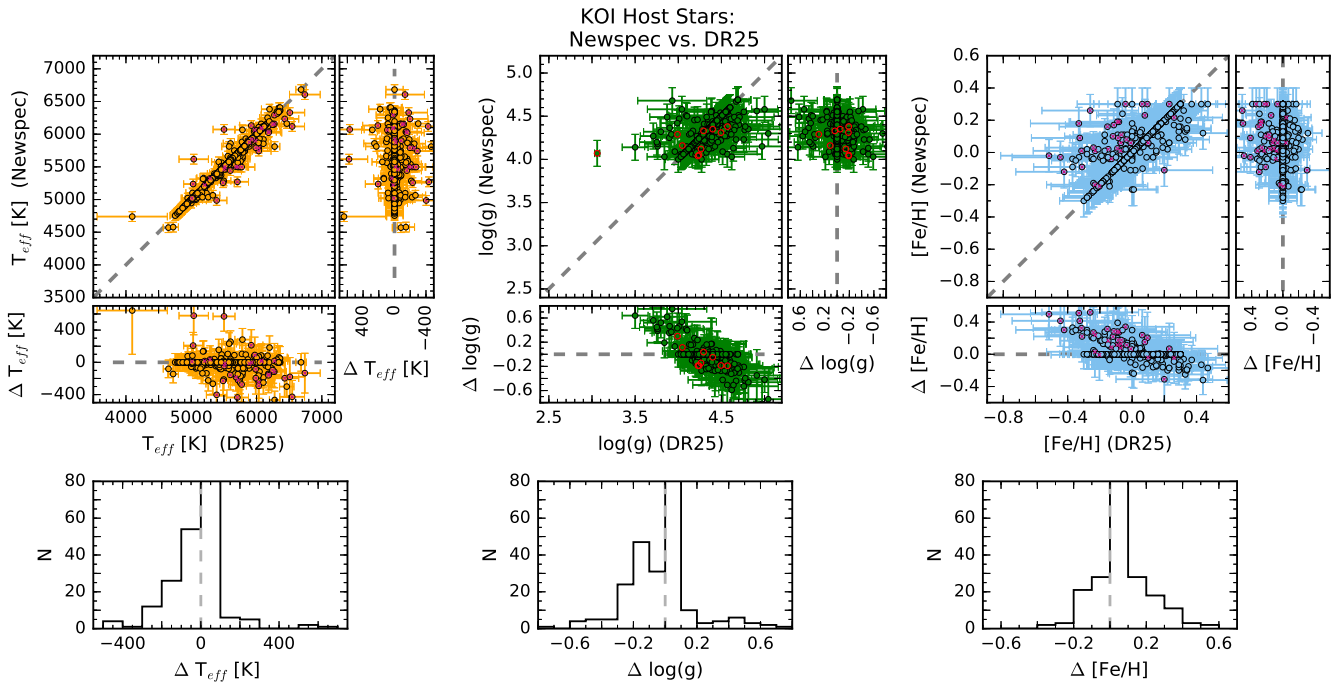


Figure 14.4. Similar to Figure 14.1, but for KOI host star parameters determined with NewSpec.

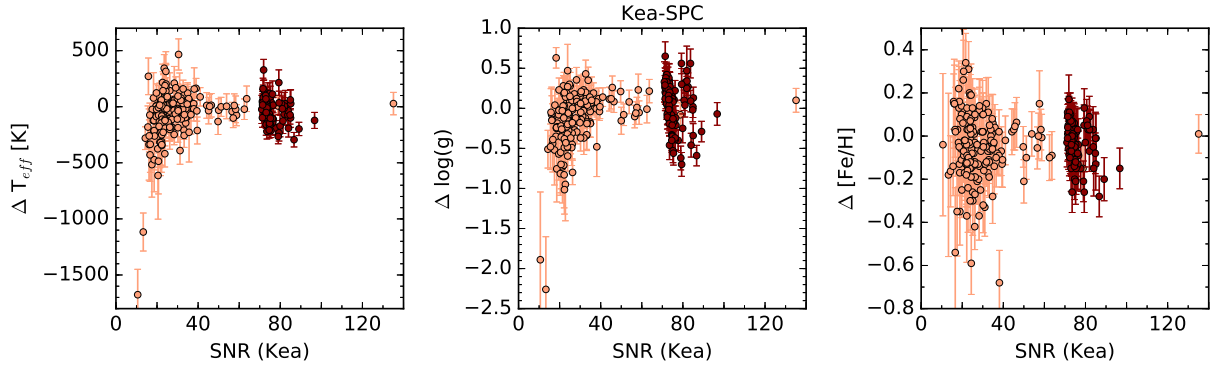


Figure 18.1. Difference of T_{eff} (left) $\log(g)$ (middle), and $[\text{Fe}/\text{H}]$ (right) values determined with SPC and Kea vs. the signal-to-noise of the spectra used as an input for Kea. Stellar parameter differences for KOI host stars are shown in a lighter color, while those for the standard stars are shown in a darker color.

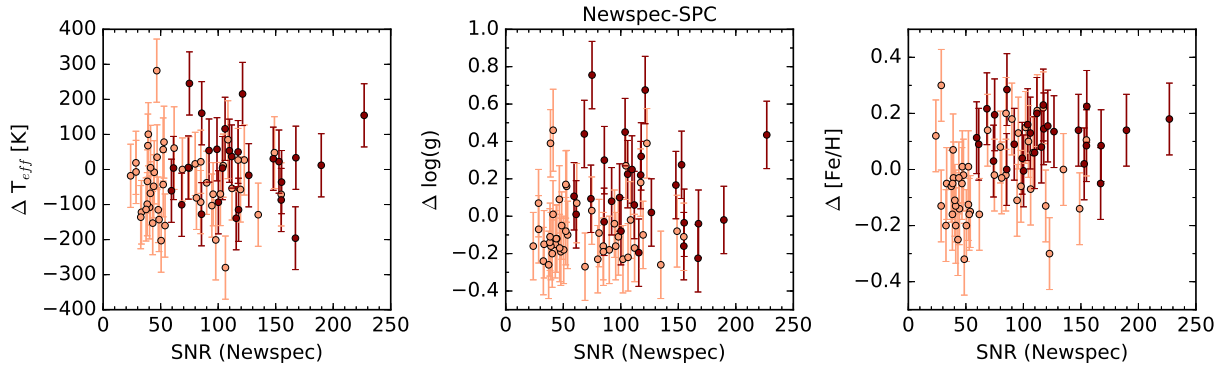


Figure 18.2. Difference of T_{eff} (left) $\log(g)$ (middle), and $[\text{Fe}/\text{H}]$ (right) values determined with SPC and Newspec vs. the signal-to-noise of the spectra used as an input for Newspec. The colors of the symbols have the same meaning as in Figure 18.1.

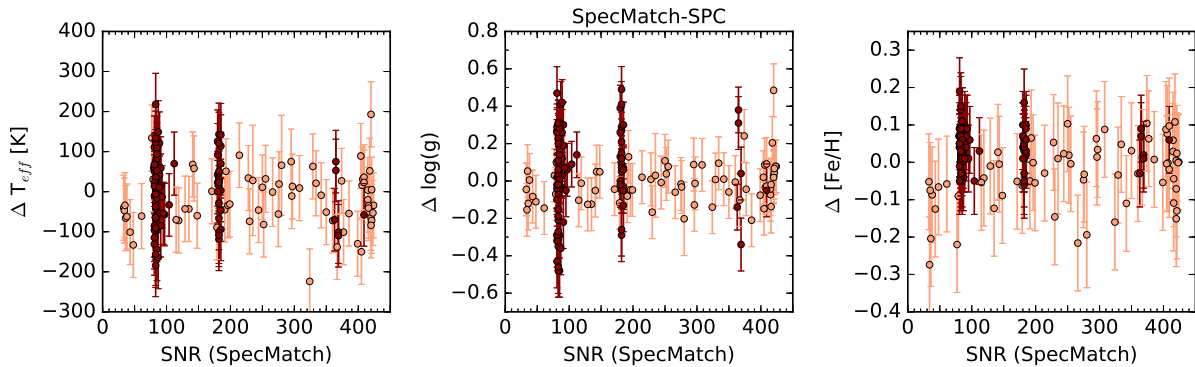


Figure 18.3. Difference of T_{eff} (left) $\log(g)$ (middle), and $[\text{Fe}/\text{H}]$ (right) values determined with SPC and SpecMatch vs. the signal-to-noise of the spectra used as an input for SpecMatch. The colors of the symbols have the same meaning as in Figure 18.1.

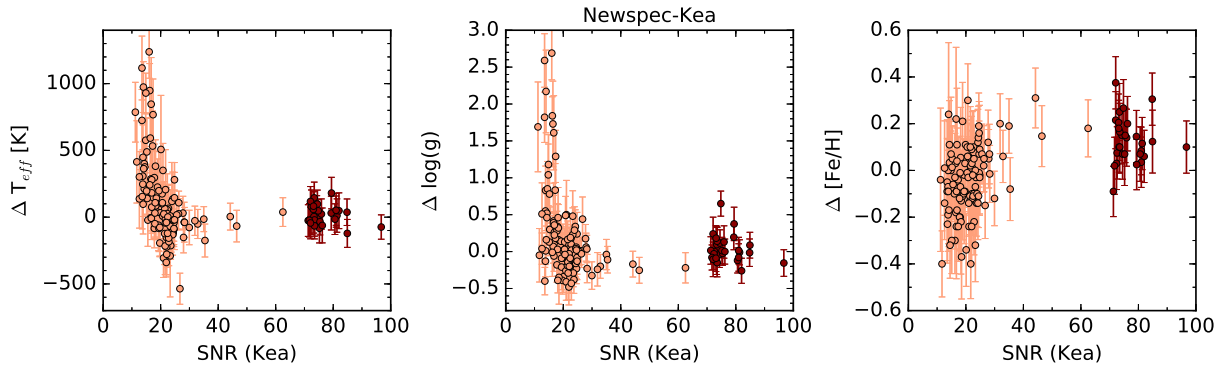


Figure 18.4. Difference of T_{eff} (left) $\log(g)$ (middle), and $[\text{Fe}/\text{H}]$ (right) values determined with Kea and Newspec vs. the signal-to-noise of the spectra used as an input for Kea. The colors of the symbols have the same meaning as in Figure 18.1.

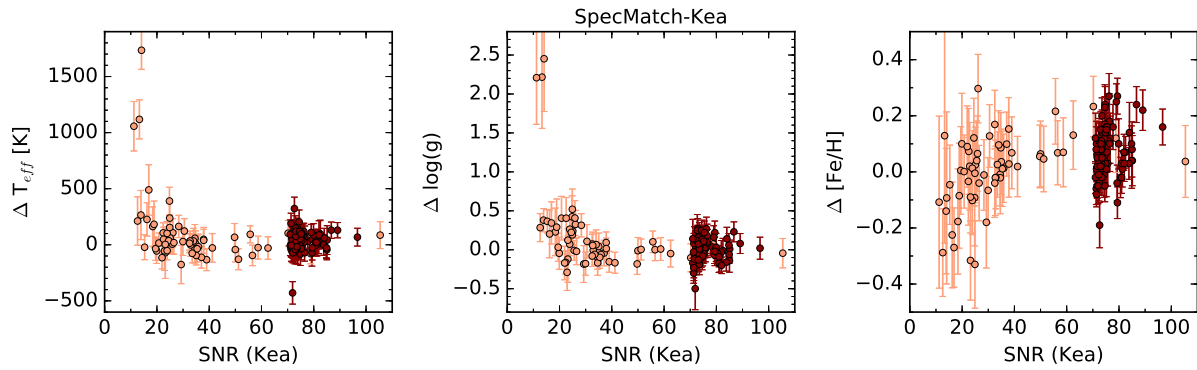


Figure 18.5. Difference of T_{eff} (left) $\log(g)$ (middle), and $[\text{Fe}/\text{H}]$ (right) values determined with Kea and SpecMatch vs. the signal-to-noise of the spectra used as an input for Kea. The colors of the symbols have the same meaning as in Figure 18.1.

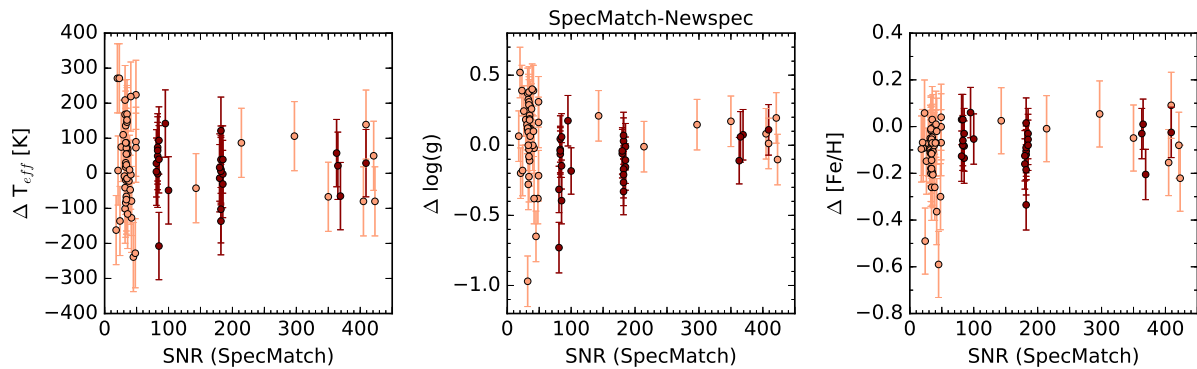


Figure 18.6. Difference of T_{eff} (left) $\log(g)$ (middle), and $[\text{Fe}/\text{H}]$ (right) values determined with Newspec and SpecMatch vs. the signal-to-noise of the spectra used as an input for SpecMatch. The colors of the symbols have the same meaning as in Figure 18.1.